



<https://theses.gla.ac.uk/>

Theses Digitisation:

<https://www.gla.ac.uk/myglasgow/research/enlighten/theses/digitisation/>

This is a digitised version of the original print thesis.

Copyright and moral rights for this work are retained by the author

A copy can be downloaded for personal non-commercial research or study,  
without prior permission or charge

This work cannot be reproduced or quoted extensively from without first  
obtaining permission in writing from the author

The content must not be changed in any way or sold commercially in any  
format or medium without the formal permission of the author

When referring to this work, full bibliographic details including the author,  
title, awarding institution and date of the thesis must be given

Enlighten: Theses

<https://theses.gla.ac.uk/>  
[research-enlighten@glasgow.ac.uk](mailto:research-enlighten@glasgow.ac.uk)

THE ROYAL COLLEGE OF SCIENCE AND TECHNOLOGY, GLASGOW

DEPARTMENT OF MINING

"FLUCTUATING PRESSURE, IN THE MINE VENTILATING  
CIRCUIT, CAUSED BY SINGLE CAGE WINDING"

by

Ronald Stewart, B.Sc.

October, 1961

ProQuest Number: 10656291

All rights reserved

INFORMATION TO ALL USERS

The quality of this reproduction is dependent upon the quality of the copy submitted.

In the unlikely event that the author did not send a complete manuscript and there are missing pages, these will be noted. Also, if material had to be removed, a note will indicate the deletion.



ProQuest 10656291

Published by ProQuest LLC (2017). Copyright of the Dissertation is held by the Author.

All rights reserved.

This work is protected against unauthorized copying under Title 17, United States Code  
Microform Edition © ProQuest LLC.

ProQuest LLC.  
789 East Eisenhower Parkway  
P.O. Box 1346  
Ann Arbor, MI 48106 – 1346

## A C K N O W L E D G E M E N T S

The author wishes to express sincere thanks to Professor G. Hibberd, Ph.D., A.R.C.S.T., M.I.Min.E., F.R.S.E., who supervised this work, for his advice and guidance throughout.

Thanks are also expressed to :

Mr. A.W.K. Stewart, Senior Lecturer, and other members of the staff of the Mining Department, The Royal College of Science and Technology, Glasgow, for their help and encouragement.

Mr. A. Chattel, for his assistance in the preparation of apparatus.

The Department of Scientific and Industrial Research, for granting a Research Studentship.

The National Coal Board, who sponsored this work, for financial assistance.

## P R E F A C E

This thesis describes work carried out in the Mining Department of the Royal College of Science and Technology, Glasgow, during an investigation into disturbances in the mine ventilation circuit caused by single cage winding. Winding with a single cage instead of two smaller balanced cages had a very noticeable effect on the ventilation of a North of England colliery and the substance of a report by the Area ventilation staff, describing these effects, is included in the thesis in order that these effects may be more clearly understood. The colliery, the ventilation of which is described in the report, is Ryhope colliery and is referred to in the thesis as colliery R.

The investigation described in the report was, naturally, very limited in scope, due to the small number of factors which could be varied, so it was decided to construct a model in which the effects could be simulated, and in which more factors could be varied. The considerations influencing the design of the model are explained and the model is described.

The methods of measurement used and the instruments involved are described, and tests which were performed to assess the limitations of the pressure recorder are included, together with the conclusions to which they lead.

The tests carried out on the model fall into two groups. The first is concerned with the pressure drop produced by the cage, and

the factors which affect it. The second deals with the effects on the ventilation system of communicating this pressure drop to the large volume of air contained in the underground workings. The tests in each group are described in full and the conclusions are drawn.

Having described the work connected with the model the thesis then deals with theoretical methods of predicting the effects. The investigation leading to the method used is fully explained and the method is given in detail. Many examples have been solved using the method and the results and conclusions have been given.

An alternative method of solution is indicated and its advantages and limitations discussed.

In the conclusions an assessment is made of the phenomenon in the light of the knowledge which has been gained from both sections of the work. All factors which may influence the effects are considered and their relative merits discussed.

The limitations of the present investigation are indicated and suggestions are made as to how the work may be extended.

C O N T E N T S

	<u>Page</u>
Preface	1
Contents	3
List of Symbols	4
Chapter 1 Introduction	7
Chapter 2 Ventilation Disturbances at Colliery R	10
Chapter 3 Description of the model	14
Chapter 4 Description of the Instruments and Methods of Measurement	21
Chapter 5 The Laws of Similarity	28
Chapter 6 Model Tests - 1. Stationary Cage Tests	32
Chapter 7 Model Tests - 2. Moving Cage Tests	40
Chapter 8 Model Tests - 3. Velocity Fluctuations Produced by the Moving Cages	44
Chapter 9 Theoretical Prediction of Velocity Disturbances - Method 1.	52
Chapter 10 Theoretical Prediction of Velocity Disturbances - Method 2.	64
Chapter 11 Conclusions	74
Appendix A	
Appendix B	
References	

LIST OF SYMBOLS

a	ft/sec.	velocity of sound
A	$= \frac{a}{a_0}$	non-dimensional form of a
b		coefficient of fill
$c_p$	B.T.u./lb, °R	specific heat at constant pressure
C	farads	capacitance
d	feet	diameter
e	volts	voltage
E		Laplace transform of e
f		coefficient of friction
$f_1$	c/s	resonant frequency of system
$f_0$	c/s	resonant frequency of connecting tube alone
$F_f$	lbs	friction force
g	ft/sec <sup>2</sup>	gravity
i	amps	current
I		Laplace transform of i
J	ft/lb./B.t.u.	mechanical equivalent of heat
k		ratio of specific heats
$l$	ft	length
m	lbs	weight
M	ft <sup>2</sup>	area

$p$	lbs/ft <sup>2</sup>	pressure
$p_f$	lb/ft <sup>2</sup>	friction pressure drop
$P$	$= \frac{2}{k-1} A + U$	Riemann constant
$Q$	$= \frac{2}{k-1} A - U$	Riemann constant
$q$	B.t.u./lb.	heat added per unit weight
$R$	ft.lb/slug, °R	gas constant
$Re$	$= \frac{w \rho u}{\gamma}$	Reynolds number
$R_p$	m.m. W.G.	pressure drop due to cage in air velocity of 100 ft/sec.
$s$	B.t.u./lb, °R	specific entropy
$S$	$= \frac{s}{c_p (y-1)} = \frac{gJs}{yR}$	non-dimensional form of $s$
$t$	secs.	time
$T$	$= \frac{t a_0}{l_0}$	non dimensional form of $t$
$u$	ft/sec.	velocity of air
$U$	$= \frac{u}{a_0}$	non-dimensional form of $u$
$v$	ft/sec.	velocity of cage
$V$	ft <sup>3</sup>	volume
$w$	lb/ft <sup>3</sup>	density of air
$x$	ft.	distance
$X$	$= \frac{x}{l_0}$	non-dimensional form of $x$

$\gamma$  lbs/ft.sec.

viscosity

$z = f_1/f_0$

ratio of resonant frequencies

$\phi$  °R

temperature

### Subscripts

a

acoustical

e

conditions inside duct, at duct end

E

conditions in region external to duct end

I

instrument

o

reference

T

tube

### Operators

$$\frac{D}{Dt} = \frac{\partial}{\partial t} + u \cdot \frac{\partial}{\partial x}$$

derivative along a particle path

$$\frac{D_{\pm}}{Dt} = \frac{\partial}{\partial t} + (u \pm a) \frac{\partial}{\partial x}$$

derivative along a characteristic.

Mining Ventilation is one aspect of mining which readily lends itself to systematic study, both in the mine and in the laboratory. Moreover many of the laws which apply in a mine have been extensively studied in other fields. It is not surprising, therefore, that the laws of ventilation are, in general, familiar and well understood. These laws apply, however, only to steady state conditions when the air velocity at any point does not vary with time. The assumption of steady state conditions is reasonable in normal mining circumstances when variations of velocity are slight.

The work described here is concerned with investigating the behaviour of the ventilating air under the unsteady conditions produced by the movement of a single large cage in one of the shafts. Under these conditions the application of the steady state laws may give very misleading results.

Unsteady flow conditions occur all the time underground when doors are opened and closed, when tubs or mine cars suddenly enter a roadway and change its resistance, when explosives are being fired or when the cages move. Many other incidents produce varying degrees of unsteady flow but it is the movement of the cages and, in particular, of a single cage which produces the most serious disturbances.

In the past, men and materials have been raised and lowered in mine shafts by means of a system whereby two similar cages travel

in opposite directions. This has meant that any pressure disturbance around one cage was counteracted by a similar disturbance around the other cage and hence any pressure variation was limited to the distance between the cages and to a short distance beyond them. Consideration of winding systems in the light of modern techniques and economics has meant that, in certain cases, it has been advantageous to use a single large cage and counterweight. The frontal area of the counterweight is generally less than 2% of that of the cage so that the effect of the counterweight on the ventilation system may be neglected. It is this single cage, therefore, having approximately twice the frontal area of each cage in the balanced cage system, producing a pressure disturbance not offset by any other pressure disturbance, which is, in certain cases, causing a serious disturbance of the steady air flow.

Work done in the field can be invaluable in studying the disturbance but it is more likely that so few results can be obtained and so few factors varied that a true picture is difficult to obtain. In the study of mine ventilation it has been found, in general, more useful to do tests on models where many factors may be varied and to verify the results of the model tests by a few field tests. This technique is now well established for steady flow studies and the laws relating the results in the model to those in the field have been determined. In the case of non-steady flow additional factors must be considered, and the laws relating the model and the

field work must be re established. For these reasons it was proposed, in this investigation, to construct a model in which a similar effect could be produced and studied with a view to determining the important factors concerned and the laws connecting these factors in the model to those in the field.

The report describing a disturbance in colliery B similar to the disturbances being investigated is the only reference [ref. 1], containing the results of fieldwork, which could be traced. The design of the model has therefore been based, to a large extent, on this report.

Towards the end of the investigation a second report [ref. 14] describing a similar phenomenon became available. In this case there was a second shaft in parallel with the first, hence this report is discussed in the conclusions, where a parallel shaft is considered as a method of reducing the disturbances.

At colliery R. a major reorganization included a changeover in the winding system from a drum winder, winding balanced cages, to a multirope friction winder, winding a single cage and counterweight in the downcast shaft. A cross section of the shaft and equipment after the changeover is shown in Fig. 1.

Fig. 2 shows the position of the various insets in the shaft. It became obvious immediately after the changeover that some disturbance to the air flow was taking place in the 5/4 inset. The disturbance was apparently associated with the movement of the cage and measurement taken by the colliery ventilation staff indicated that reversal of the air flow was taking place during part of the winding cycle. This conclusion prompted the Area ventilation staff to carry out a series of tests designed to yield more detailed information on the nature of this reversal.

A full description of these tests and results is included in ref. 1 but the following details are given here to facilitate description of the phenomenon. In the first series of tests observers were stationed at the 5/4 level 10 yards from the shaft in the main intake airway, 1,000 yards inbye from this position and in the main return adjacent to the upcast shaft. Using two Velometers (one for flow in the reverse direction) they noted the air velocity at 5 second intervals during several complete winding cycles. A manometer connected directly across the shafts at the 5/4 level was similarly read at 5 second intervals. The cage was

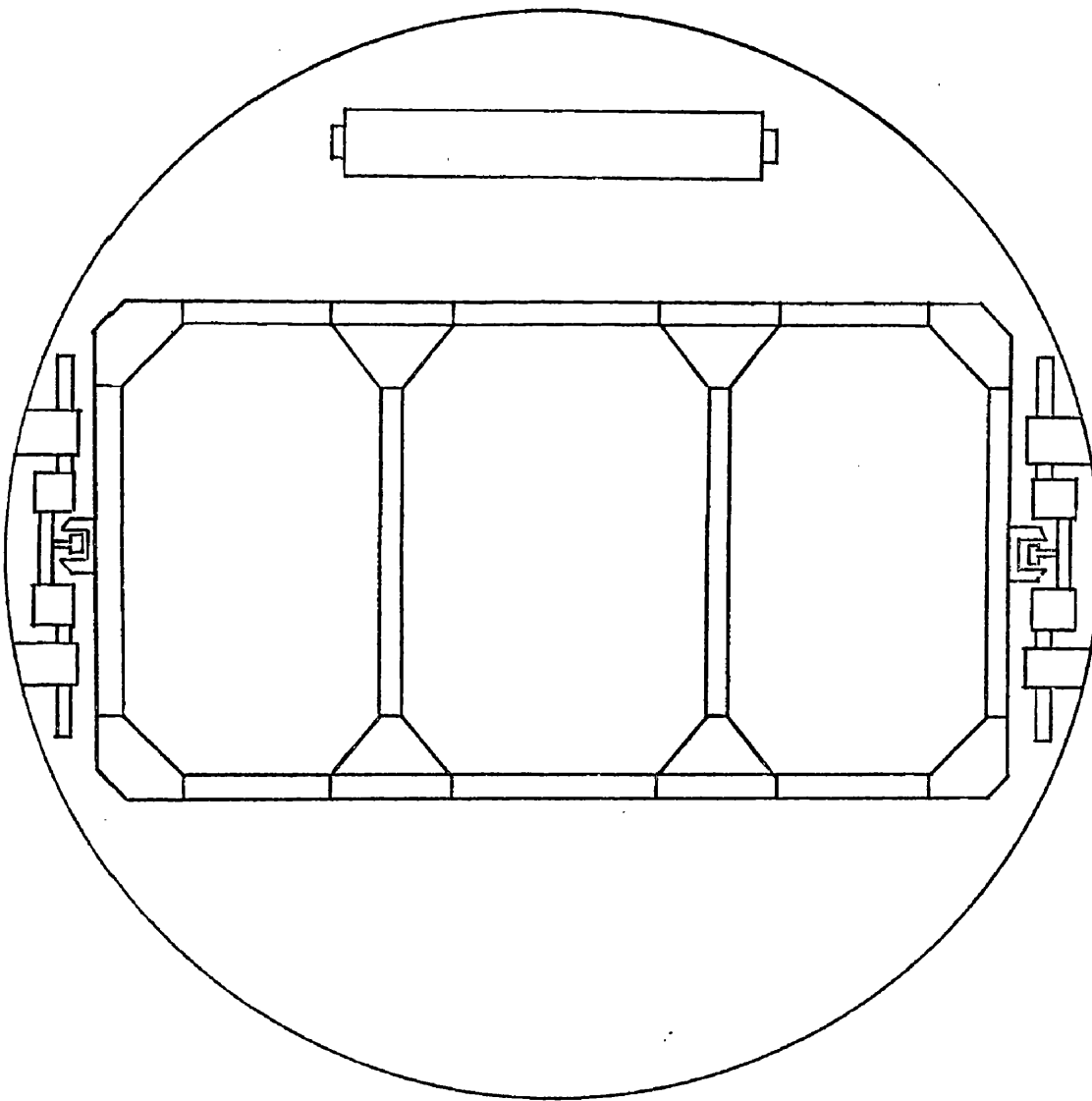


Fig.1. Cross-section of shaft and equipment at colliery R after the change-over.

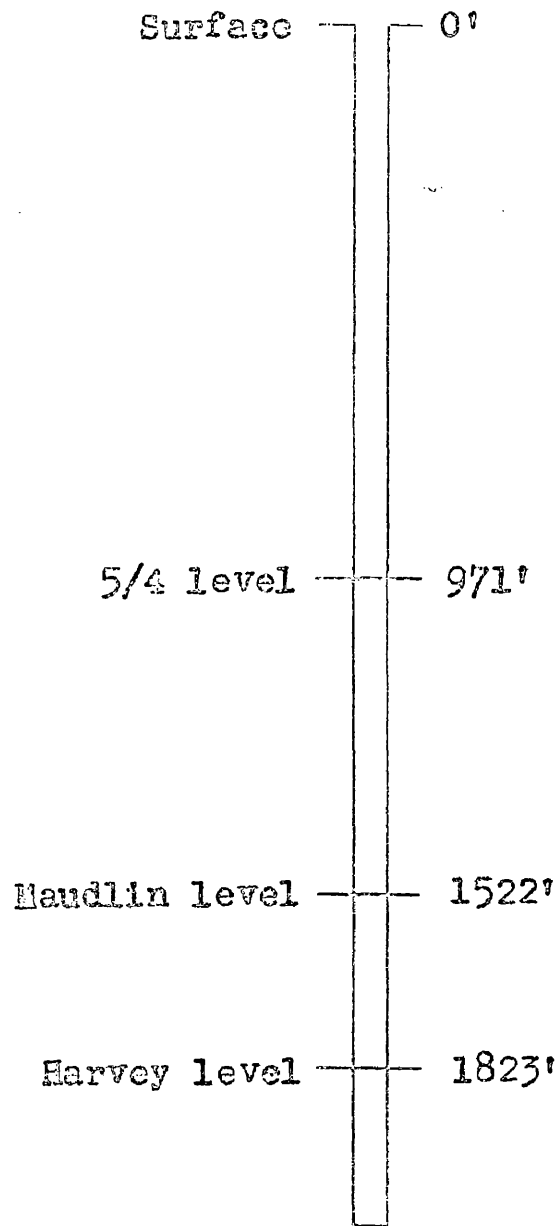


Fig. 2. Downcast shaft section.

wound from the 5/4 level and the Harvey level at both normal speed (40 ft/sec.) and slow speed (20 ft/sec.) and completed several winding cycles, at 5 minute intervals for normal speed winding and 10 minute intervals for slow speed winding. The observers were synchronized with each other and with the movements of the cage.

In a second series of tests the air velocity was recorded 10 yards from the downcast shaft at each level at 5 second intervals while the cage completed several winding cycles at normal speed from the Harvey level.

The first series of tests is represented by Figs. 3-6 inclusive. To facilitate comparison the three velocities and the shaft pressure difference have been plotted on one diagram for each type of winding cycle. Velocities have been plotted as a percentage of normal flow, with due regard to direction, and the pressure difference has been plotted directly in inches of water gauge. The second series is represented by Figs. 7-9 inclusive where velocity is again plotted as a percentage of normal flow.

The other data recorded during these tests are given below :

Area of shaft	176 ft <sup>2</sup>
Area of cage	91 ft <sup>2</sup>
Area of buntens	6 ft <sup>2</sup>
Area of counterweight	6 ft <sup>2</sup>

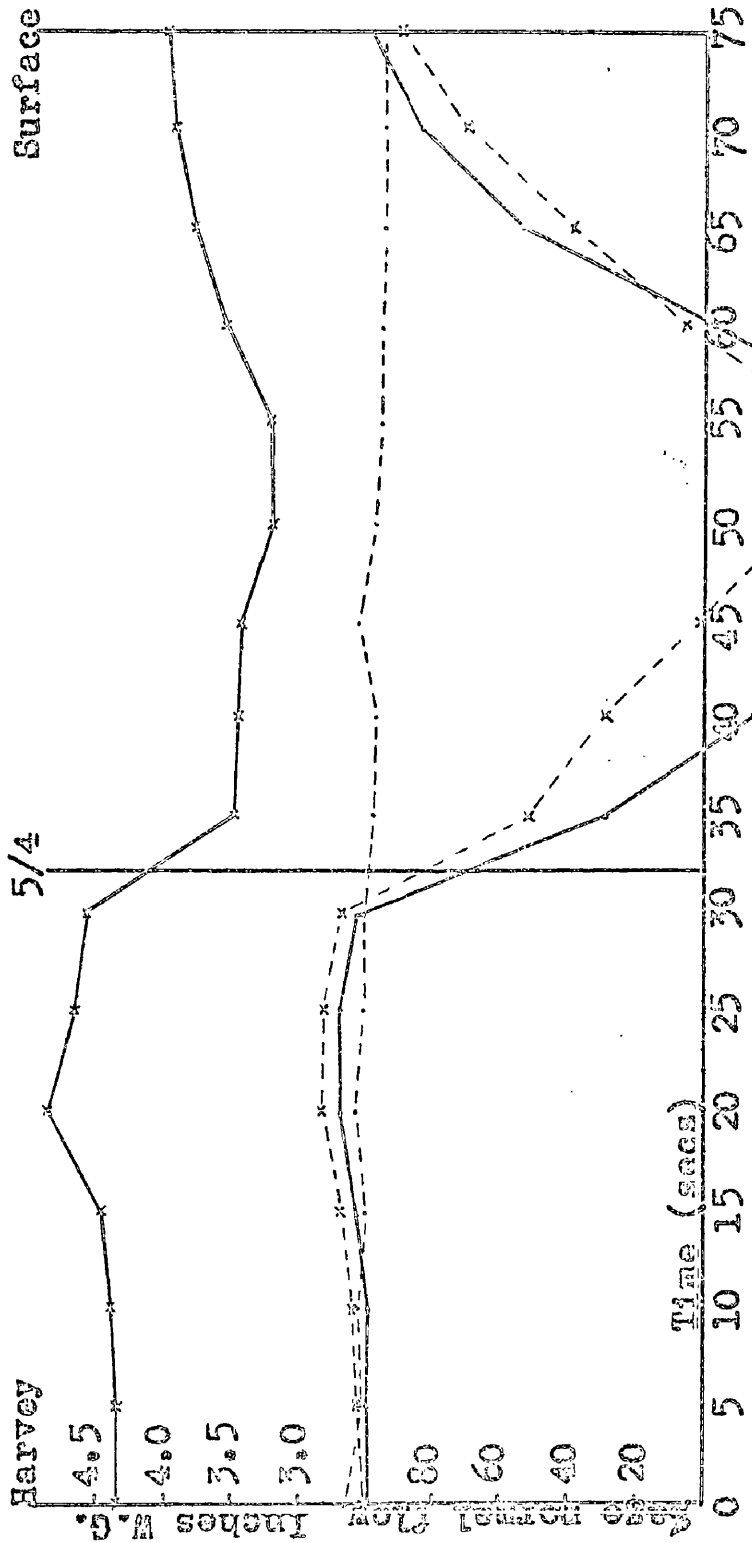


Fig. 3(a). The effect on the ventilation in the 5/4 seam when the cage ascends from the Harvey at 40ft./sec. Air velocity (a) — at inset (b) --- in intake (c) ···· in return adjacent to upcast. Pressure difference between the shafts at the 5/4 level ····.

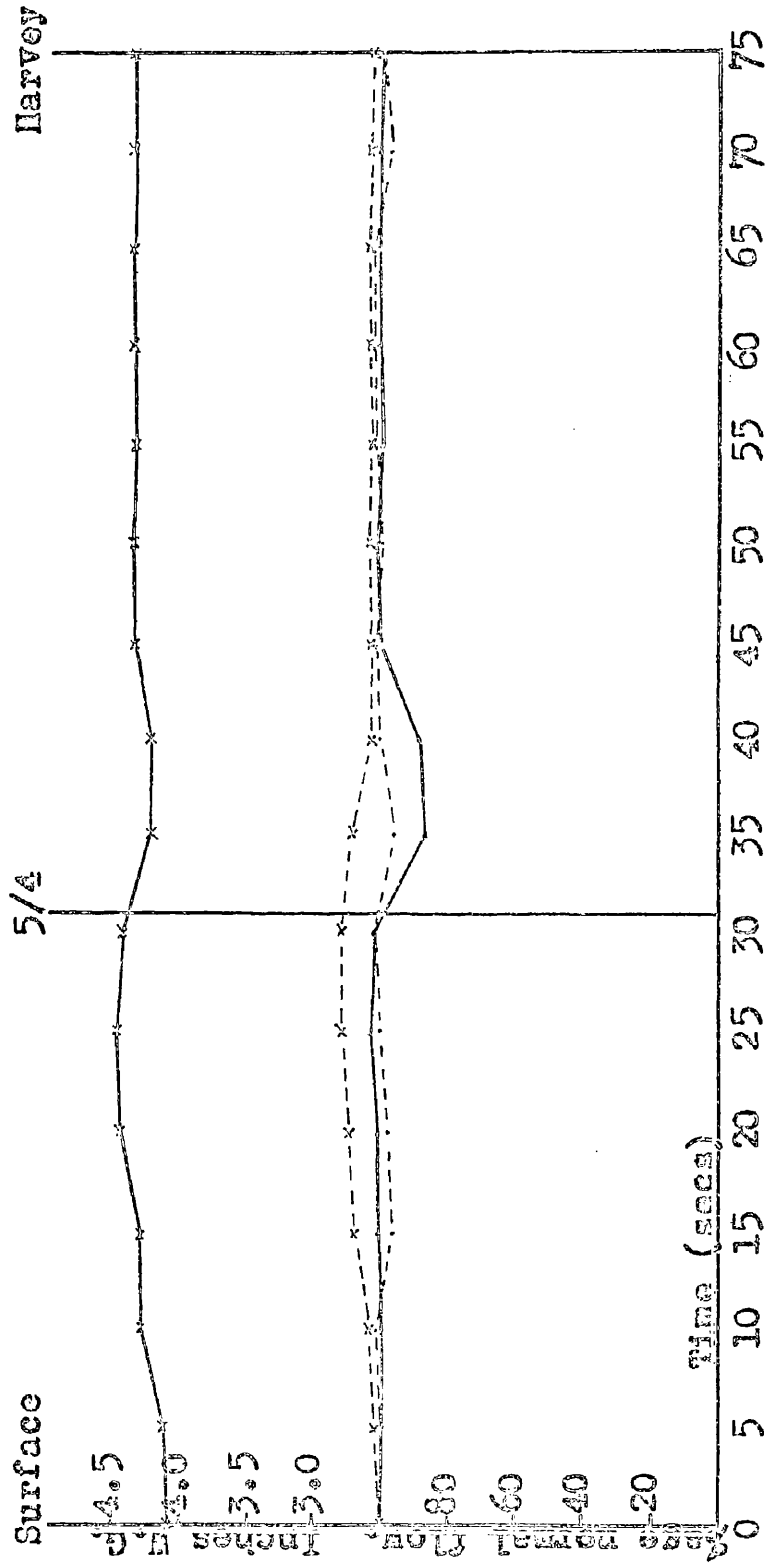


FIG. 3(b). The effect on the ventilation in the 5/4 seam when the cage descends to the Harvey level at 40ft./sec. Air velocity (a) — at inset, (b) x---x 1100 yards intake, (c) -.-.- in return adjacent to upcast. Pressure difference between shafts at the 5/4 level x---x.

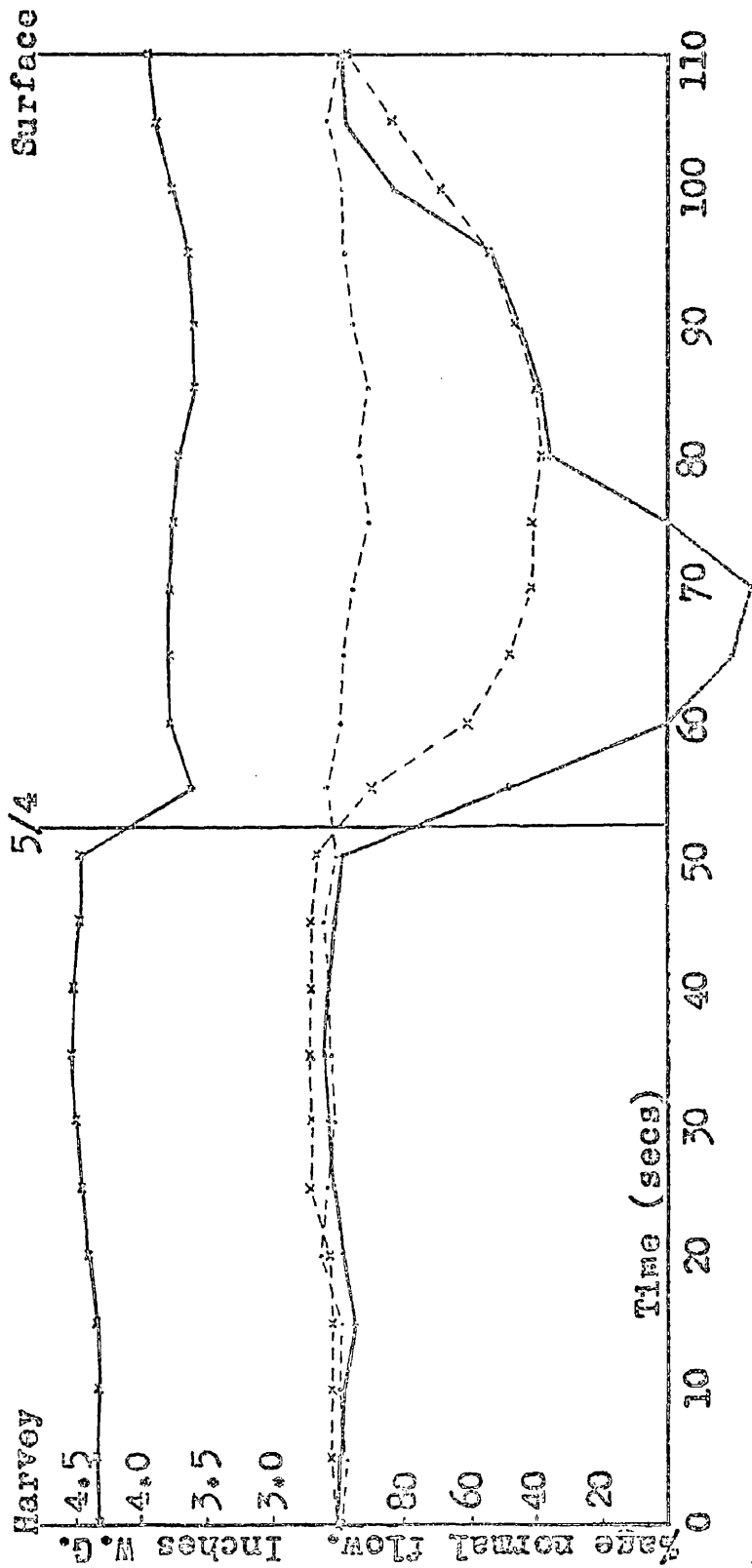


Fig. 4(a). The effect on the ventilation in the 5/4 seam when the cage ascends from the Harvey level at 20 ft./sec. Air velocity (a) — at inset. (b) x---x 1100 yards inbye in intake. (c) — in return adjacent to upcast. Pressure difference between shafts at the 5/4 level x---x.

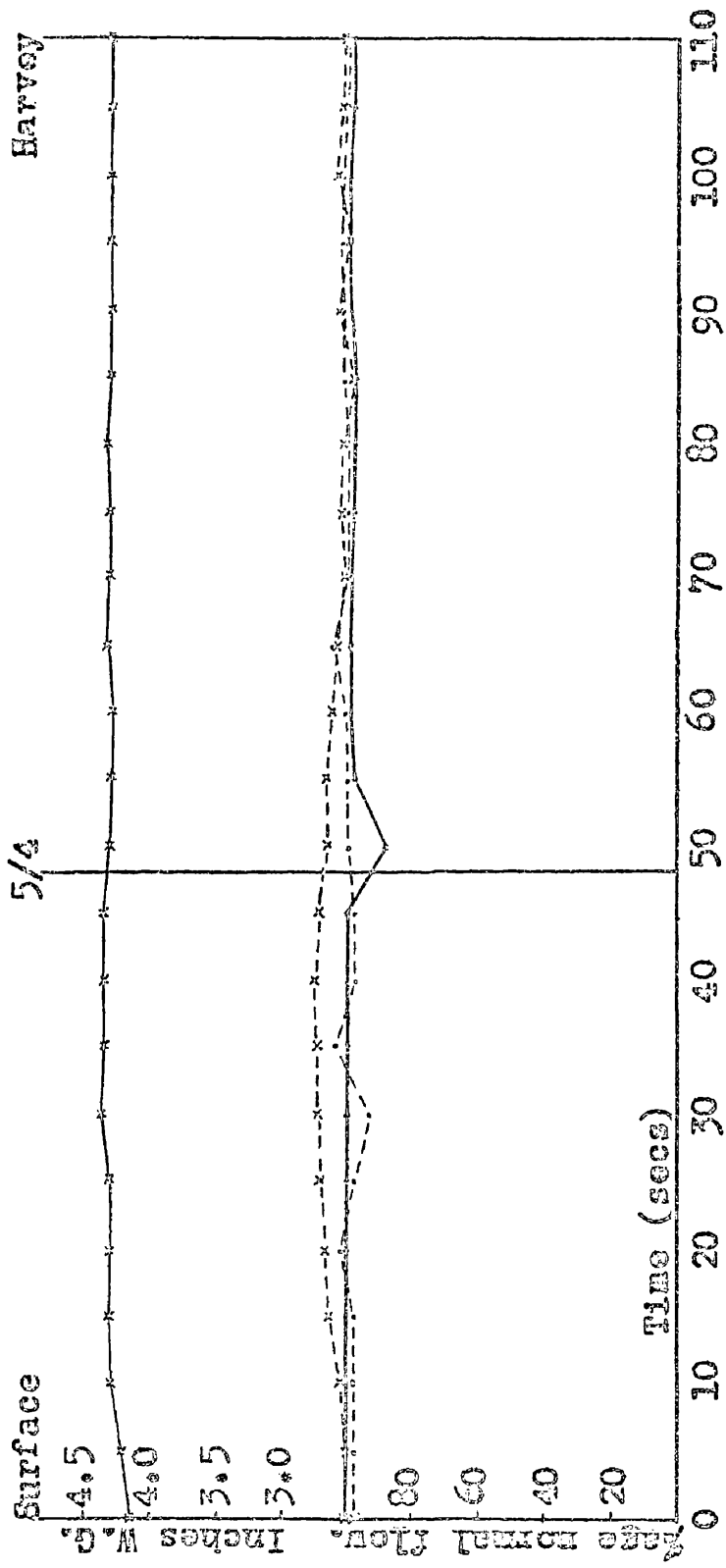


Fig. 4(b). The effect on the ventilation in the 5/4 seam when the cage descends to the Harvey level at 20 ft./sec. Air velocity (a) — at inset. (b) x-x 1100 yards inbye in intake. (c) ···· in return adjacent to upcast. Pressure difference between shafts at the 5/4 level x-x-x.

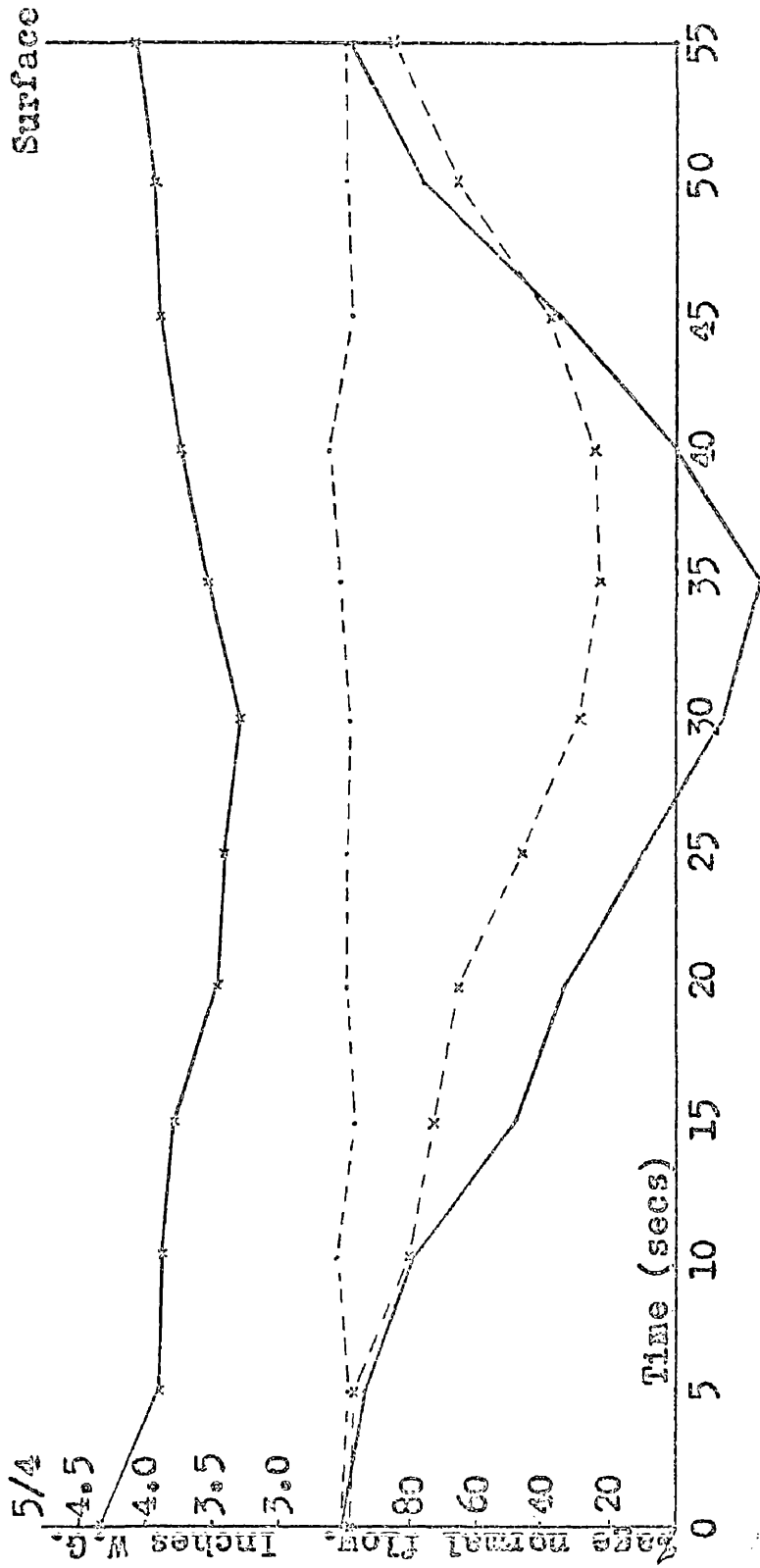


Fig. 5(a). The effect on the ventilation in the 5/4 seam when the cage ascends from the 5/4 level at 40 ft./sec. Air velocity (a) — at inset, (b) x---x 1100 yards inbye in intake, (c) ·-·-· in return adjacent to upcast, Pressure difference between shafts at the 5/4 level x---x.

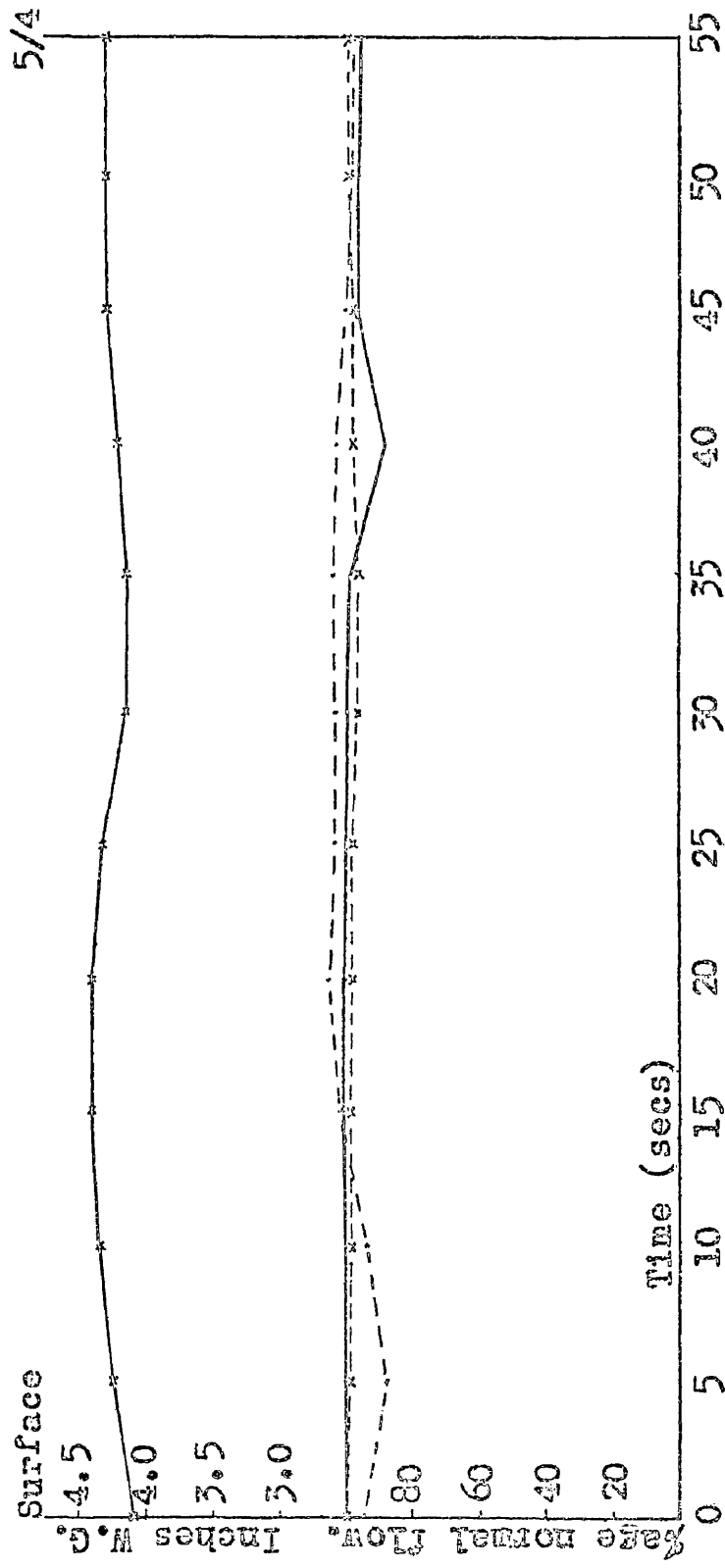


Fig. 5(b). The effect on the ventilation in the 5/4 seam when the cage descends to the 5/4 level at 40 ft./sec. Air velocity (a) — at inset. (b) x--x 1100 yards inbye in intake. (c) ···· in return adjacent to upcast. Pressure difference between shafts at the 5/4 level x---x.

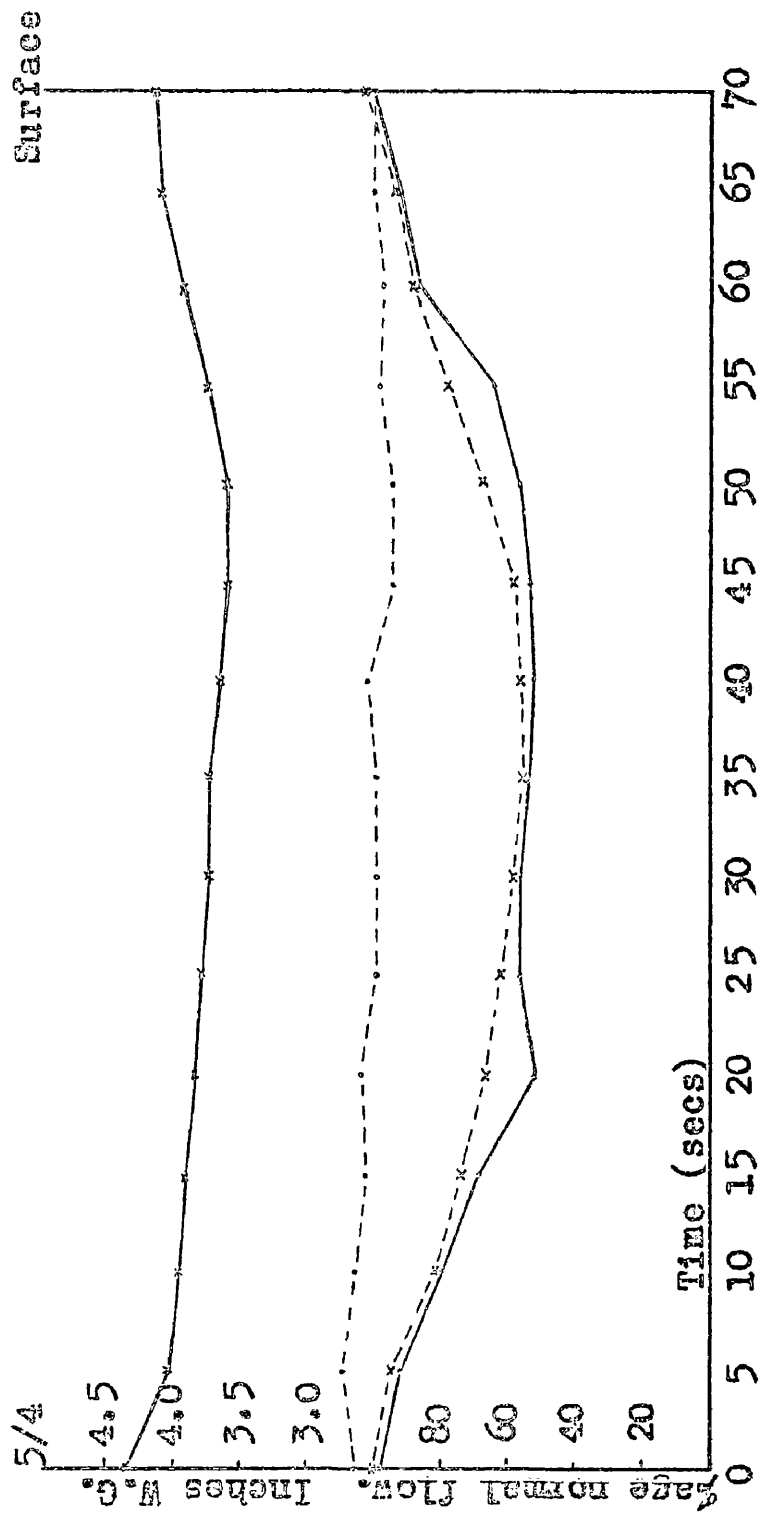


Fig. 6(a). The effect on the ventilation in the 5/4 seam when the cage ascends from the 5/4 level at 20 ft./sec. Air velocity (a) ——— at intake. (b) x---x 1100 yards inbye in intake. (c) ·---· in return at upcast. Pressure difference between shafts at the 5/4 level x---x.

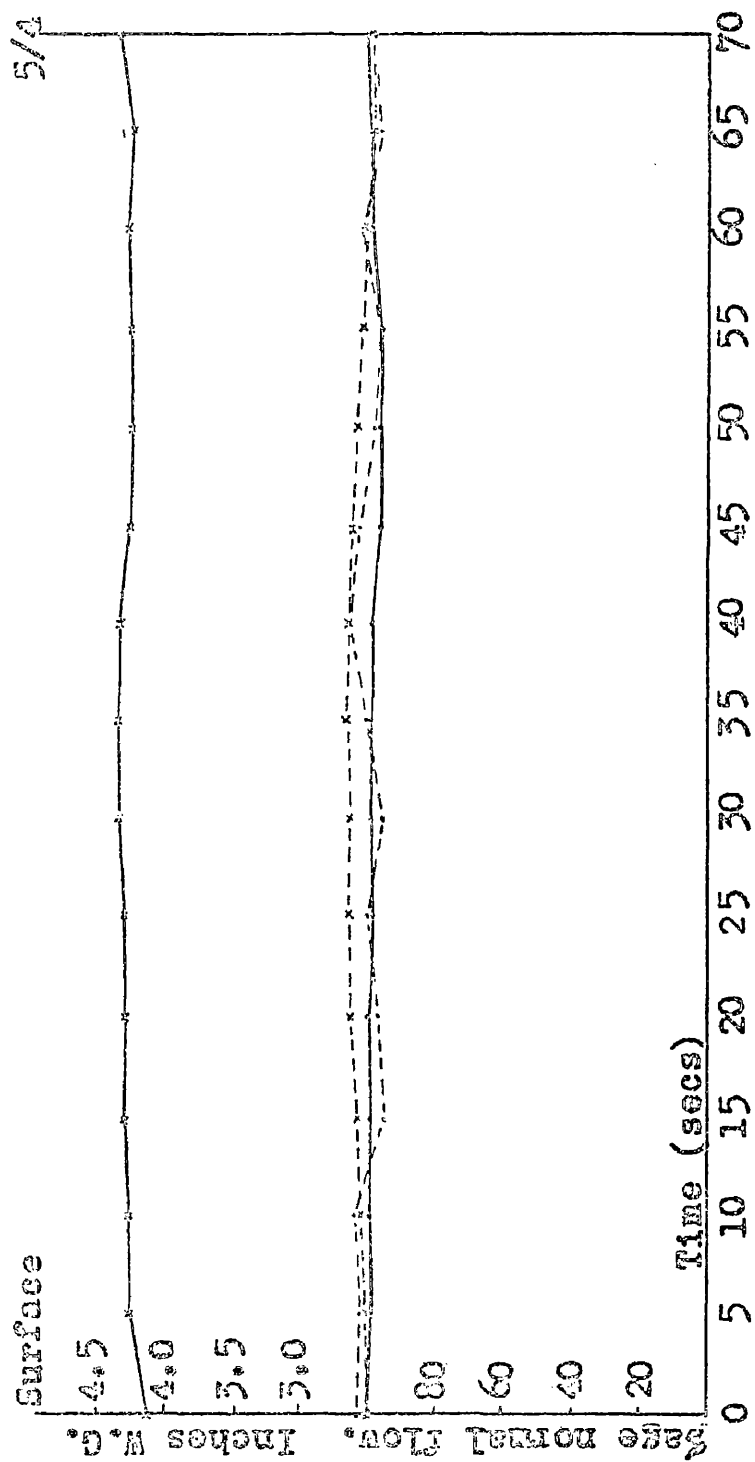


Fig. 6(b). The effect on the ventilation in the 5/4 seam when the cage descends to the 5/4 level at 20 ft./sec. Air velocity (a) —•— at inset. (b) \*---\* 1100 yards inbye in intake. (c) ---- in return at upcast. Pressure difference between shafts at the 5/4 level \*---\*.

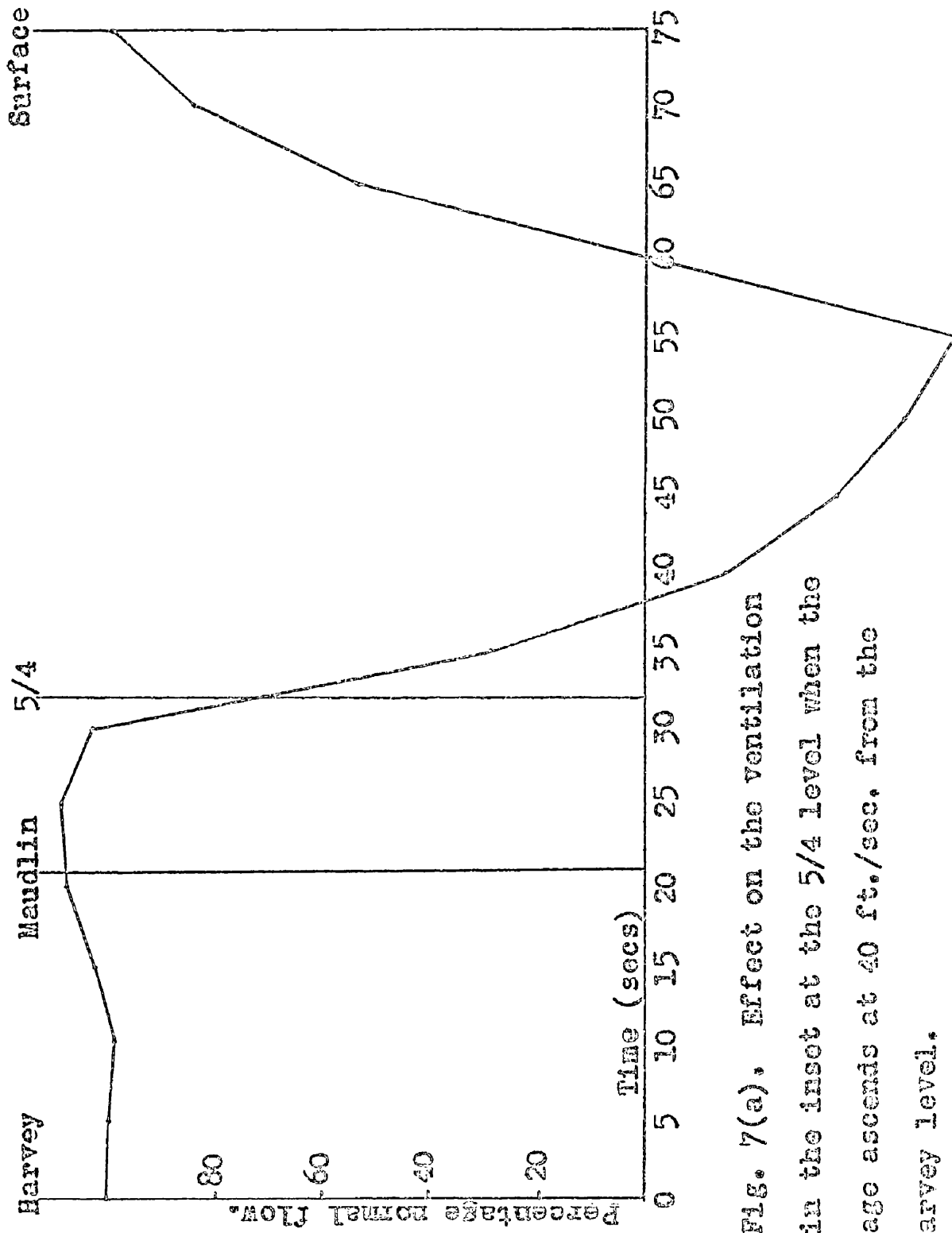


Fig. 7(a). Effect on the ventilation in the inset at the 5/4 level when the cage ascends at 40 ft./sec. from the Harvey level.

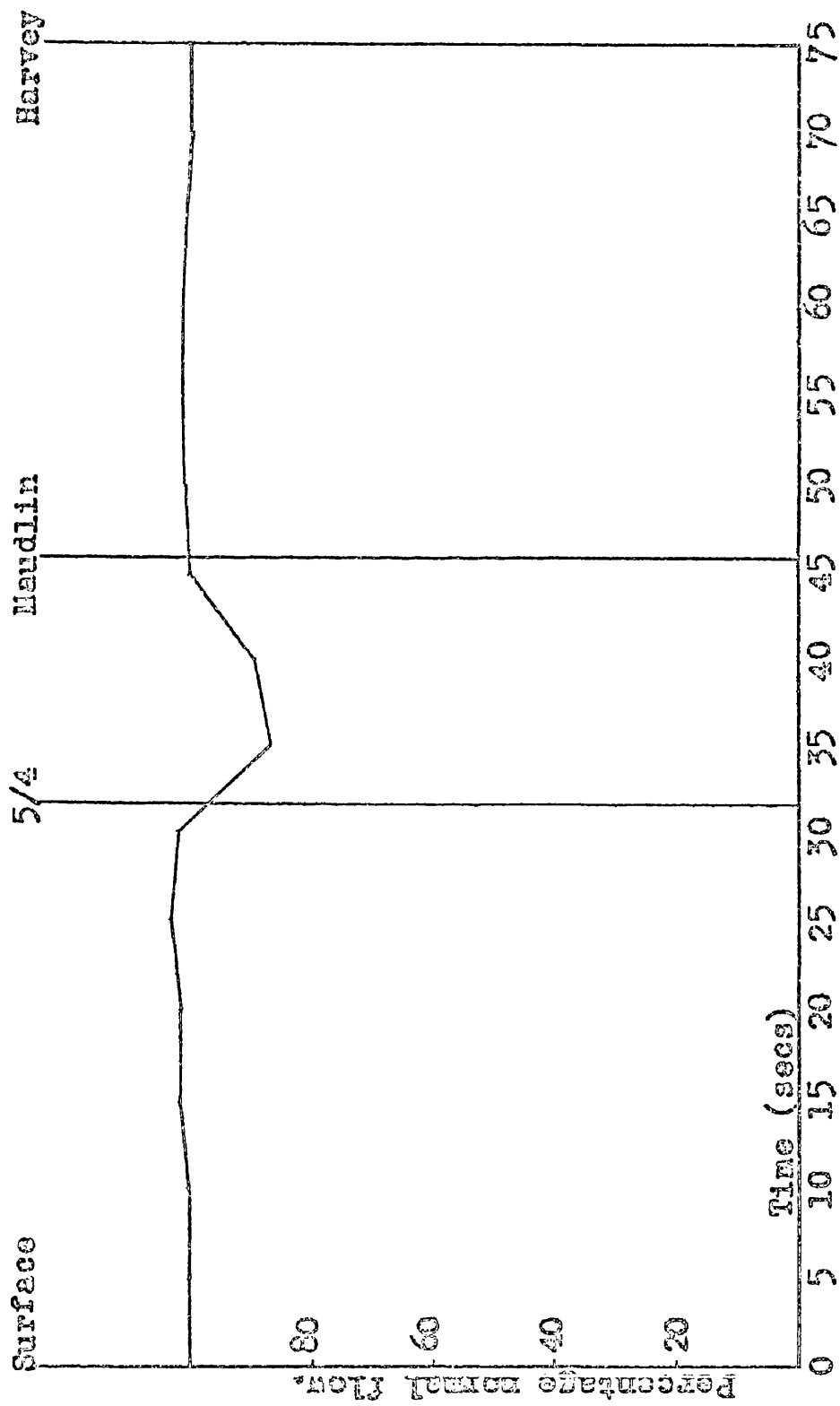


Fig. 7(b). Effect on the ventilation in the inset at the 5/4 level when the cage descends at 40 ft./sec. to the Harvey level.

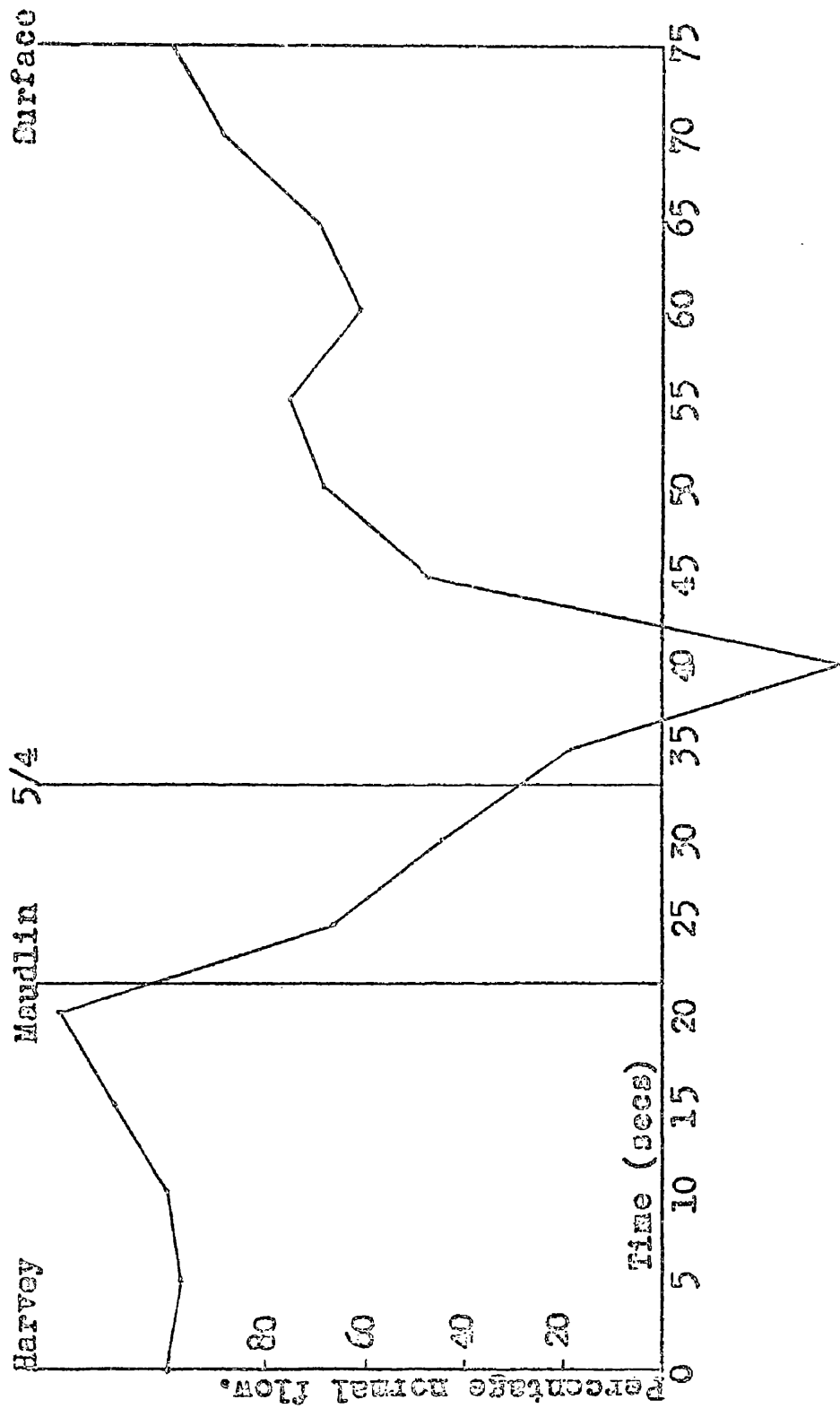


Fig. 8(a). Effect on the ventilation in the inset at the Maudlin level when the cage ascends at 40 ft./sec. from the Harvey level.

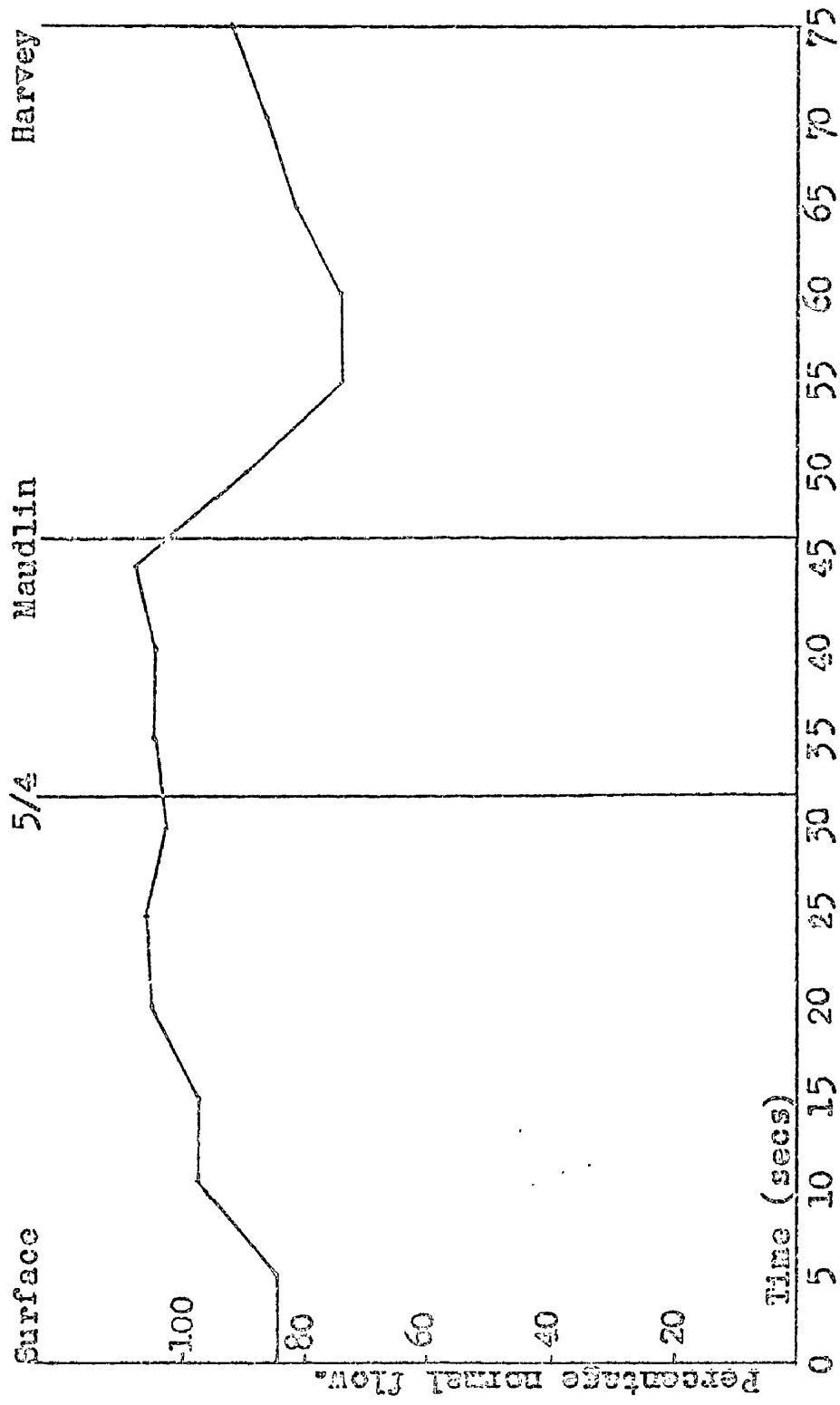


Fig. 8(b). Effect on the ventilation in the inset at the Maudlin level when the cage descends to the Harvey level at 40 ft./sec.

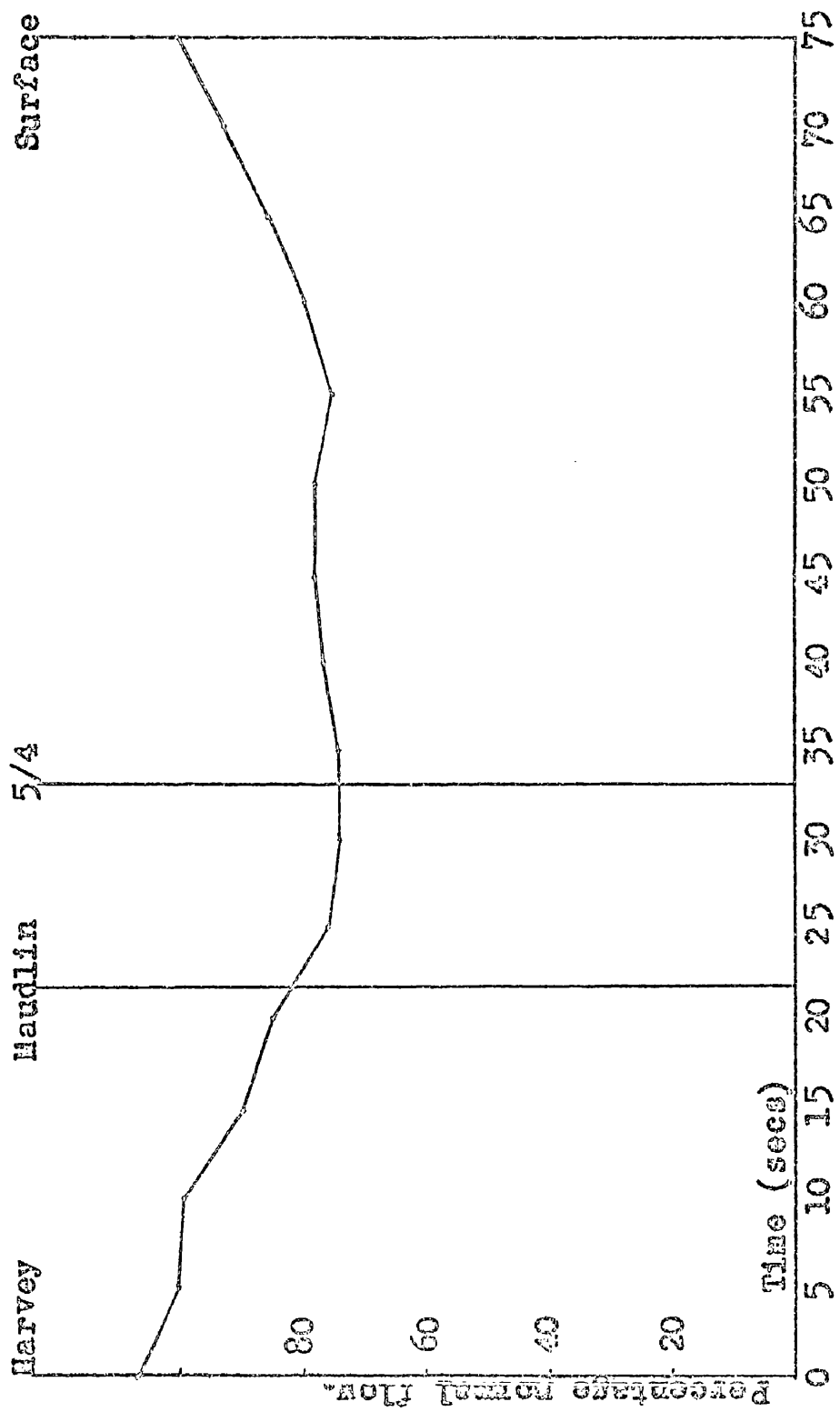


Fig. 9(a). Effect on the ventilation in the inset at the Harvey level when the cage ascends at 40 ft./sec. from the Harvey level.

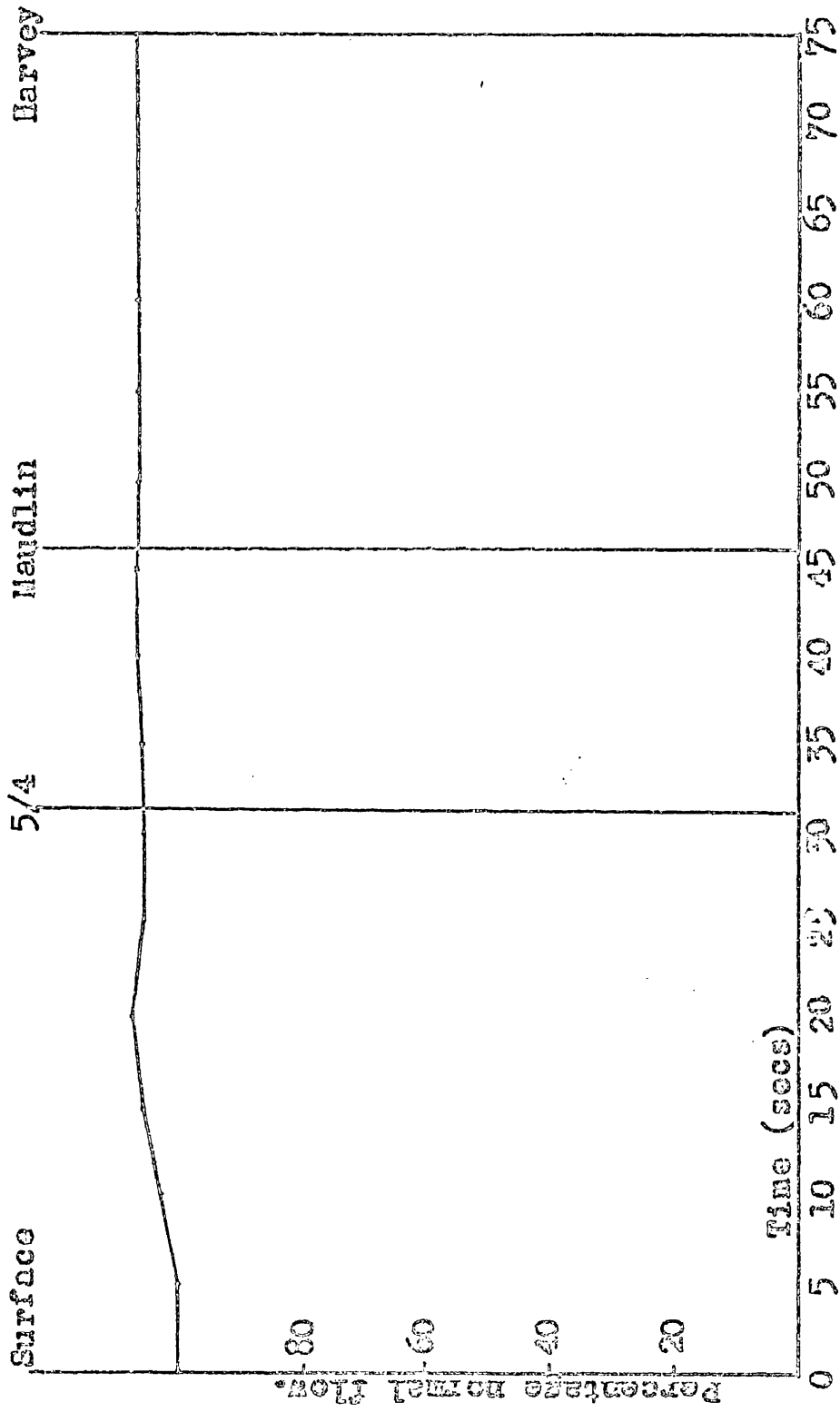


Fig. 9(b). Effect on the ventilation in the inset at the Harvey level when the cage descends at 40 ft./sec. to the Harvey level.

	Air quantities (c.f.m.)	
	<u>Seam</u>	<u>Shaft. between seams</u>
Surface	212,000	208,500
5/4	48,000	155,500
Maudlin	29,000	125,500
Hutton	16,000	108,500
Harvey	108,000	

Note: Average shaft quantities have been corrected for temperature and compression effects.

Several conclusions can be drawn immediately from the diagrams. The magnitude of the disturbance appears to bear some relation to the cage pressure drop, so that when the cage is descending, and therefore has a low velocity relative to the air, the cage pressure drop is small and so, therefore, are the disturbances. Thus the following observations are made from the graphs of the ascending cage.

When winding from the 5/4 level the shaft pressure difference appears to follow the cage movements very closely, dropping slowly as the cage accelerates and recovering as the cage slows down. When winding from the Harvey level we see that the pressure drops very suddenly as the cage passes the inset, although the method of measurement used was not able to show exactly how suddenly. These observations show that the pressure disturbances follow the movements of the cage faithfully.

The drop in pressure produced by the cage at the inset is propagated along the roadway to the workings causing the air to expand. It would appear to be this expansion of the air which causes the velocity disturbances and reversal of flow. We note that little or no change of velocity is detected adjacent to the return, while 1,000 yards from the source it is attenuated to a greater or lesser degree.

It is this attenuation which causes most surprise. In two cases the attenuation at 1,000 yards is very slight, while in other two it is severe. There appears to be no obvious explanation and no connection can be seen between the attenuation and the speed of the cage, or the speed at which the pressure pulse is applied to the inset. It was hoped that the further insight gained during the experimental and theoretical work undertaken would provide some explanation.

By integrating the volume of air affected by the pressure changes it is possible to estimate the volume of the workings, assuming a simple Boyle's Law relationship. In the case of winding at normal speed from the Harvey level the excess air flowing from the 5/4 level is approximately 25,000 cu.ft. and the pressure drop is approximately 1" W.G. This would suggest that  $10^7$  cu.ft. of air has been affected which is not an unrealistic figure for the volume of workings in the 5/4 level.

Having gained this information from the colliery investigation it was decided to attempt to simulate these disturbances in a model

so that, having greater control over all factors, the effect of these factors could be carefully studied.

### Chapter 3

### DESCRIPTION OF THE MODEL

From the investigations at colliary R the following conclusions may be drawn.

1) The variation of the velocity of the air flowing through the workings at any level corresponds closely to the pressure difference between the two shafts at that level. Since the flow in the return, adjacent to the upcast shaft, is seen to be little affected we may assume that the pressure in the upcast shaft is constant. Since the pressure at the top of the downcast shaft is constant and the shaft quantity varies little, we may deduce that the velocity disturbance corresponds closely to the pressure drop produced by the cage in the downcast shaft. This pressure drop is obviously a function of, among other things, the cage velocity and the air velocity in the downcast shaft.

2) The velocity disturbance is propagated inbye to a considerable distance. Attenuation of the disturbance takes place but the factors governing this attenuation are not evident from the small number of results available.

On these conclusions, it was decided, would be based experimental tests designed to determine

- (a) How the pressure disturbance was produced,
- (b) How this pressure disturbance produced a velocity, disturbance, and
- (c) How the velocity disturbance was propagated.

In order to investigate how the pressure disturbance was produced it was planned to construct a model system which would closely resemble the arrangements at colliery R. When investigating the pressure drop produced by the cage it was necessary to have available cage speeds which were of the same order as the air speeds, since such a relationship is common in practice. This meant, if the air velocity were to satisfy the conditions of turbulent flow, relatively high cage speeds. To obtain these the scale of the model was necessarily small. A diameter of  $3\frac{1}{2}$ " was considered a convenient size for the model shaft and this gave a scale factor, compared with colliery R, of 52 times.

The shaft was 33' long with a 13' Perspex section centrally placed. The ability to see where the cage was at any instant was very useful and avoided the need for complicated control arrangements. The shaft, on either side of the central section was opaque Polythene the bore of which was not quite uniform and, for this reason, all measurements were confined to the Perspex section.

To ensure that the cage would travel safely at the speeds

planned it was necessary to pay particular attention to the guides and shoes. In the arrangement adopted the guides were brass sections in the shape of a rectangular C and the shoes were small pulleys in a spring mounting. The rope was attached to a draw bar inside the cage so that the rope tension was not carried by the cage. These cage mounting arrangements are shown in Fig. 10.

With these arrangements it was found that the cage could be safely driven at speeds up to 12 ft/sec. At this speed the cage traversed the Perspex section in approximately one second, which meant that measurement taken while the cage was moving had to be taken with an instrument having a fairly good dynamic response. This was found to be the factor which limited the cage speed.

The cage was driven by a single phase electric motor and a continuously variable reversible gear which gave a smooth accurate control of speed.

The model arrangements, for determining how the pressure drop due to the cage was produced, were completed by the addition of a small centrifugal fan which enabled air to be exhausted from the shaft at speeds up to 32 ft/sec. The air velocity was controlled, initially, by means of a cylindrical shutter concentric with the main shaft, which fitted inside the shaft and slid in front of the fan drift.

When taking preliminary measurements with the pressure recorder it was noticed that the velocity of the air fluctuated at about 12 c/s. This was seen to be resonance of the air in the shaft and was aggravated by the sliding shutter. It was found, however, that this

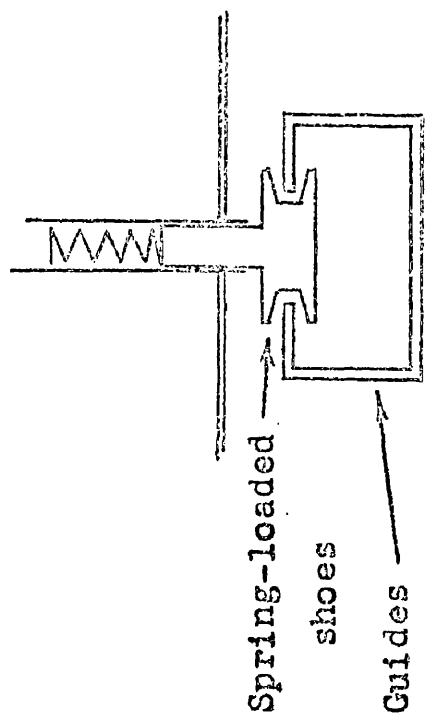
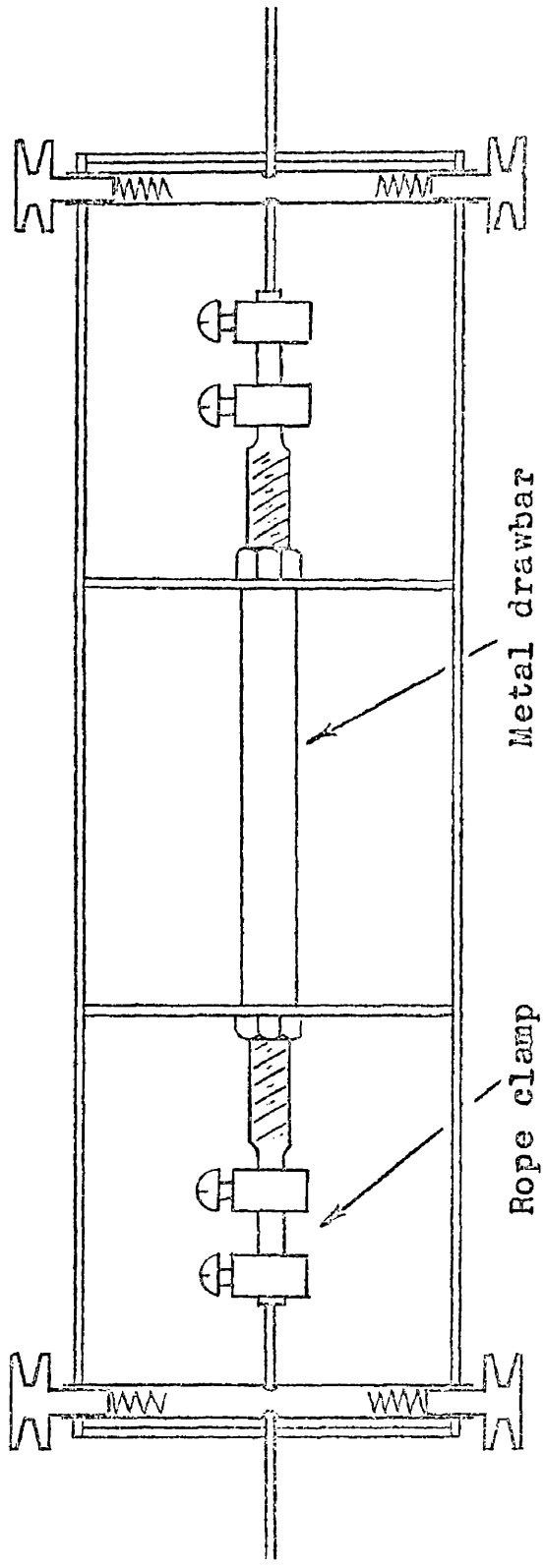


Fig. 10. Case mounting arrangements.

fan was, for reasons given later, not suitable and the investigation into the pressure drop produced by the cage was carried out using a much larger fan.

In order that the ability of a pressure disturbance to produce a velocity disturbance could be studied, the Perspex section of the shaft had fitted, at its centre, a T piece junction. This allowed any pressure disturbance produced by the cage to be communicated elsewhere. It was then evident that if a large volume were connected to this T piece, and if the cage were immediately downstream from the T piece, the pressure of the air in the volume would be that which is normally upstream from the cage. If the cage were then moved to a position immediately upstream from the T piece the pressure in the volume would be lowered by an amount equal to the pressure drop produced by the cage. At this lower pressure the original mass of air must occupy a larger volume and hence air must flow out of the T piece as the cage changes position.

Calculation showed this air flow to be 0.5 ft sec/deg. which may be 100 ft/sec. for 1/200 sec. or 1/10 ft/sec. for 5 seconds. Attempts to detect this flow of air with the pressure recording equipment met with complete failure. Since there could be no doubt about the fact that air flowed out, it must, then, have flowed either too quickly or too slowly to be detected. The resistance offered to air flowing out of the volume was very small, hence it was assumed that the air had flowed out too rapidly. The solution to this particular problem might have been to increase the

resistance to the outflowing air.

It was realised, however, that this simple arrangement was not sufficiently realistic, and that it would be necessary to include the volume in one branch of a ventilation circuit. When this was done it would be necessary to have ample power in the fan to allow a wide range of resistances in the circuit, since the relationship between the resistances of the various components of the circuit appeared to be of importance. It was therefore decided to suspend preliminary testing until a larger fan was installed.

A 20 H.P. fan already available was coupled to the model shaft but it was necessary to allow the fan to draw air other than from the shaft so that it would operate on a suitable portion of the characteristic curve. Tests immediately showed that severe pulsations existed. A chamber, the cross sectional area of which was 130 times that of the shaft, was interposed between the shaft and the fan, effecting a slight improvement, but it was finally decided to obtain a fan designed to suit the particular conditions. The fan which was installed was a backward bladed centrifugal fan designed to produce up to 18" W.G. at approximately 350 c.f.m. Control of quantity was by speed control of the fan. An electric motor and variable speed drive allowed a continuous variation of the fan speed over a wide range. This fan and speed control were found to be eminently suitable for all tests and allowed Reynolds numbers up to 200,000.

It was found, with this fan, that resonance of the air in the shaft still occurred, at a frequency of 14 c/s now due to a different

length of connection between the shaft and the fan. But the magnitude was such that it could be damped out without seriously affecting the lower frequencies which were being measured.

Other equipment associated with the model included two 'volumes', one of 45 cu.ft. and the other of 250 cu.ft., both rectangular boxes. They were designed to simulate the workings but, since the volume of the workings is difficult to estimate and since geometrical similarity might be of no advantage in this case, the actual volume had no meaning at the design stage.

In order to investigate fully the pressure drop produced by a cage, a series of model cages was constructed giving a range of variable factors. The factors investigated were the number of decks, the frontal area, the length to breadth ratio and the effect of completely closing the sides of the cage. The terms used in relation to a cage are shown in Fig. 11 and Table I gives the dimensions for the series being tested. The model cages are seen in Plate 1.

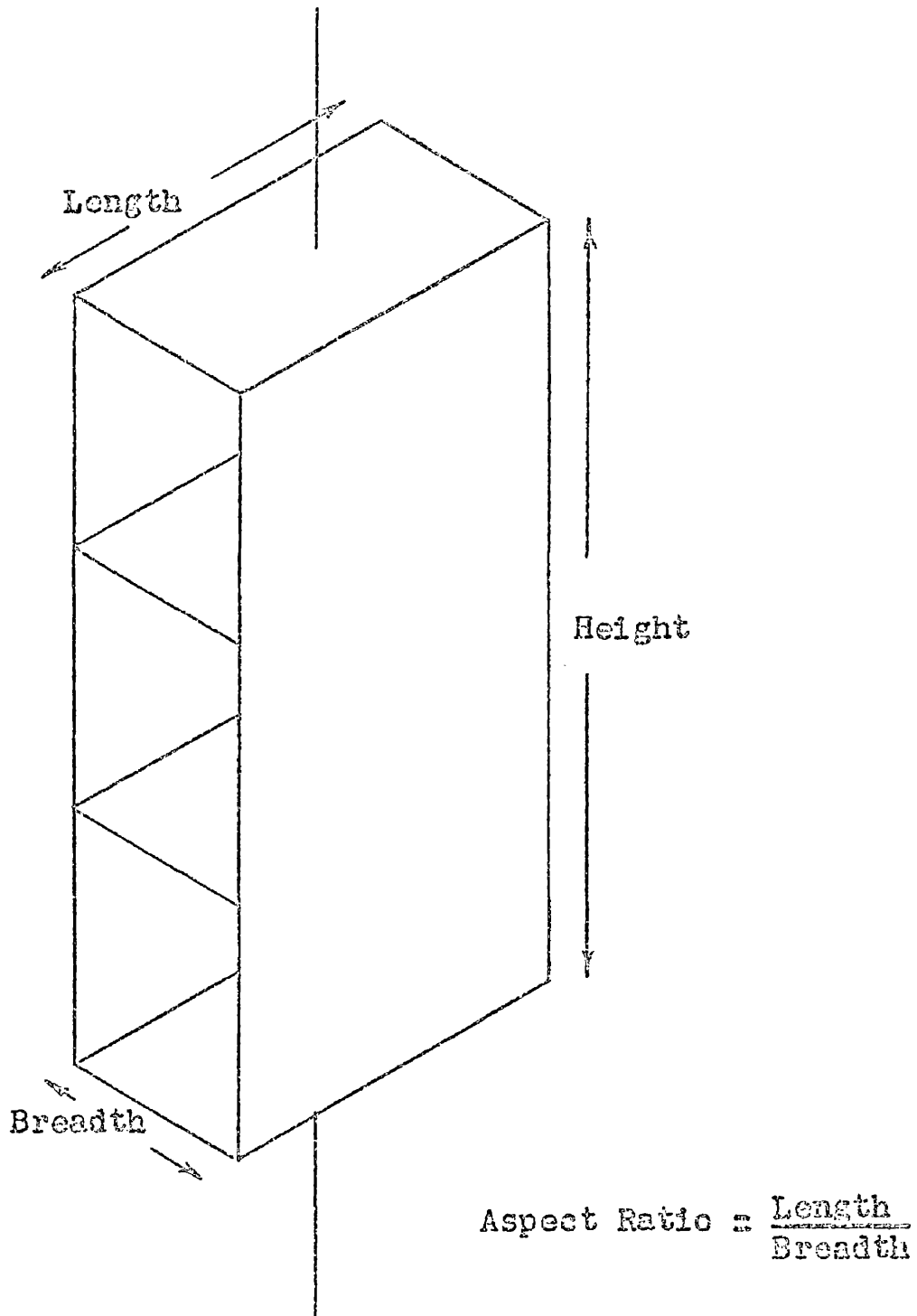


Fig. 11. Cage Nomenclature.

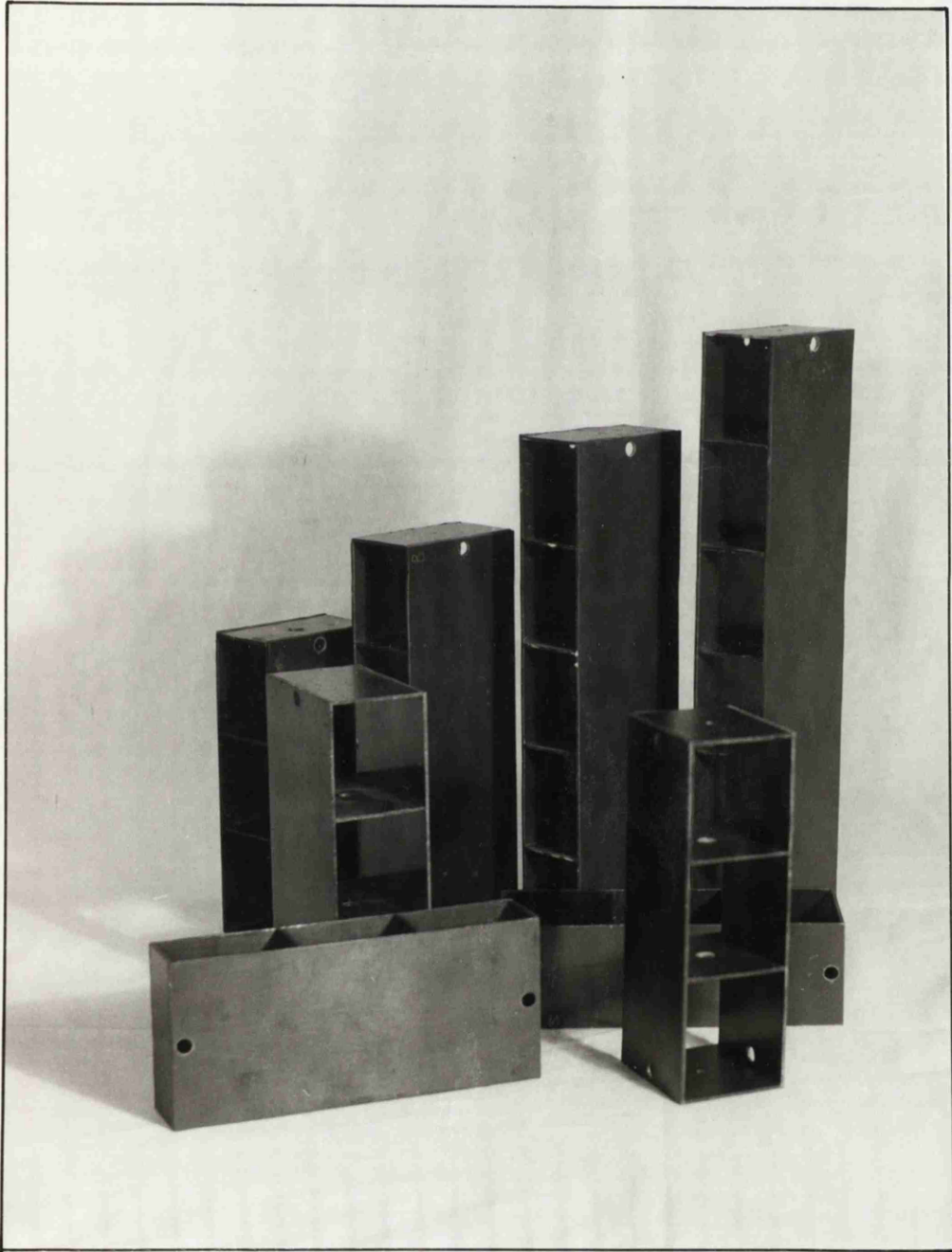


PLATE I.

TABLE 1

Cage	Number of decks	Height (ins.)	Length (ins.)	Breadth (ins.)	Frontal Area (sq. ins.)	Aspect Ratio
A	3	6	2.75	1.50	4.12	1.83
B	4	8	2.75	1.50	4.12	1.83
C	5	10	2.75	1.50	4.12	1.83
D	6	12	2.75	1.50	4.12	1.83
E	3	6	2.75	1.75	4.81	1.57
F	3	6	2.75	1.25	3.44	2.20
G	3	6	2.25	1.84	4.14	1.22
H	3	6	1.88	2.2	4.12	0.85

The model equipment was completed by adding a cage position indicator so that the position of the cage could be seen from remote controlling positions.

Chapter 4      DESCRIPTION OF THE INSTRUMENTS AND  
METHODS OF MEASUREMENT

In all the tests in this investigation the basic quantity being measured was pressure, whether it represented an energy loss or the velocity of the air flow. In some cases it was steady pressure while in others it was fluctuating pressure. For general steady pressure readings the Betz manometer (Plate 2) was used. This direct reading instrument was found to be very simple to read, reliable and accurate. For very accurate work, for example when determining the accuracy of other instruments, the Chattock Ray tilting manometer (Plate 3) was used. This has a much more limited range than the Betz and is not so easy to read, but the accuracy is greater.

To measure and record fluctuating pressures a recording manometer developed in the Mining Department of the Royal College of Science and Technology was used. A description of the development work can be found in reference 2. The sensitive element was a thin brass diaphragm stretched taut and clamped between two steel rings. This diaphragm was so arranged as to divide into two compartments an air chamber. One wall of the chamber was a heavy brass plate which acted as the stationary plate of a variable condenser, the thin diaphragm being the other plate. A difference in pressure between the two compartments caused the thin diaphragm to be deflected, producing a change in capacitance between the two plates. The capacitance of the two plates was arranged to act as one arm of a

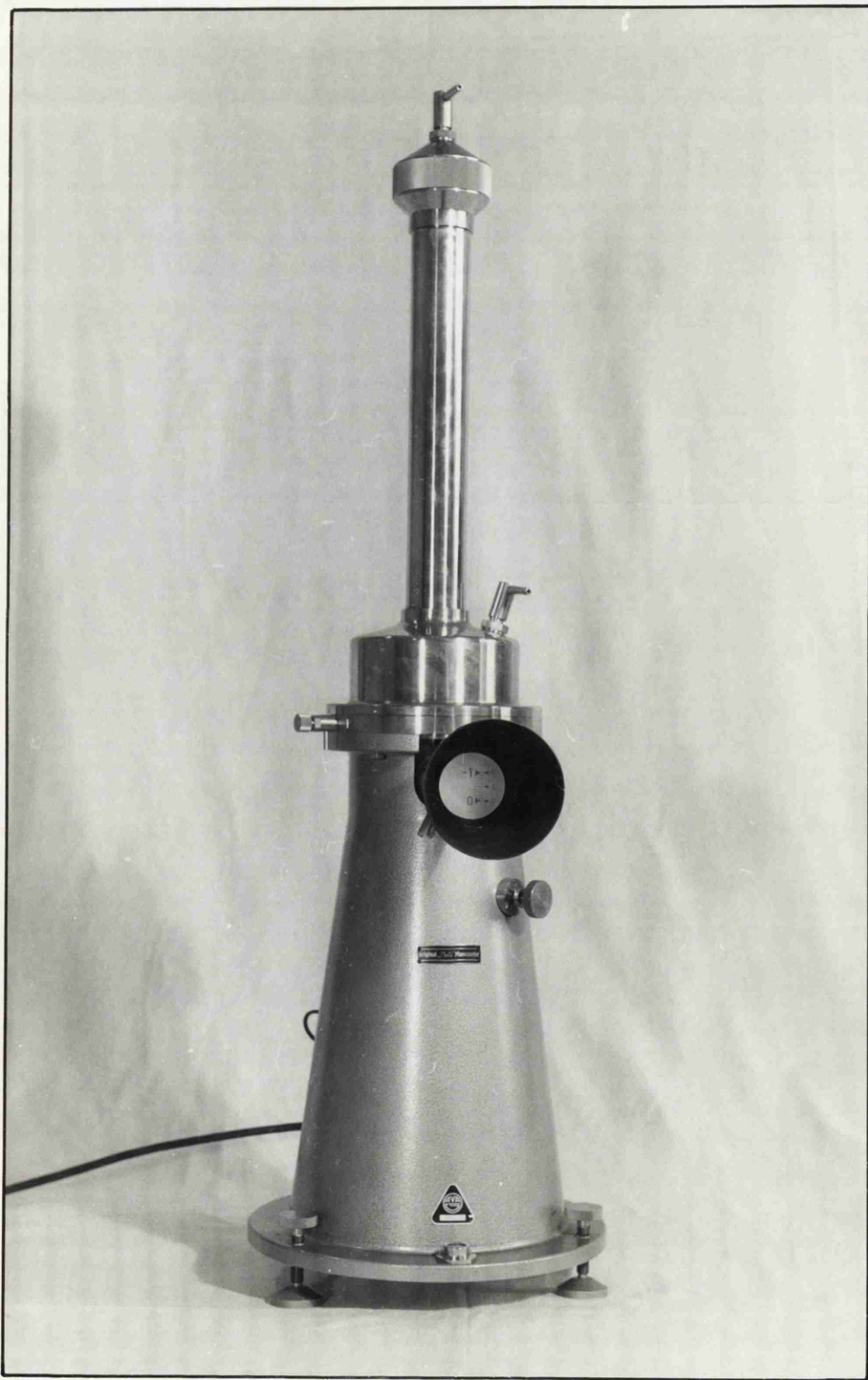


PLATE 2.

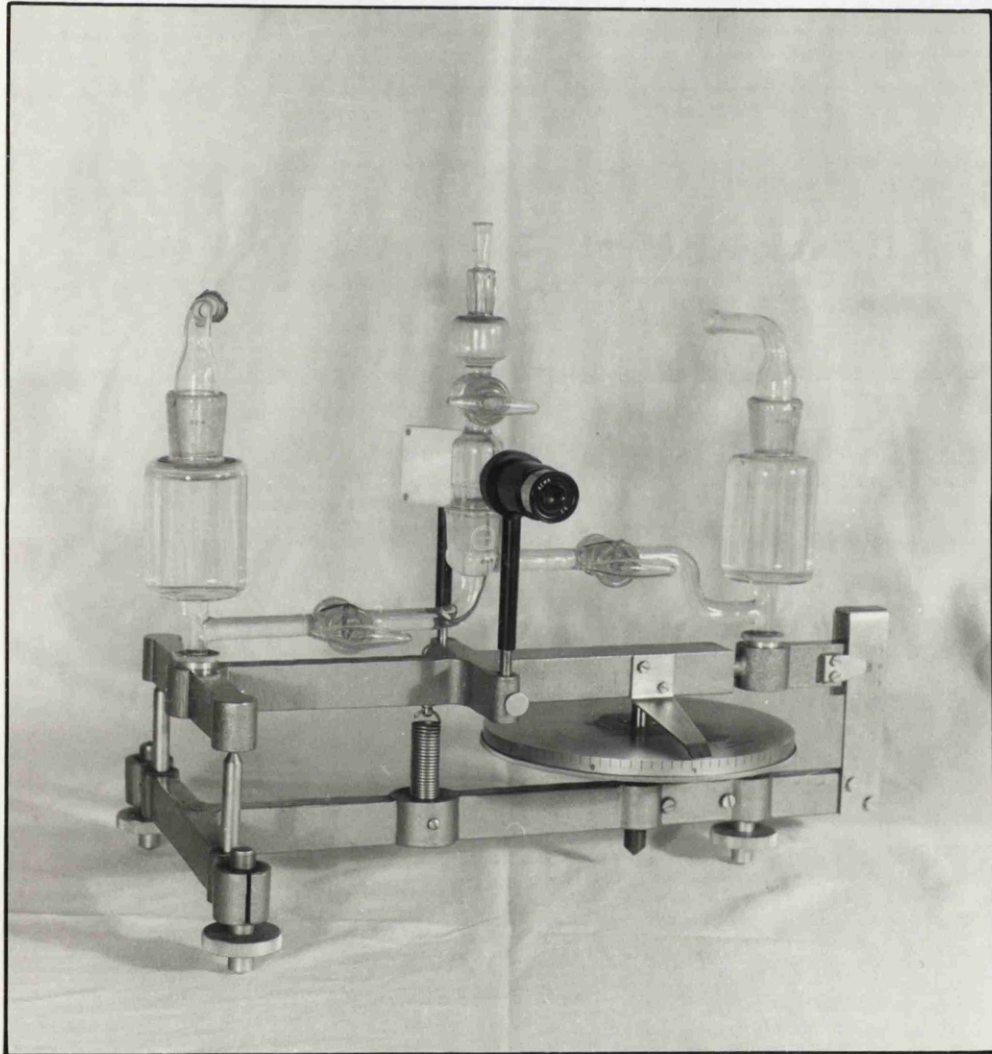


PLATE 3.

capacitance-inductance bridge so that any change in capacitance produced an output voltage from the previously balanced bridge. This output voltage was amplified, rectified and fed to one channel of a twelve channel galvanometer recorder. Film speeds of up to 5 inches/sec. enabled a continuous record to be obtained of the differential pressure applied to the sensitive element.

This principle has been found to be very satisfactory and capable of stability and accuracy consistent with the purposes of the tests. Sensitive elements with brass diaphragms of thicknesses 0.015" (for pressures up to 14" W.G.) and 0.005" (for pressures up to 5" W.G.) were already available but it was felt necessary to construct a more sensitive element with brass 0.0015" thick. The brass was stretched by cementing it to a large aluminium ring and then heating this ring to a temperature of 100° C. The brass was clamped between two smaller, 4" diameter, steel rings while the aluminium was at that temperature. It was found that the amount of tension so produced was sufficient to cause the thin brass diaphragm to return to the neutral plane accurately after each application of pressure, while having a sensitivity such that 3.5 m.m. W.G. produced a full scale deflection of the recording galvanometer. This pressure sensing element is known in any later description as the 3.5 m.m. diaphragm.

The voltage amplifier had a variable amplification control and this allowed adjustment so that full scale deflection of the galvanometer corresponded to the pressures being measured.

Fig. 12 shows a calibration curve for the most sensitive diaphragm. The galvanometer deflection has been plotted against the pressure in m.m. W.C. as measured by the Chatteck Fry tilting manometer. It will be seen that there is, in actual fact, no straight line portion although two straight lines would cover the range with little error. It will also be noticed that the scatter of the points is slight — less than 0.6% of full scale deflection. However, it was found that the overall slope tended to vary about a mean slope by  $\pm 4\%$  from calibration to calibration. For this reason it was decided to calibrate the apparatus over the range of pressures being used immediately before and after any test or series of tests. This allowed a straight line calibration to be used for the most useful part of the curve and eliminated the effects of long period drift.

The response of the pressure recorder to fluctuating pressures was, to a certain extent, unknown although calculations had shown (ref. 2) that the natural frequency of the diaphragm itself would be greater than 200 c/s. No instrument of known response was available for comparison and it was necessary to carry out several tests which, it was hoped, would provide some assurance that the frequencies being measured were not severely attenuated.

Taback (ref. 3) has developed a relationship between instrument volume  $V_g$ , connecting tube volume  $V_t$  and the ratio  $z$  of the combined lowest resonant frequency of the system  $f_1$  to the lowest resonant frequency of the connecting tubing  $f_0$ . This relationship

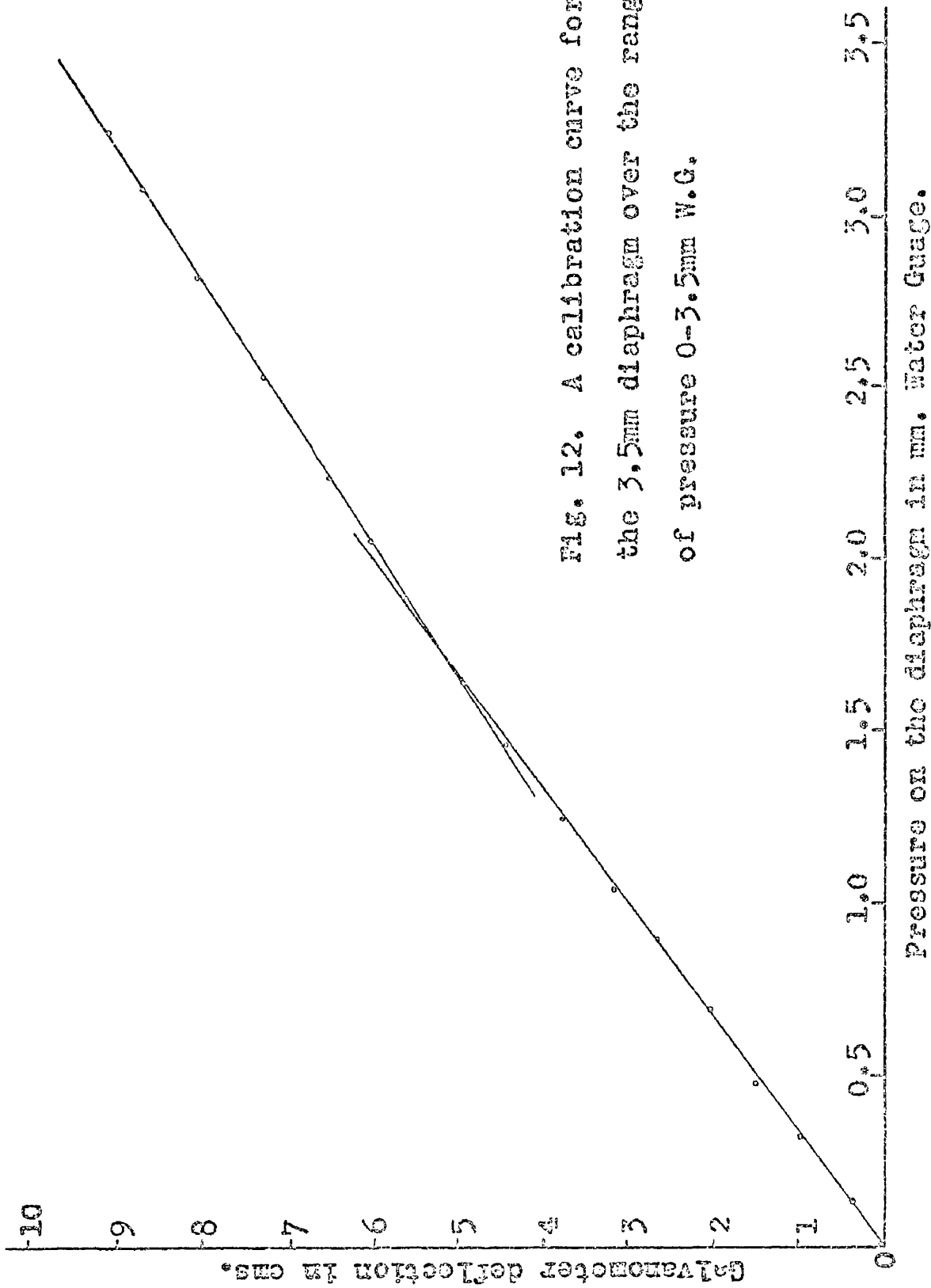


FIG. 12. A calibration curve for the 3.5mm diaphragm over the range of pressure 0-3.5mm W.G.

is given as

$$\frac{V_1}{V_T} = \frac{\cot \frac{\theta}{2} s}{\frac{\theta}{2} s} \quad \text{Equn. 1}$$

In this case  $V$  was estimated to be 10-15 ccs. and the shortest length of 8 m.m. bore tubing which could be used was 2". Allowing for the volume of the static plate and connection to the sensitive element inside the instrument  $V_T$  was approximately 4 ccs. Solution of Equn. 1 with these figures gives  $\theta = 0.276$ . The lowest resonant frequency of the connecting tubing is given by  $f_0 = \frac{a}{4L}$  where  $a$  is the velocity of sound and  $L$  is the length of the tubing. The total connecting length was no greater than 6" which gives  $f_0 = 560$  c/s indicating that the lowest resonant frequency of the system would be approximately 150 c/s.

This simplified theory is based on the assumption that the friction effect of the tubing was negligible. This, according to Taback, is reasonable in the case of the 8 m.m. tubing being used, hence the attenuation of frequencies below 15 c/s would be negligible and measurements taken with a 2" connecting length were assumed to be accurate.

During the investigation a commercial pressure recording instrument became available but it was limited to one degree of sensitivity. A high degree was chosen and it was used to record fluctuations in velocity when the steady velocity was less than 20 ft/sec. The instrument is shown in Plate 4 and is referred to



PLATE 4.

as the micro-manometer. The sensitive element volume of the instrument was 0.0015 ccs. which ensured that if a short length of connecting tube were used the natural frequency of the measuring system would be very high — about 500 c/s. Hence the measurements obtained when this instrument was connected by 2" of 8 m.m. bore tubing to a static plate were taken as standard and the responses of other measuring systems were compared with it. Fig. 13 shows the pressure at a point in the model, measured as above, and taken as standard. Two major frequencies, one of 17.5 c/s and the other of 53 c/s, are readily noticed. A similar trace was obtained using the  $3\frac{1}{2}$  m.m. diaphragm and a similar short piece of connecting tubing. When this measurement was repeated with 30" of 8 m.m. bore tubing the 17.5 c/s component was not attenuated noticeably while the 53 c/s component was greater. Thus we see that in order to avoid resonance effects at the higher frequencies very short lengths of tubing must be used. When 9" of tubing was used both frequencies showed slight attenuation. The responses appeared to be the same when the tests were repeated using 6 m.m. bore tubing.

The 17.5 c/s component was due to resonances in the model and was always present. It tended to mask the effect which was being measured and a method of attenuating it was sought. The insertion of various lengths of capillary tube in the connecting tubing was tried and it was found that any length longer than 1" gave very severe attenuation. A length of 1" attenuated the 17.5 c/s component to different degrees, depending on the length of connecting tubing

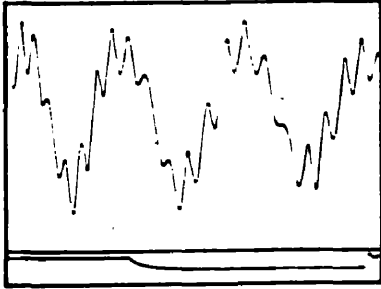


Fig. 13. Pressure recorded with micromanometer connected by 2" of 8mm. bore tubing to the static plate.

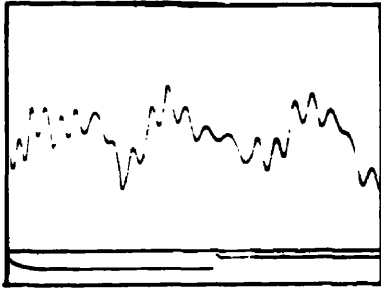


Fig. 14. Pressure recorded with micromanometer connected by 2" of 8mm. bore tubing and 1" of capillary tube to the static plate.

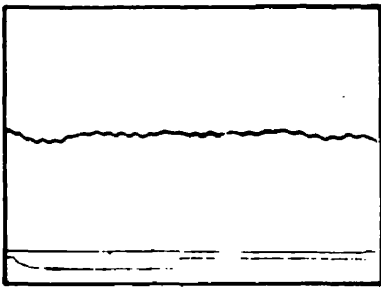


Fig. 15. Pressure recorded with  $3\frac{1}{2}$ mm. diaphragm connected by 2" of 8mm. bore tubing and 1" of capillary tube to the static plate.

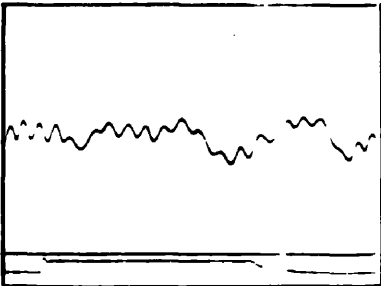


Fig. 16. Pressure recorded with micromanometer connected by 2" of 8mm. bore tubing to a 4mm. pitot-static tube.

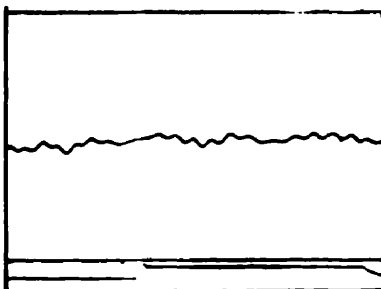


Fig. 17. Pressure recorded with micromanometer connected by 2" of 8mm. bore tubing to a 3mm. pitot-static tube.

and the volume of the instrument. Fig. 14 shows the pressure recorded with the static plate connected to the micromanometer (instrument volume 0.0015 ccs.) by 2" of 8 m.m.-tubing and 1" of capillary tube. A moderate degree of attenuation is noticeable compared with the standard. Fig. 15 shows the same pressure similarly connected to the  $3\frac{1}{2}$  m.m. diaphragm (instrument volume 10 - 15 ccs.) and here we notice the very severe attenuation.

The variation in pressure which it was intended to measure had a frequency of approximately 1 c/s and it was found that 1" of capillary tube did not attenuate this frequency to any noticeable degree when using the  $3\frac{1}{2}$  m.m. diaphragm. This capillary was therefore used when measuring these pressures. The 1" length of capillary tube did not sufficiently attenuate the 17.5 c/s component when using the micromanometer but the instrument had a fixed degree of electrical damping which could be switched into circuit. This was found to produce the required effect, attenuating the 17.5 c/s component severely and the 1 c/s component little.

The pressures in these tests were measured with a static plate because the attenuating effect of the static holes in a pitot-static tube is very severe, attenuating even the low frequency component. Fig. 16 is the pressure recorded with a 4 m.m. pitot-static tube connected by 2" of 8 m.m. bore tubing to the micromanometer. Fig. 17 is the same pressure recorded with a 3 m.m. pitot-static tube. The severe attenuation is evident in both cases.

The conclusions to be drawn from these tests are that the

length and bore of tubing connecting the instrument to the pressure will not affect the response of the system to frequencies as low as 1 c/s. Unwanted frequencies may be suppressed in this case by inserting 1" of capillary tube in the connecting tubing when using the  $3\frac{1}{2}$  m.m. diaphragm and by using the micromanometer with the electrical damping in circuit.

The other quantity with which the investigations were concerned was the speed of the cage. This was measured at the instant when the cage interrupted a beam of light to a photo-electric cell. This produced a record on the film of the cage speed at a known position. The maximum nominal value of the film speed was 5 inches/sec. but that varied slightly from day to day due to the inability of the motor to maintain a constant speed in the face of the varying friction in the system, and a time base was recorded on another channel so that the cage speed could be determined accurately. At a cage speed of 12 ft/sec. and a film speed of 5 inches/sec. the length of the interrupted portion of the photo-electric trace was about 5 m.m. This could be measured, if necessary, to an accuracy of better than 1% using a travelling microscope. It was, however, considered that the accuracy given by normal methods of measurement, about 5%, was sufficient.

The use of models as an aid to predicting pressure losses in ventilation circuits has been common practice for many years and the principles are now well established. If we assume that the pressure drop due to air passing over a surface is dependent only on (a) the density of the air,  $w$  (b) the viscosity of the air,  $\gamma$  (c) the velocity of the air,  $u$ , and (d) the size of the surface as represented by a length dimension,  $l$ , we find, using dimensional analysis, that

$$\text{Friction force } P_f \propto w l^2 u^2 \left( \frac{\gamma}{w l u} \right)^{1/n}$$

The dimensionless group  $\frac{u l u}{\gamma}$  is known as Reynolds number,  $Re$ .

Hence the friction pressure drop  $p_f$  is given by

$$P_f = K w u^2 (Re)^n$$

and the ratio of the friction pressure drop in the model to that in practice is given by

$$\frac{P_m}{P_p} = \frac{w_m}{w_p} \left( \frac{u_m}{u_p} \right)^2 \left( \frac{Re_m}{Re_p} \right)^n$$

If we use the same fluid, air, and arrange the model velocity such that  $u_m l_m = u_p l_p$  we get the simple relationship,

$$P_m = P_p \left[ \frac{u_m}{u_p} \right]^2$$

In the type of model testing used in mining ventilation it is not generally possible to arrange that  $u_m l_m = u_p l_p$  (i.e.  $Re_m = Re_p$ ). However, very extensive model testing has shown that when  $Re$  is

above a certain value, which varies with the roughness of the surface, it has no further effect on the friction pressure drop. In mining practice the combination of  $R_g$  and surface roughness is such that  $R_g$  is above this value. If we ensure that, in the model,  $R_g$  is above the value corresponding to the model surface roughness, we may neglect the effect of  $R_g$  in any comparison between the model and actual practice.

Any pressure losses due to shock, sudden expansion etc. . will also be proportional to  $u^2$  so that, combining the losses, we have,

$$\text{total loss}_{\text{practice}} = \text{total loss}_{\text{model}} \cdot \left( \frac{u_p}{u_m} \right)^2$$

This assumes that the model is a scale model, identical in every respect, even to the surface roughness.

So, in the model shaft where  $R_g$  up to  $2 \times 10^5$  is possible, we are able to carry out tests on cages and predict the pressure losses which will be obtained in practice.

When we come to investigate how these pressure drops produce velocity disturbances, and how these velocity disturbances are propagated, we meet a different set of conditions. One major problem is the fact that a scale model of the workings is not a practical proposition. It would mean a scale factor of approximately 500 which, in turn would mean a shaft diameter of 0.35". At this diameter the speeds necessary for high Reynolds numbers would involve compressibility effects. In addition, the experimental techniques

would no longer be those which are familiar.

Another factor which introduces difficulties of similarity is the shape of the volume representing the workings. This determines whether the volume is evenly distributed throughout the length or whether the greater part is concentrated at one part of the workings. As the pressure pulse travels through the workings it expands the air as it reaches it. If, at one point, it reaches a large proportion of the total volume, then additional outflow will take place at a corresponding time. It will take a pressure pulse 24 seconds to travel a distance of 5 miles underground, whereas in the model it will have reached all the air in approximately  $1/100$ th of a second. The inertia of the air is such that the rate of outflow in the model will be controlled only by the resistance through which it has to flow and not by the shape of the volume. This appears as a serious drawback to the simulation of real conditions and until it can be circumvented any velocity disturbance in the model can be related to actual practice only in a very loose fashion.

It was hoped, in this investigation, to simulate those aspects of the workings which were of most importance, namely volume and resistance, and to make corrections for the errors which would be introduced. It was found, as the experiments proceeded, that resonances of various components of the ventilation circuit play a very important part in determining the experimental results. It was generally possible to see, by comparison of frequencies and lengths, which component or components were resonating, but it was

considered that predictions as to whether similar resonances were likely to occur in practice would be very tentative.

The cage produces two major pressure peaks, one at either end, and the rate at which these pass the inset may determine, together with the natural frequency of the system, how severe any resonance will be. At the colliery these pressure peaks pass in approximately  $1/10$  of the time constant of the roadways. A similar relationship in the model would mean that the cage would be travelling at 85 ft/sec.

For these reasons comparison of model conditions and those in practice will have to be made with caution and much preliminary investigation will be necessary before methods of overcoming these difficulties can be found.

Chapter 6      MODEL TESTS - STATIONARY CAGE TESTS

The further insight into the problem gained as a result of the theoretical investigation which was proceeding simultaneously indicated that complete similarity would be difficult to obtain. This is due to the fact that the shape of the volume representing the workings and roadways is as important as the distribution of resistance throughout this volume. It is sufficiently difficult to decide what this relationship is in practice but it is equally difficult to plan how this may be simulated in a model. Two methods come to mind but both are fairly complicated and do not readily lend themselves to control. The first method is simply to represent the workings by a series of small volumes connected together in various combinations by means of connecting pieces which are, in fact, variable resistances. The other method would appear to allow a greater variation of resistance, but less of shape. In this case a volume is constructed to represent the roadways and workings. The factor which is important in the design of this volume is that the cross sectional area at any distance from the entry bears the proper relationship to the total cross sectional area of all the roadways and workings at the corresponding distance from the mine shaft. Having constructed this volume it is then filled with a framework of gauzes at right angles to the line of airflow. In its simplest form this would mean gauzes across the section of the volume, variously spaced throughout the length.

These gauzes might have different mesh sizes and hence different values of resistance to air flow. Since time was not available to try these complex methods, and therefore complete similarity was abandoned, it was decided to split the problem.

The first part was concerned with the pressure drop produced by the cage. This included such factors as cage speed, air speed and cage dimensions. The second part was concerned with the manner in which the pressure disturbances produced by the cage produced a velocity disturbance and how this velocity disturbance was propagated.

To begin the investigation into the pressure drop of the cage it was decided to determine the resistance to air flow of all the cages while stationary. This involved measuring the pressure drop produced by the cage and the length of shaft in which it stood and then subtracting that pressure drop which was due to the shaft. This was done at many velocities over a wide range so that the law of resistance could be determined.

To measure the velocity a pitot-static tube station was constructed 25 shaft diameters downstream from the cage position. A 3 m.m. pitot-static tube was used, together with the Betz manometer, to determine the velocity of the air across a diameter of the shaft. Repeating this at many velocities enabled a graph to be plotted of the velocity head, in m.m. W.G., as measured by a pitot-static tube at the centre of the shaft, and the mean velocity in ft/sec. Some anomalous results were obtained using this velocity measuring station and it was found that the cage affected the velocity distribution,

even at 25 diameters. The measuring station was moved to a point 40 shaft diameters downstream and recalibrated. No further trouble was experienced and this was used to measure steady state velocity in all tests.

The pressure drop due to 147" of Perspex shaft was measured over a range of velocities up to 100 ft/sec. and the results are plotted in Fig. 18. It is found that the shaft pressure drop was proportional to the velocity to the power 1.83 which would indicate that the lined shaft was acting as a smooth pipe at these Reynolds numbers (up to  $2.0 \times 10^5$ ). It might be mentioned here that when carrying out a similar test with the 20 H.P. fan it was found that the pressure drop was proportional to the velocity to the power 1.67, when the velocity fluctuations were approximately 10% of the steady state velocity. While outwith the scope of this investigation it is noteworthy due to the magnitude of the discrepancy.

The graphs showing the pressure drop due to cage against velocity are shown in Figs. 19 and 20 for cages A to H. From these graphs and the dimensions of the cages Table II is produced.

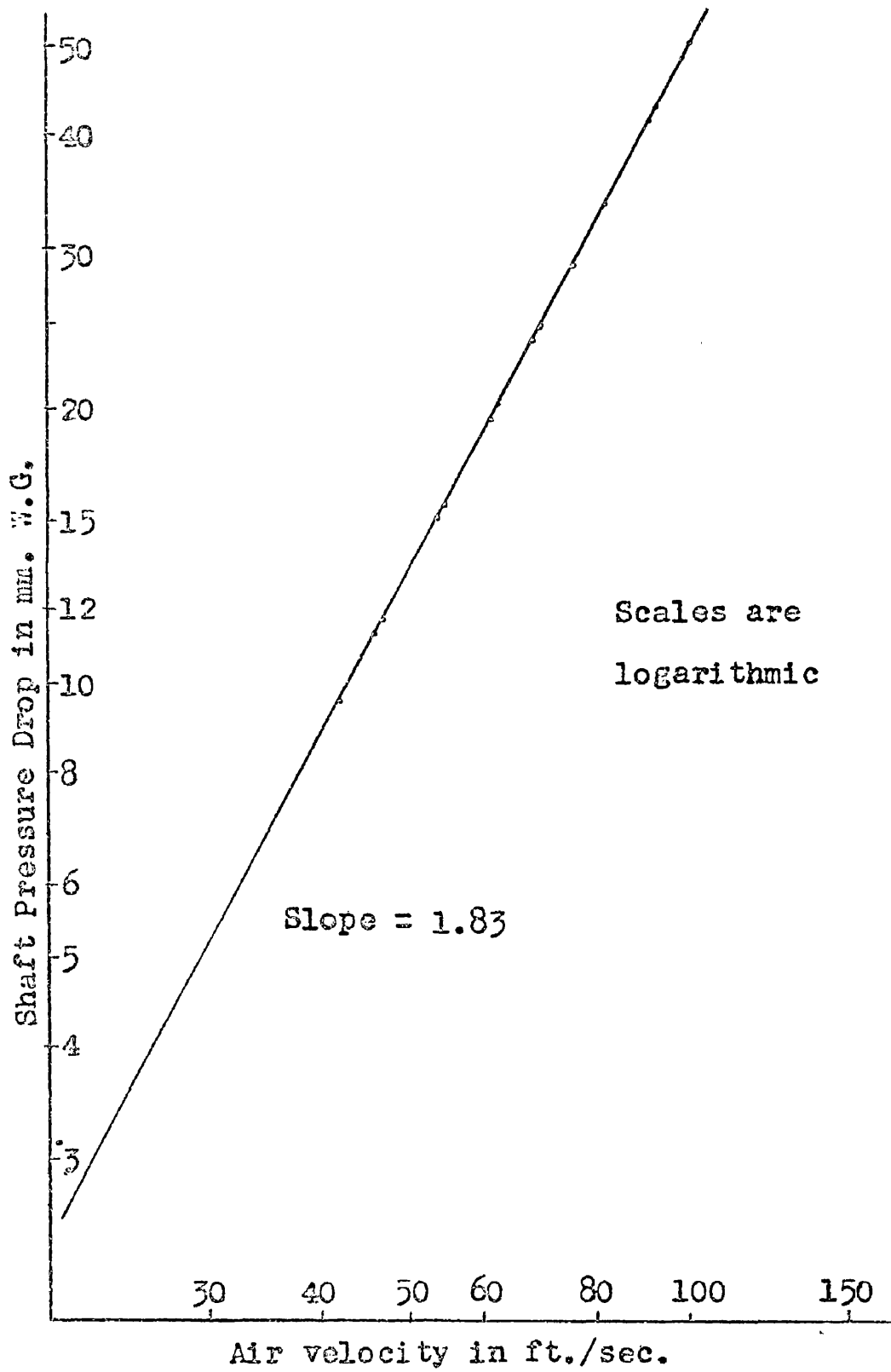


Fig. 18. Resistance law of model shaft.

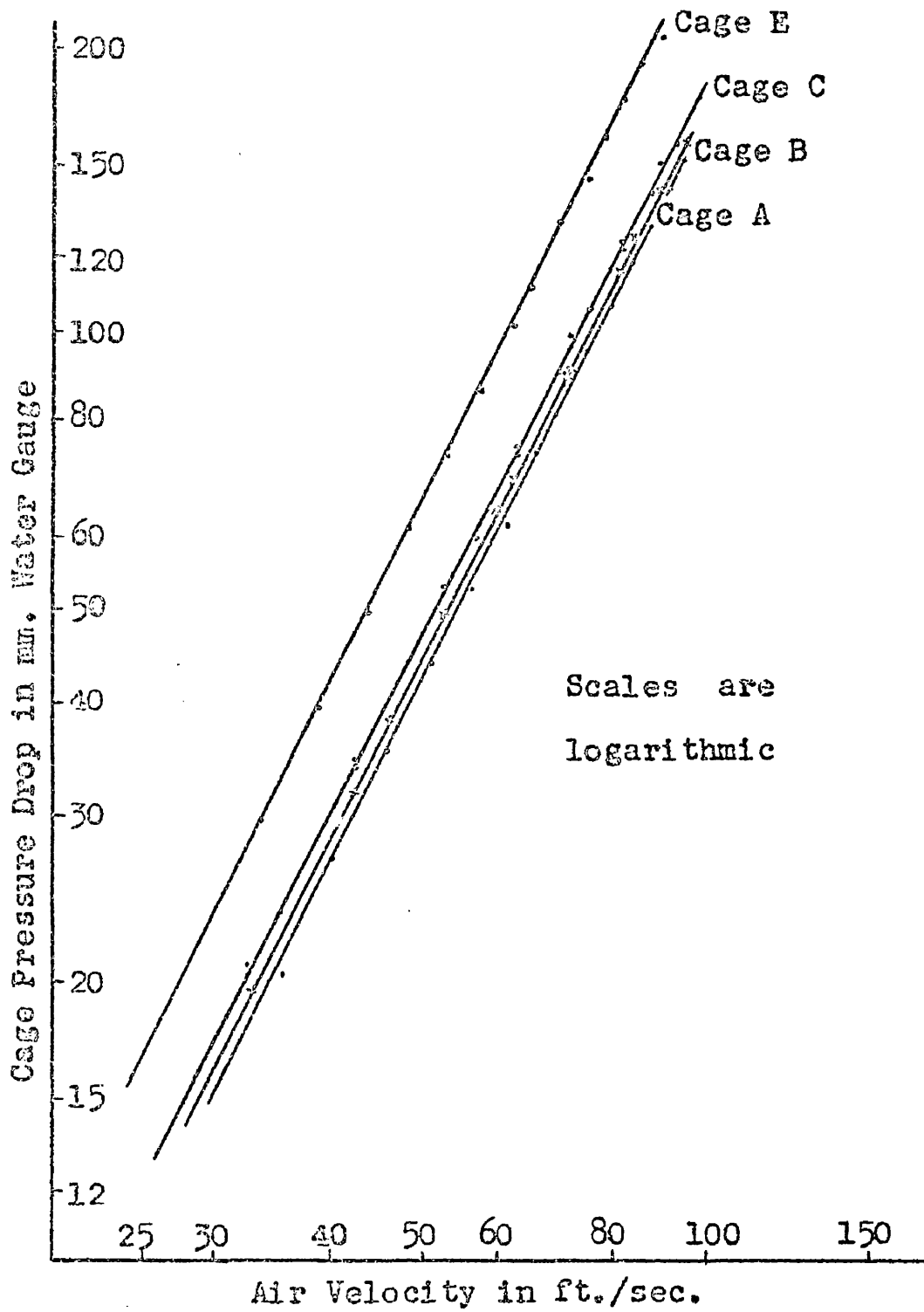


Fig. 19. Pressure drop due to cages.

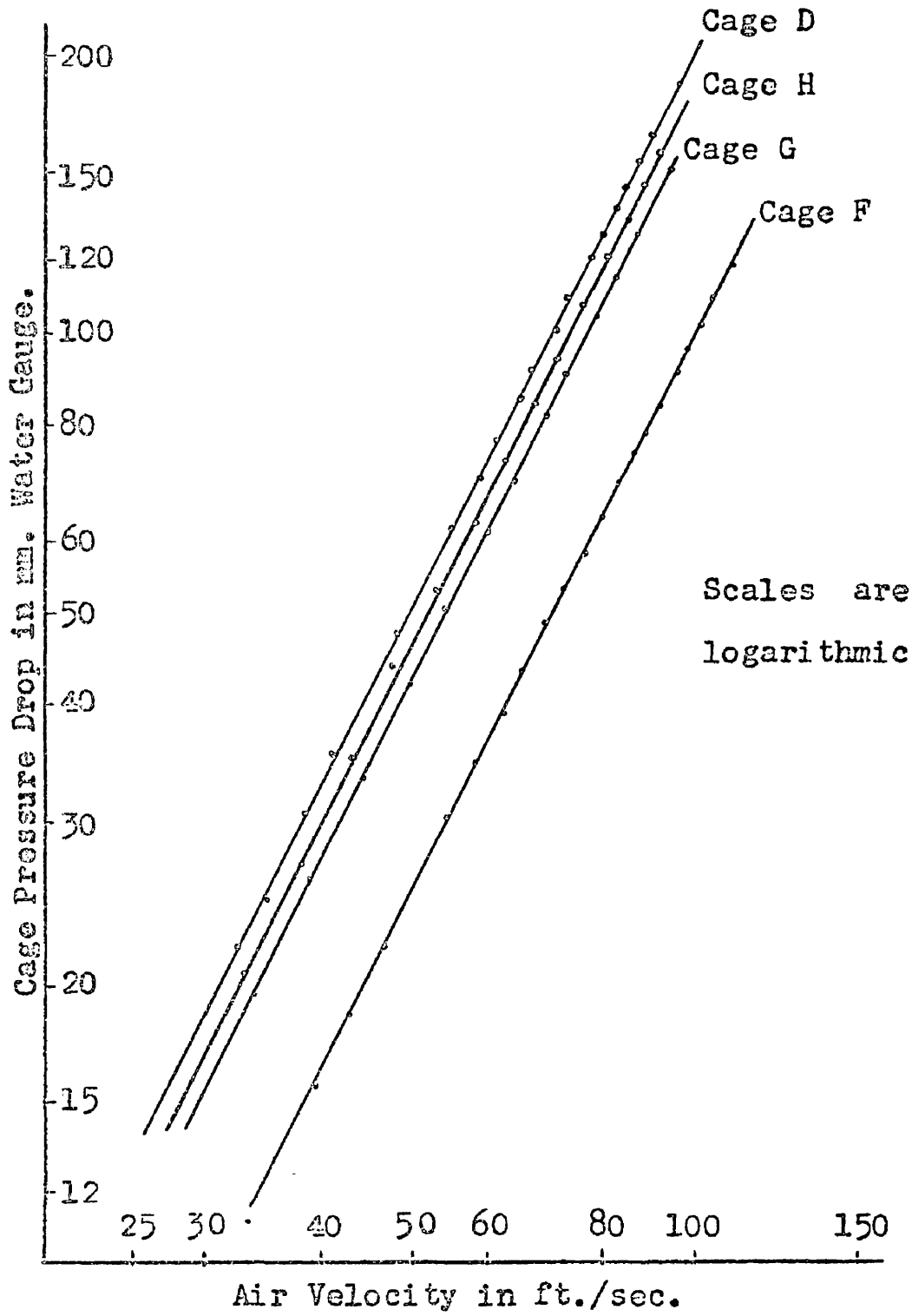


Fig. 20. Pressure drop due to cages.

TABLE 11

Cage	Frontal Area	Number of Decks	Aspect Ratio	K	K'	p.d. in m.m. W.G. $Re = 1.8 \times 10^5$
A	4.12	3	1.83	0.018	1.99	170
B	4.12	4	1.83	0.020	1.97	178
C	4.12	5	1.83	0.022	1.97	187
D	4.12	6	1.83	0.023	1.97	201
E	4.81	3	1.57	0.028	1.99	267
F	3.44	3	2.20	0.012	1.97	100
G	4.14	3	1.22	0.020	1.97	170
H	4.12	3	0.85	0.020	1.99	185

Note: K and K' in Table 11 refer to the equation  $p.d. = Ku^{K'}$  when p.d. is the cage pressure drop in m.m. W.G. and u is the air velocity in ft/sec.

In comparing the resistance of cages the pressure drop at  $Re = 1.8 \times 10^5$  ( $u = 100$  ft/sec.) has been used. Other authors (ref. 4) have used terms to denote resistance which assumes that the pressure drop is proportional to the second power of the air velocity. Assuming an index of 2.00 instead of 1.97 at  $u = 100$  ft/sec. leads to an error of 13%. For the purposes of description the pressure drop at 100 ft/sec. due to the cage will be called the resistance pressure drop ( $R_p$ ). From Table 11 we are able to plot  $R_p$  against

(a) the number of decks (Fig. 21)

(b) the ratio known as the coefficient of fill (b), which is defined as the cage frontal area divided by the shaft cross sectional area (Fig. 22)

(c) the aspect ratio (Fig. 23)

The increase in  $R_p$  with an increase in the number of decks is shown in Fig. 21. The increase in  $R_p$  is as would be expected except for the 6 deck cage. The pressure having increased linearly up to 5 decks there appears to be no reason why it should increase more rapidly with a greater number of decks. An error in measurement is immediately suspected, but the figure used is obtained from approximately 20 points the scatter of which is negligible. To investigate further would entail constructing a 7 deck cage. It was considered that little useful information would be gained since cages with more than four decks are rare in this country.

The graph of coefficient of fill (b) against  $R_p$  indicates that  $R_p = K b^{2.9}$ . On the same graph are results obtained by Blaho in a paper concerning the drag of trains in tunnels (ref. 5). His results indicate that  $R_p = K b^{3.1}$  which is a good measure of agreement. We note that a single cage replacing two cages and having twice the frontal area of each cage has a  $R_p$  equal to 4 times the combined  $R_p$  of the two cages.

In Fig. 23 is plotted the  $R_p$  of three cages against their aspect ratios. No precise conclusions can be drawn due to the small number of cages available, but it would appear that  $R_p$  is

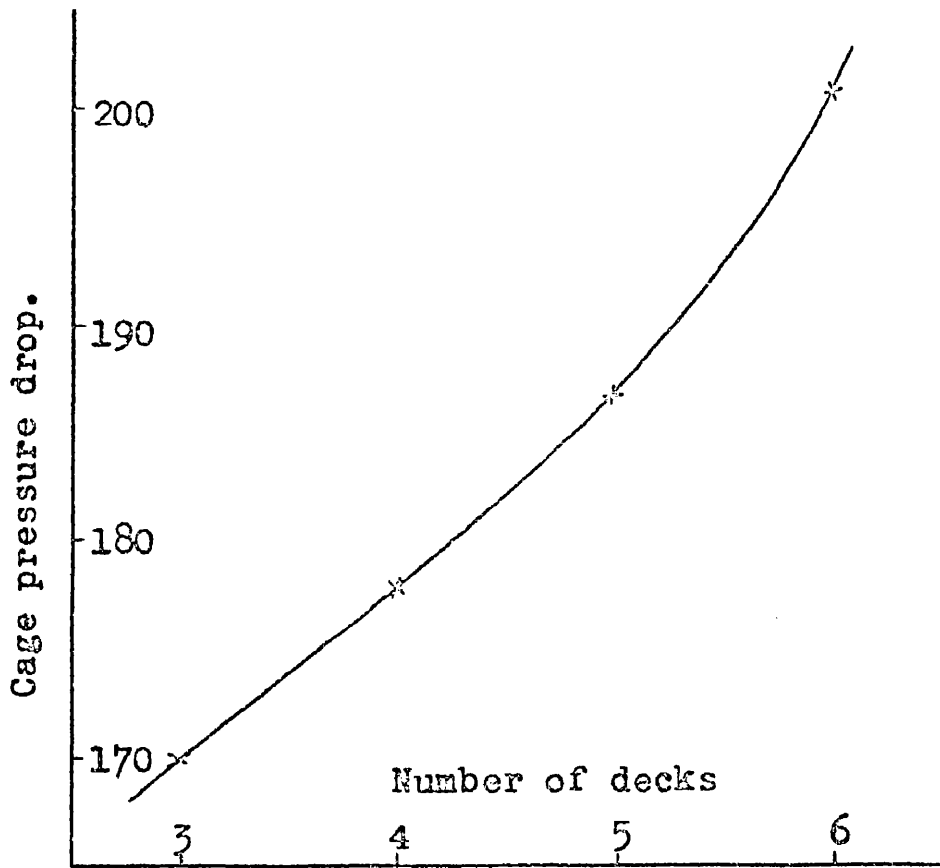


Fig. 21. Effect of number of decks on cage resistance

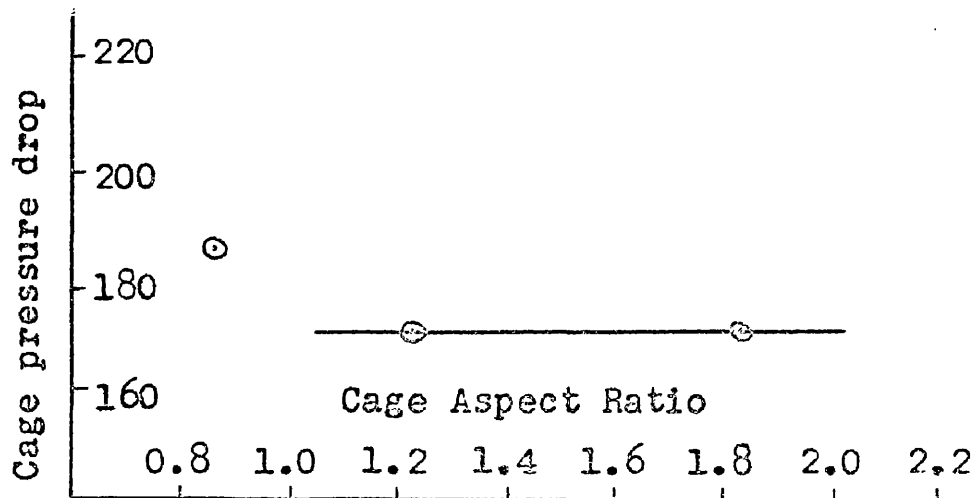


Fig. 23. Effect of aspect ratio on cage resistance.

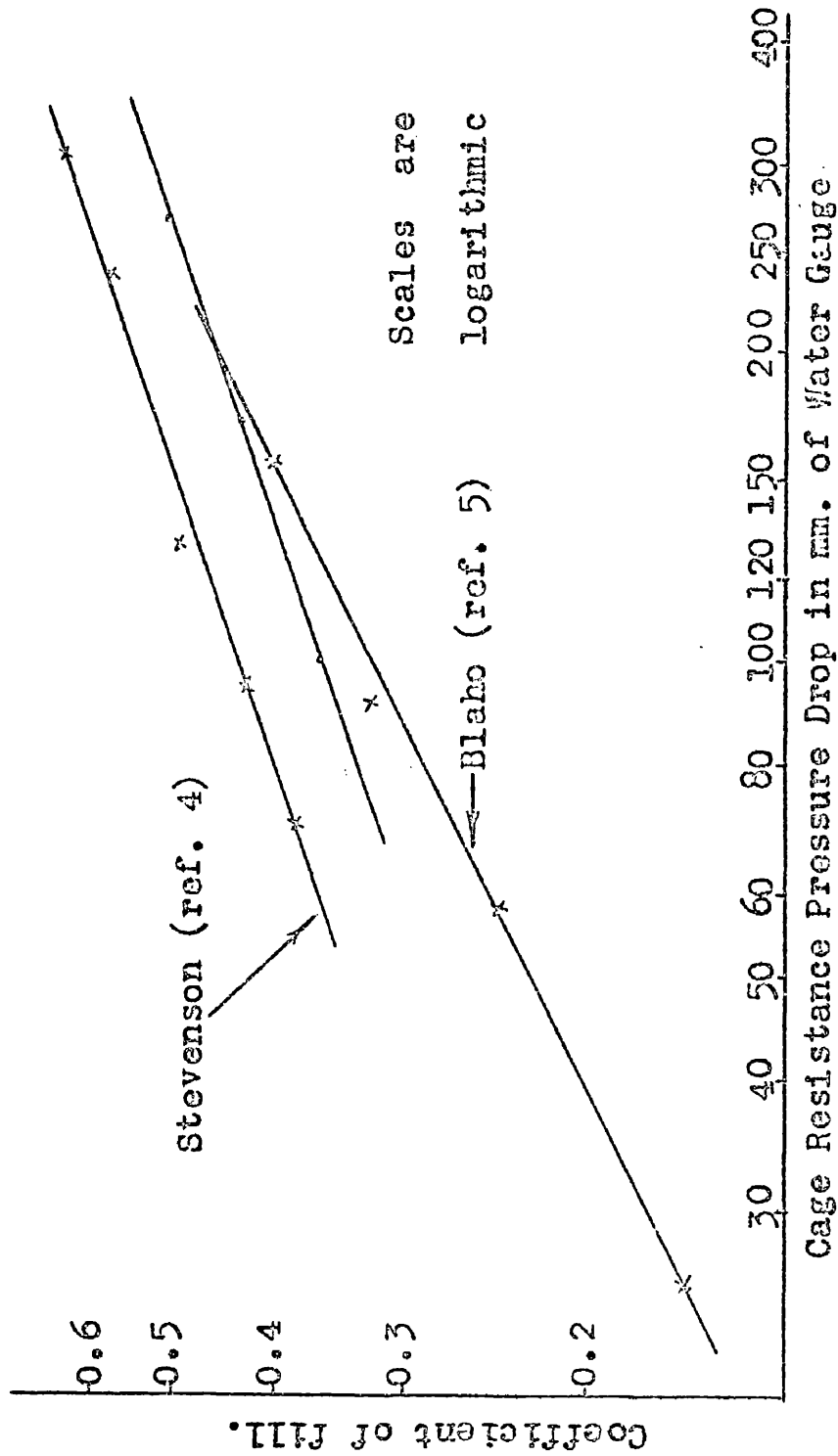


Fig. 22. The effect of coefficient of fill on cage pressure drop. Blaho's results are not comparable in magnitude, due to his method of presenting the results, but the slopes may be compared.

independent of this ratio within the limits of the ratio which are likely to be used.

From these tests it can be seen that the  $R_p$  due to a cage can be kept to a low value by having a greater number of decks rather than a large frontal area. This would entail simultaneous decking arrangements if a high winding tonnage were contemplated. The extensive excavations necessary might make this one of the less attractive methods for minimising velocity disturbances due to the movement of the cage.

To investigate how the pressure drop produced by the cage was constituted it was proposed to plot the total pressure drop along the length of the cage, on both major axes. It was soon found that this was not very easy due to the eddies produced by each deck. Pieces of thread attached to the end of the cage showed eddies at the downstream end existing for approximately  $1\frac{1}{2}$  cage lengths. To align the total head tube in the direction of maximum velocity was, in some places, not feasible.

It was therefore accepted that a static pressure survey would be easier while still providing much information. It might be argued that static pressure measurements would be no more valid than those of total pressure since the static holes would not be at right angles to the direction of maximum velocity at all times. However, the eddies involved were large by comparison with the pitot-static tube being used. Therefore the direction of maximum velocity would be the same on one side of the pitot-static tube as on the

other so that any positive velocity component on one side would have a corresponding negative component on the other side.

The static pressure was measured halfway between the cage and the shaft wall, past the open decks and also past the sides of the cage. The open decks were then completely closed in and the pressure distribution was measured past these closed decks. This was done twice at each of three velocities for the eight cages.

The first conclusion to be drawn from these tests is that the pressure distribution does not vary with velocity. That is, the pressure losses at all points are proportional to the same power of velocity. This means that by dividing the static pressure at any point by the square of the mean velocity we obtain one curve for each cage at all velocities. These curves are so similar that only those for cage A (the scale model of the cage at colliery R) and cage D are shown. These illustrate how the pressure varies over the cage.

Fig. 25 shows the pressure distribution past cage A,

- (i) in the plane of the open decks,
- (ii) in the plane of the cage sides,
- (iii) in the plane of the decks after they have  
been completely closed in.

Fig. 25 (i), (ii) and (iii) shows the pressure distribution in the same planes respectively for cage D.

The pressure distribution is much as expected. The air, flowing past each deck, continues to accelerate until the 'vena

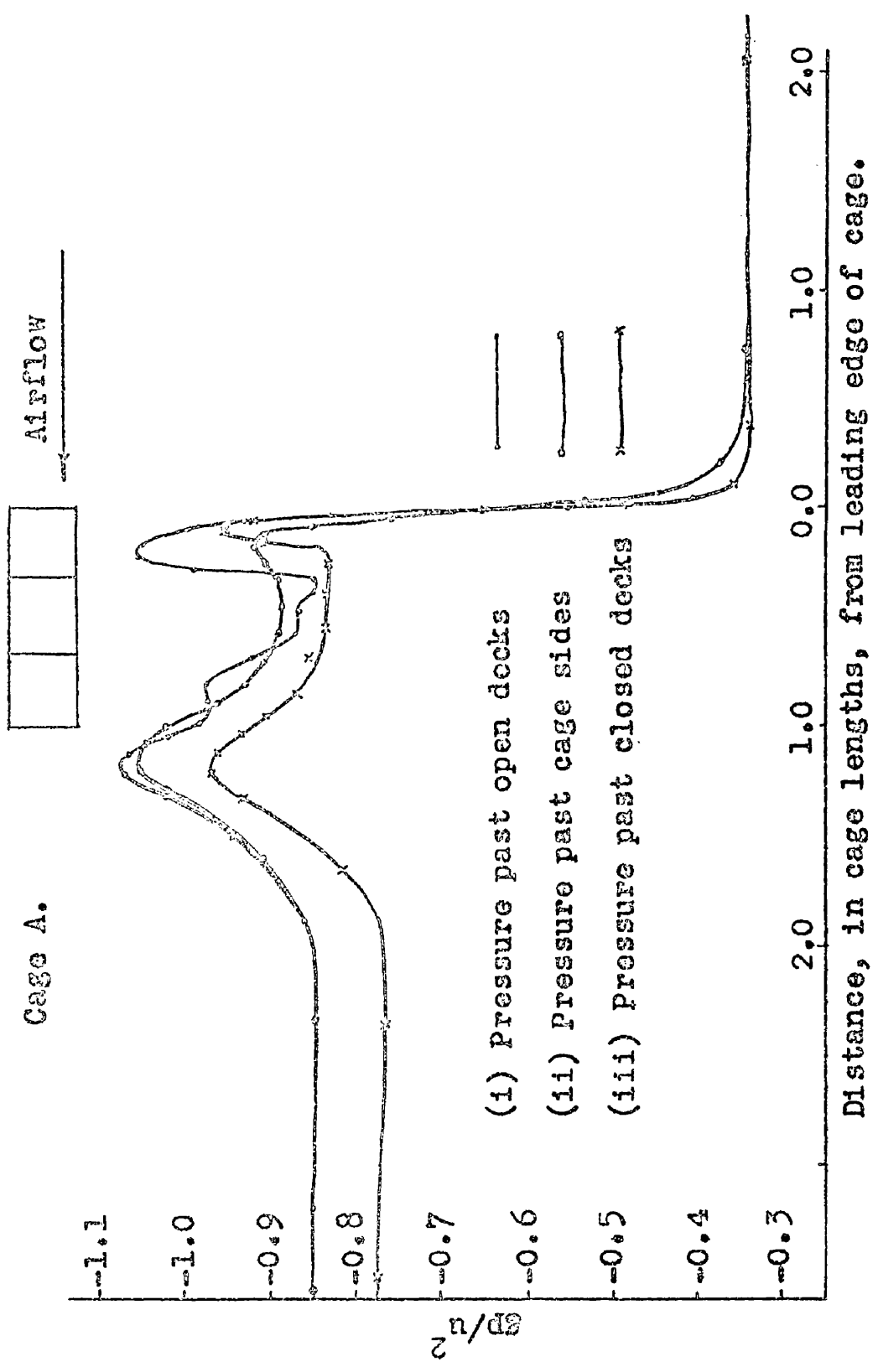


Fig. 24. The distribution of static pressure past stationary cage A.

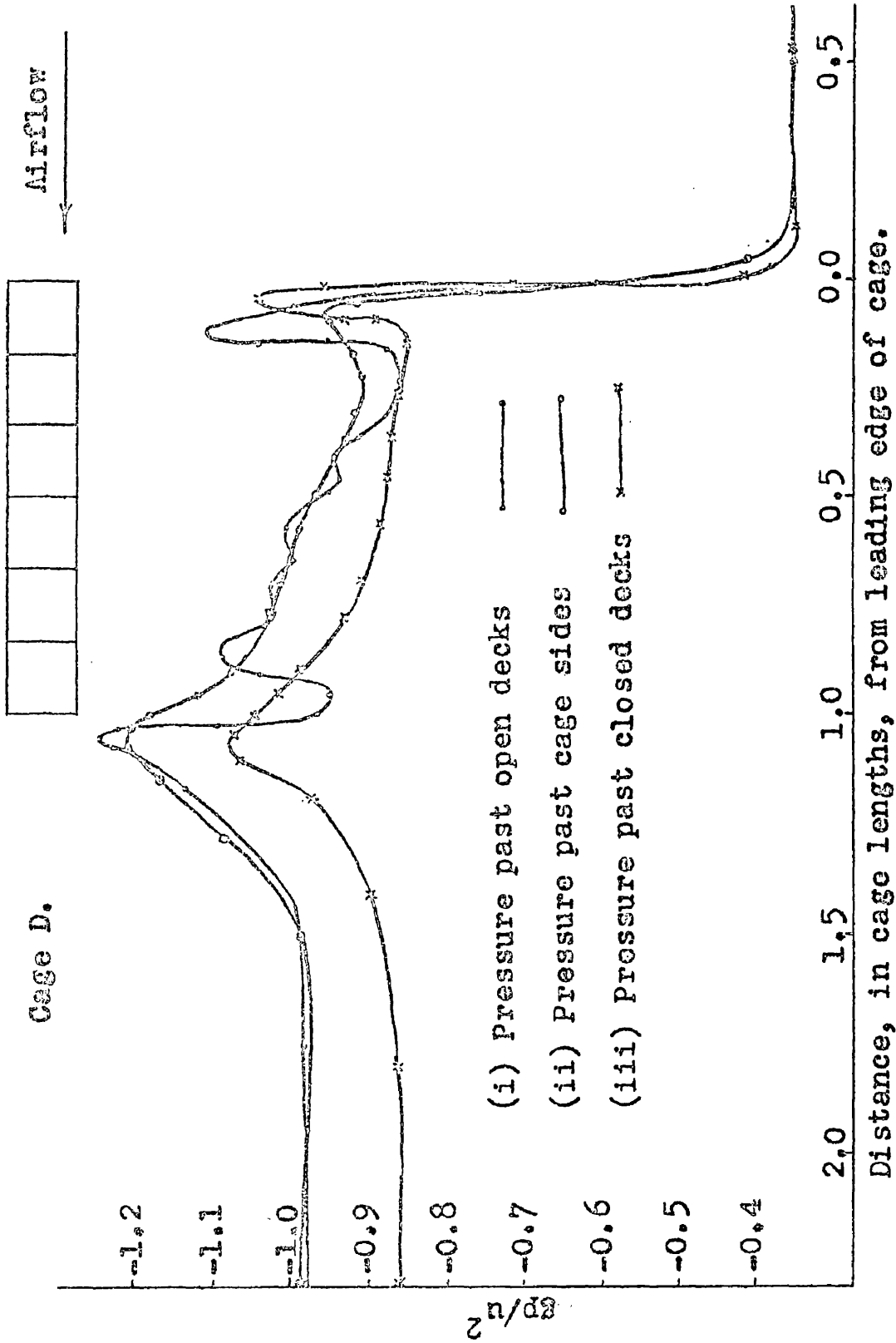


Fig. 25. The distribution of static pressure past stationary cage D.

contracts<sup>o</sup> at which point the static pressure is lowest. It then re-expands with consequent loss of energy, repeating this procedure at each deck. The distribution past the sides of the cage shows the drop in static pressure as the air accelerates into the space between the cage and the shaft wall. Then follows a steady drop in pressure due to the friction of the air against the cage and the shaft wall. The air re-expands behind the cage producing an increase in static pressure but, since there is no streamlining, a loss of energy.

The pressure distribution along the two axes can never be the same, being produced in different ways, thus air flow must take place between the sides of the cage and the open ends. This movement of air complicates the distribution of pressure and makes its prediction very difficult. When, therefore, the relationship between the air velocity, the cage velocity and the pressure drop is determined the form of the relationship is governed only by the experimental data and not by any theoretical considerations.

Figs. 24 (iii) and 25 (iii) show the distribution of static pressure past the ends of the cage when these ends are completely closed in, as they might be with properly fitting mine cars. It is seen that the static pressure drop now contains components of a higher frequency than before. These components will be more severely attenuated when this pressure waveform is propagated along the roadways. It is also noticed that the overall pressure drop is lowered by 16-18%, when the sides of the cage are completely enclosed.

From these tests it seems that streamlining the cage would be the only method of reducing pressure drop due to shock losses and sudden expansion losses. It has been shown, however, (ref. 4) that streamlining which is effective in one direction loses the greater part of this effectiveness when travelling in the opposite direction. This may not be important in a case such as is being investigated since the large pressure drop is produced when the cage and air are travelling in opposite directions. When the cage and air are moving in the same direction, their relative velocity will be very low and the pressure drop produced by the cage will not be of importance.

## Chapter 7

MODEL TESTS 2 - MOVING CAGE TESTS

The tests in this series were designed to determine the pressure drop produced by the cage when it was moving. The factors considered were the cage speed, the air speed and the cage dimensions. As explained in the previous chapter the form of the final relationship was governed solely by the experimental results, since the complex behaviour of the air round the cage made prediction difficult. For these tests the measurements necessary were (a) the air velocity, as represented by the pressure drop due to a length of shaft. It was decided to use this for the velocity determination since this

measurement was already being recorded and an accurate estimate of velocity was possible from previous tests, (b) the cage speed, measured photo-electrically, and (c) the pressure drop due to the cage, measured with the pressure recorder.

When the cage begins to move the pressure drop produced by it alters and hence the total resistance in the fan circuit is changed. This produces a change in the air velocity, dependent on the shape of the pressure/quantity curve in the fan characteristics. It was, therefore, necessary to determine this effect so that corrections could be applied. This was done by inserting a variable area orifice in the shaft and measuring the change in velocity as the area was altered to produce a different static pressure drop. It was found that if a change in area increased the static pressure drop, due to the orifice and the 147" of shaft which contained it, by  $p$ , then the pressure drop of 147" of shaft, due to the velocity, dropped by  $p/1.79$ . This linear relationship was found to hold over the range of air and cage velocities being used.

The method of determining the air velocity and cage pressure drop was, therefore, as follows. The pressure drop produced by 147" of Perspex shaft plus the stationary cage, was measured. The cage motor was started and the pressure drop produced by the same length of shaft plus the moving cage was then recorded. If the difference in these pressures was  $p$  then this is the change in static pressure produced in 147" of shaft containing a variable resistance. Hence the change in pressure drop of 147" of shaft

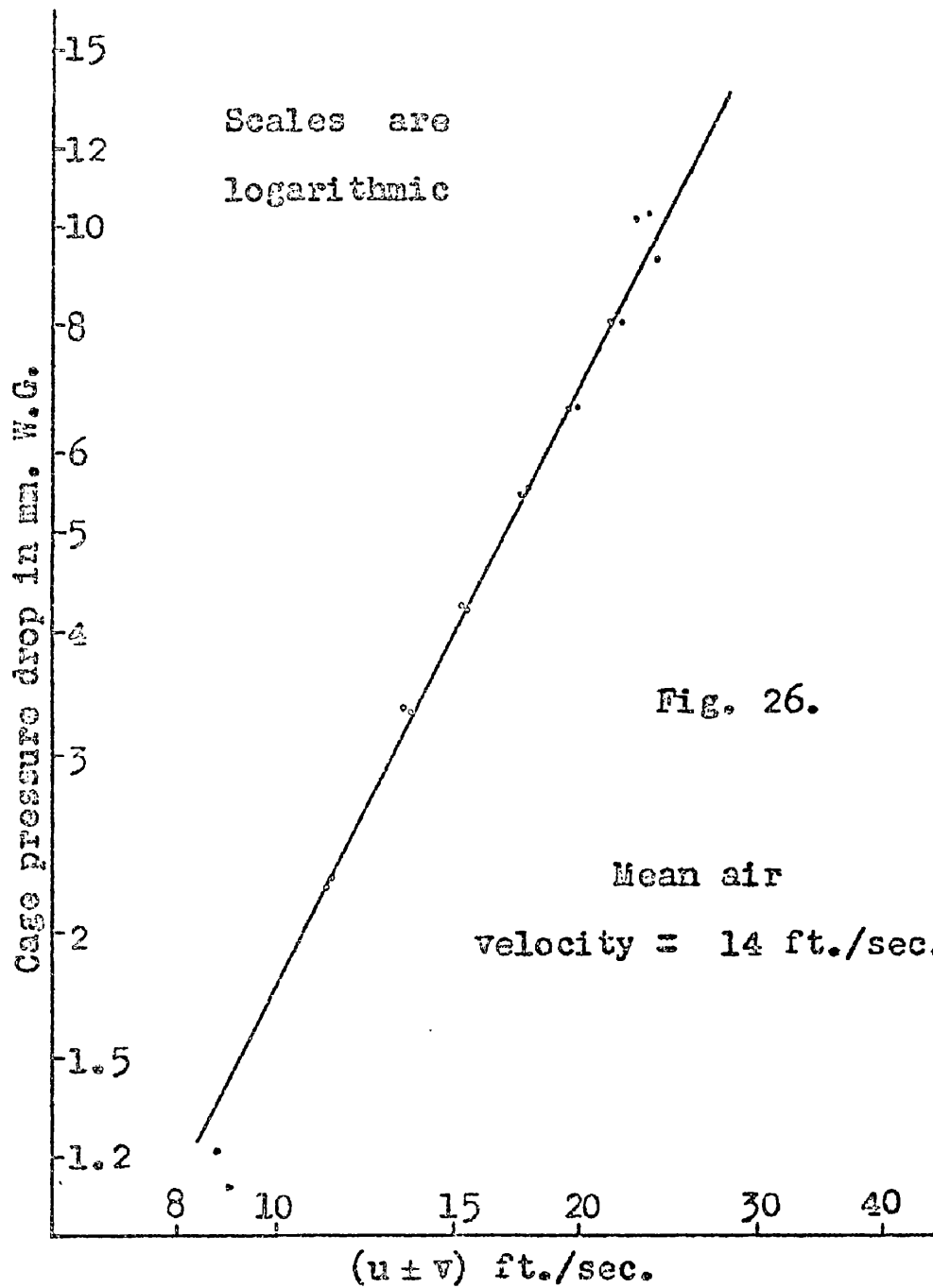
alone was  $p/1.79$ . From the previous series of tests we were able to determine the shaft component of the first measured pressure. This changed by  $p/1.79$  when the cage was moving and hence we were able to determine the new velocity and also the cage pressure drop.

At each of five air velocities the pressure drop due to the cage was measured for each of six cage speeds, using the pressure recorder. Figs. 26-30 show the pressure drop due to the cage plotted against  $(u \pm v)$  where  $u$  is the air velocity in ft/sec. and  $v$  the cage velocity. They are both positive in opposite directions. It can be seen from the straight lines that, at any  $u$ ,  $p.d. = K(u \pm v)^{K'}$ . Table IV shows  $K$  and  $K'$  for the range of velocities used.

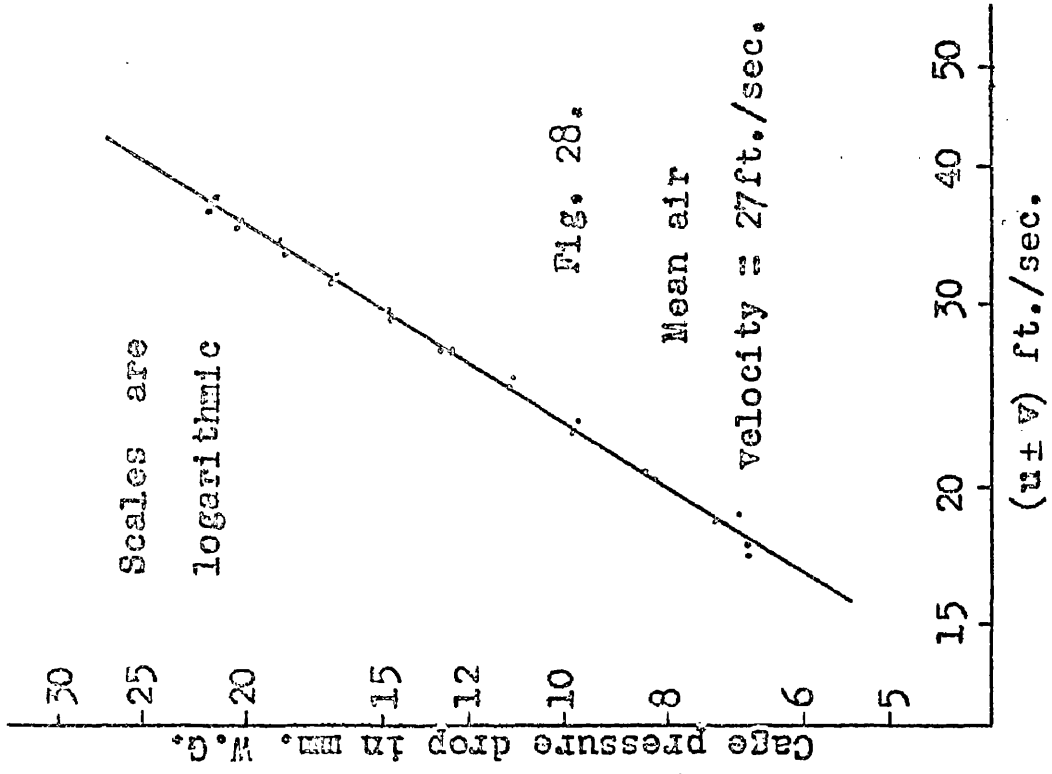
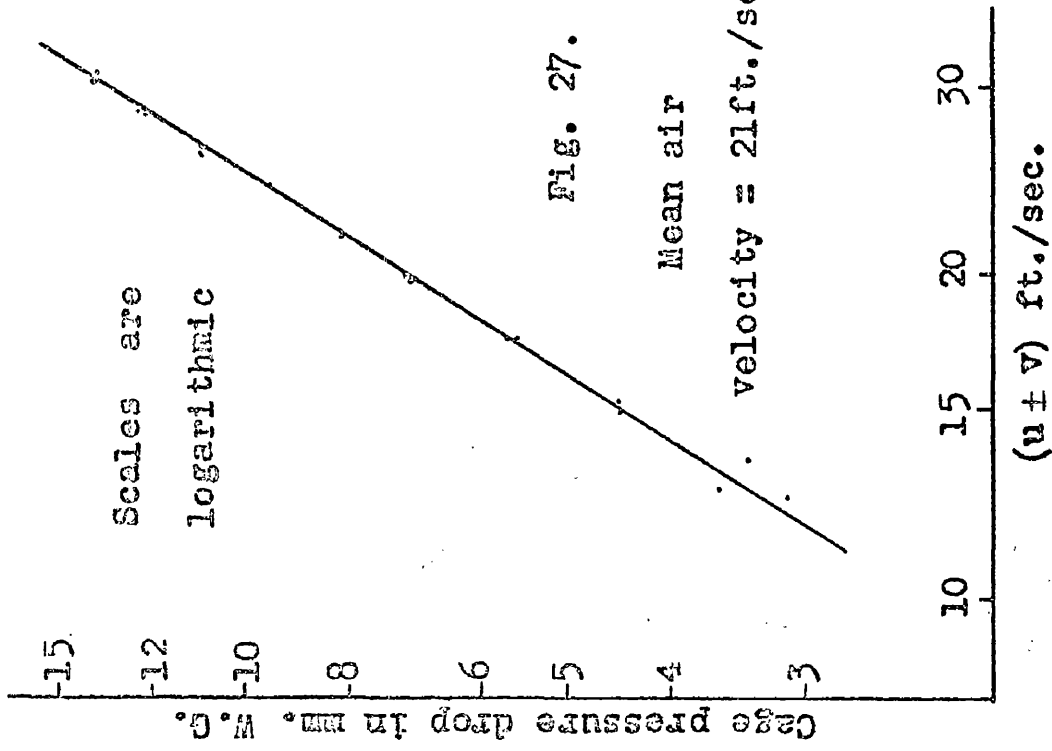
T A B L E IV

Mean Velocity (ft/sec.)	14	21	27	33	39
K	.018	.056	.062	.075	.068
K'	2.00	1.62	1.62	1.58	1.62

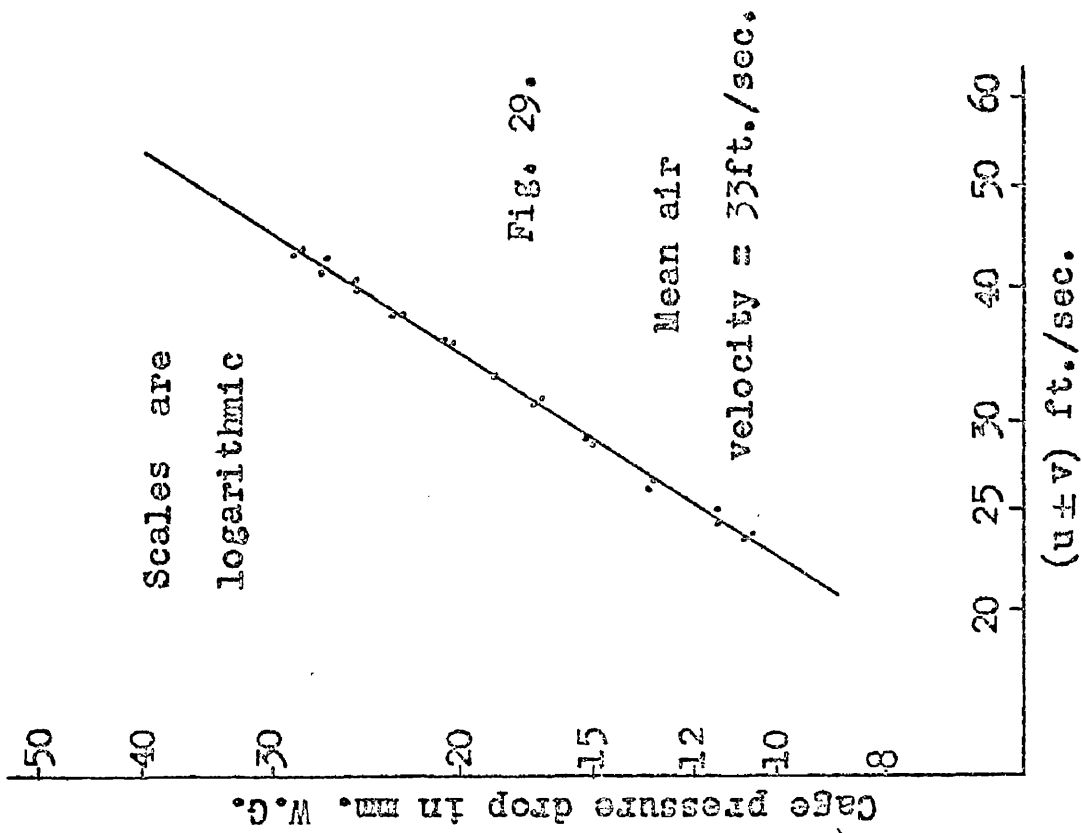
Table IV shows  $K$  and  $K'$  for the range of velocities used. The value of 2.0 for  $K'$  at the lowest mean velocity is unexplained and may be due to inaccurate measurements at such low values. Since no further investigation was possible it seemed more reasonable to shorten the range over which the results are applicable rather than attempt to cater for this anomalous result. In the range measured it is seen



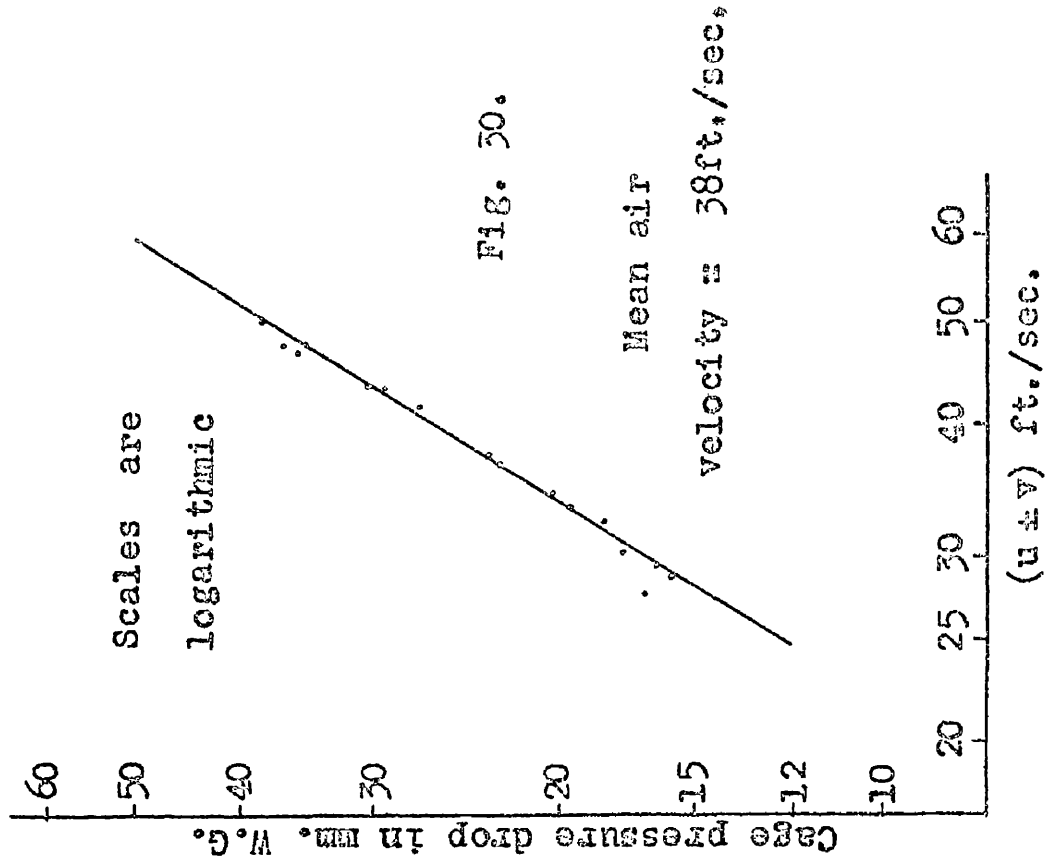
Pressure drop produced by a moving cage in an air stream.



Pressure drop produced by a moving cage in an air stream.



Pressure drop produced by a moving cage in an air stream.



Pressure drop produced by a moving cage in an air stream.

*page out of place.*

the pressure drop itself is low and gross inaccuracies in its estimation are not important for the purposes of this investigation.

## Chapter 8

MODEL TESTS 3 — VELOCITY FLUCTUATIONS PRODUCED  
BY THE MOVING CAGE

This series of tests was designed to investigate the effect of communicating the pressure drop produced by the cage to a large volume of air representing the workings. Fig. 31 shows the model arrangement which was used,  $V$  being the volume and  $R_1$ ,  $R_2$ ,  $R_3$  and  $R_4$  being variable resistances. The fan was used to exhaust air at all times. Since little was known about the behaviour of the air it was decided, in the first instance, merely to assess the qualitative effect of all the variable factors with a view to developing a theory connecting the model and actual practice. Having determined which factors are of importance it was then proposed to study them in more detail.

In the colliery investigation the disturbance in the roadway, adjacent to the shaft, was measured at a point 10 yards from the shaft. It was found, in the model, that at a corresponding point, according to the laws of geometrical similarity, eddies produced by the inset were severe. The velocity was therefore measured at a point which was four times this distance from the shaft. It was measured using a total head tube and static plate. This was necessary

that  $p.d. = K(u \pm v)^{1.62}$  where  $K$  is a function of  $u$ . It is also known, by plotting the results when  $v = c$ , that, when  $v = c$ ,  $p.d. = 0.019 u^{1.97}$  therefore  $K$  was chosen initially as  $0.019 u^{.35}$ . This was found to attach too much importance to  $u$  and a closer relationship was found, by trial and error, to be  $p.d. = 0.019 u^{.24} (u \pm v)^{1.73}$ . Due to the complex air flow pattern round the cage it is not possible to predict whether or not this is of the correct form.

It will be noticed that when  $u$  and  $v$  are equal and in the same direction, this expression predicts zero pressure drop. However, under these circumstances the air in the space between the cage and the shaft wall will be travelling at a velocity  $u$  ft/sec. and will produce a pressure drop proportional to  $u^{1.03}$ . This would suggest that the form of the expression is not quite correct and hence may account for the difference between predicted and measured results at low  $(u \pm v)$  values.

The shortcomings of this series of tests are due mainly to the low maximum speed of the cage. This was about 12 ft/sec. which, considering the frequency response of the pressure recorder, is almost a practical maximum. The frequency response is important insofar as the recorder must read the steady pressure before the cage starts decelerating. Hence, to have low  $u \pm v$  values, the velocity of the air must be 10-20 ft/sec. at which speed measurements may become inaccurate and  $Re$  is low.

It will, however, be remembered that at low  $(u \pm v)$  values

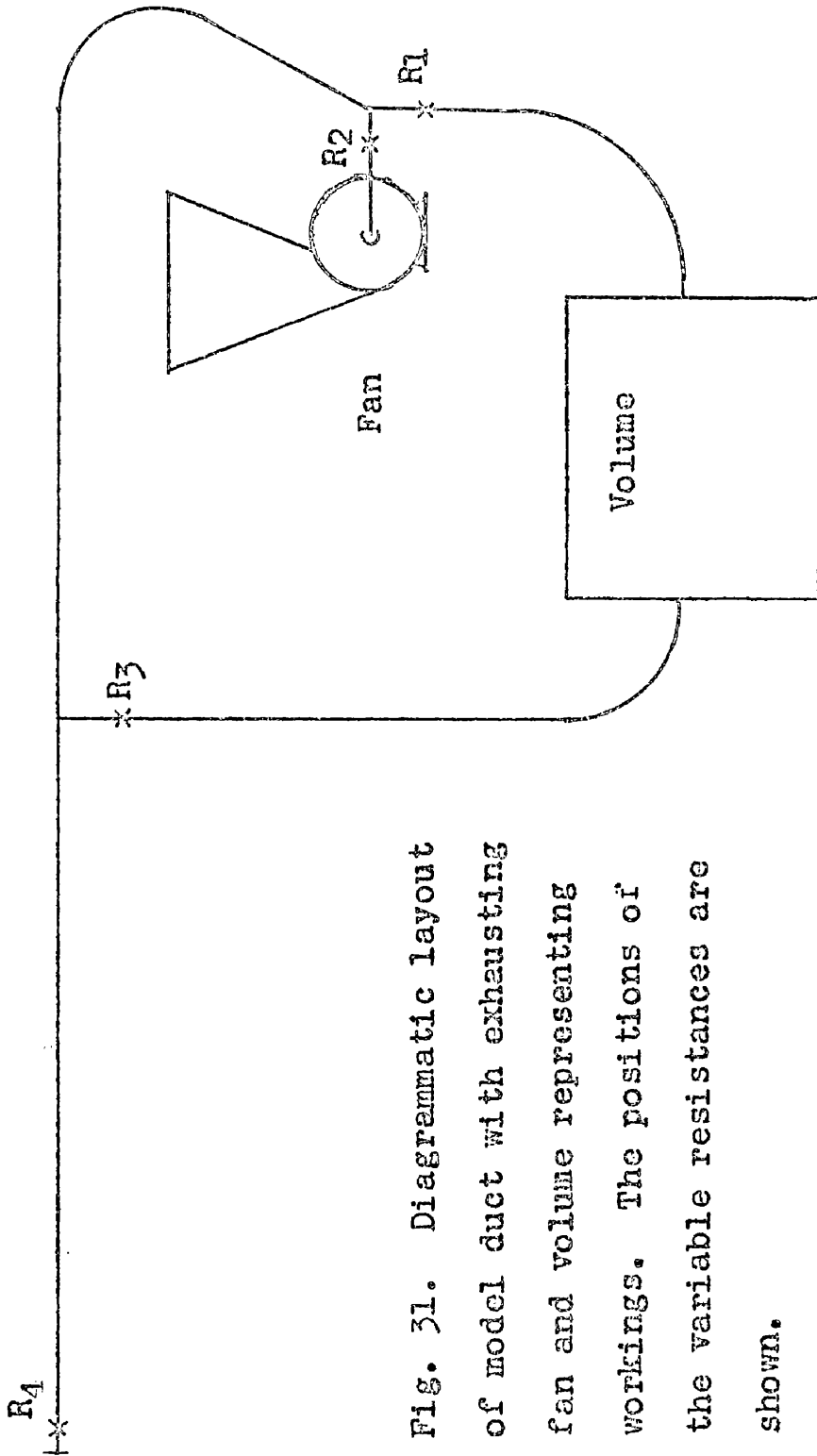


Fig. 31. Diagrammatic layout of model duct with exhausting fan and volume representing workings. The positions of the variable resistances are shown.

because the small holes of a pitot-static tube severely attenuated the fluctuating velocity as recorded by the pressure recorder. To record the velocity head both the micromanometer and the  $3\frac{1}{2}$  m.m. diaphragm were used depending on the range of pressure.

The variable resistances shown as  $R_1$ ,  $R_2$ ,  $R_3$  and  $R_4$  in Fig. 31 were simply sliding shutters which slid between the flanges of the ducting and which contained a series of holes, any of which could be inserted in the air stream. For the purpose of the qualitative tests only relative resistance was important and the holes were simply numbered 1 to 10 without attempting to determine the actual resistance. Table V gives the diameter of the hole corresponding to each number.

T A B L E V

Resistance Number	1	2	3	4	5	6	7	8	9	10
Diameter of hole in inches	$\frac{1}{4}$	$\frac{3}{8}$	$\frac{1}{2}$	$\frac{3}{4}$	1	$1\frac{1}{4}$	$1\frac{1}{2}$	2	$2\frac{1}{2}$	3

The resistances were always used at positions where the bore of the duct was  $3\frac{1}{2}$ ".

Two volumes were constructed in the form of rectangular boxes. The smaller was 5 feet long with a volume of 45 cu.ft. and the larger was 8 feet long with a volume of 250 cu.ft. The construction of the smaller box presented no difficulties and no leakage was detected. With the larger box, however, it was necessary to withstand a total

thrust of nearly 11 tons. The box, therefore, had to be braced internally with steel angle spaced one foot apart. Even with such support there was considerable movement of the box when the pressure was applied. All the joints were sealed with cellulose masking tape, but leakage occurred which could not be traced.

The usual method of tracing leaks is to pump smoke into the box and note where it emerges. This was not possible with this box as it was constructed to withstand only pressures less than atmospheric. Every joint was examined to see if it drew smoke into the box but no leak of any sort was detected. It was assumed that the resultant leakage was the sum of many small leaks which were difficult to seal. It was therefore necessary to consider the effect of this leakage at all times.

Resistance  $R_4$  represented the resistance of the downcast shaft above the inset and was kept at one value for all the tests. Resistance  $R_2$  represented the resistance of the workings at a lower level. For the purposes of similarity, therefore, it would need to be high, but if it is made high the air velocity in the shaft is severely reduced and the cage does not produce a large pressure drop. Tests were made both with  $R_2$  high ( = 7 ) and low ( = 0 ). Resistances  $R_1$  and  $R_3$  were placed on either side of the volume and represented the resistance of the workings which the volume simulated. This is one of the major points which makes complete similarity difficult or impossible. The resistance of the workings is spread throughout, and all the air is subjected to a friction effect. In

the model only the air flowing through these 'lumped' resistances is affected.

In the first tests  $R_2$  was set equal to zero so that a velocity of 90 to 100 ft/sec. was obtained in the shaft, with a consequent cage pressure drop of 8" W.G.  $R_1$  and  $R_3$  were made large so that the velocity through the volume would be low and any change would be more readily noticed. The 45 cu.ft. box was used and the velocity through it was about 30 ft/min.

The velocity head, measured in the roadway under these conditions as the cage passed the inset, is shown in Fig. 32. This shows a simple rapidly decaying oscillation with no nett movement of air. The effect of decreasing the resistance  $R_3$  is seen from Fig. 33 to be an increase in the steady velocity, the amplitude of oscillation and the decay time. Decreasing  $R_1$ , as is seen from Fig. 34, does not appear to affect the amplitude or decay time of the oscillation, but merely increases the steady flow velocity and the steady velocity fluctuations. These steady velocity fluctuations have a frequency of approximately 15 c/s and the cage would appear, in this case, merely to increase, temporarily, these oscillations. The distance, measured from the inset, through the box, to the fan, was 35 feet which could have a resonant frequency of 16 c/s. This assumes that the fan acts as an open end to the oscillations. Another, and perhaps more likely, form of oscillation is when the end of the box furthest from the inset acts as a closed end. This would have a fundamental frequency of 15 c/s. If a similar oscillation were produced under-

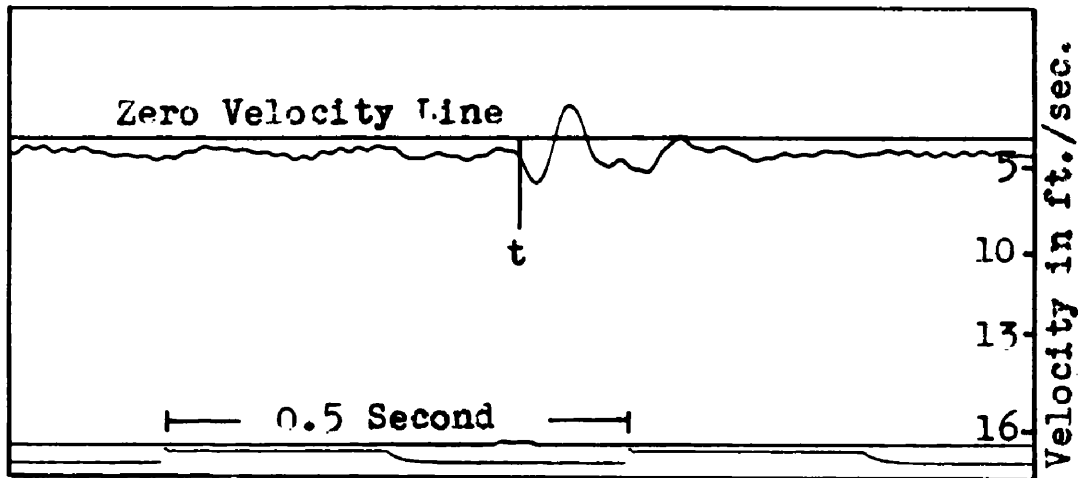


Fig. 32. Air velocity variation in the roadway. due to cage passing inset at time  $t$ .  $R_1=9$  and  $R_3=9$ . Attached volume 45 cu. ft.

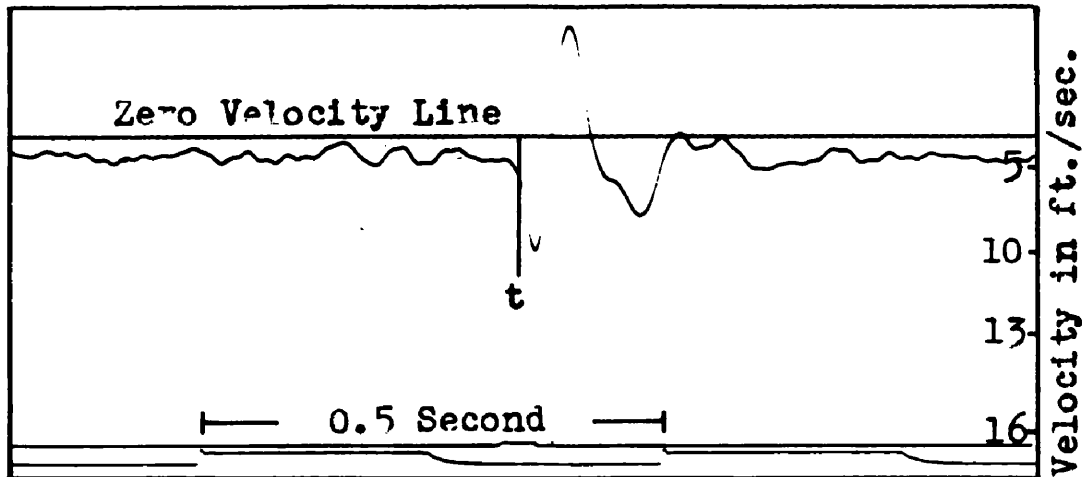


Fig. 33. Air velocity variation in the roadway. due to cage passing inset at time  $t$ .  $R_1=9$  and  $R_3=6$ . Attached volume 45 cu. ft.

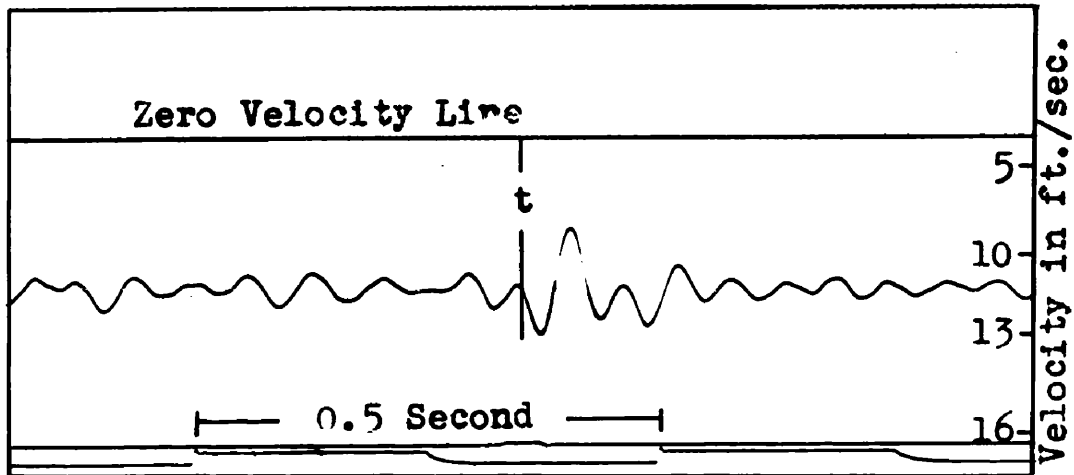


Fig. 34. Air velocity variation in the roadway, due to cage passing inset at time  $t$ .  $R_1=6$  and  $R_3=9$ . Attached volume 45 cu.ft.

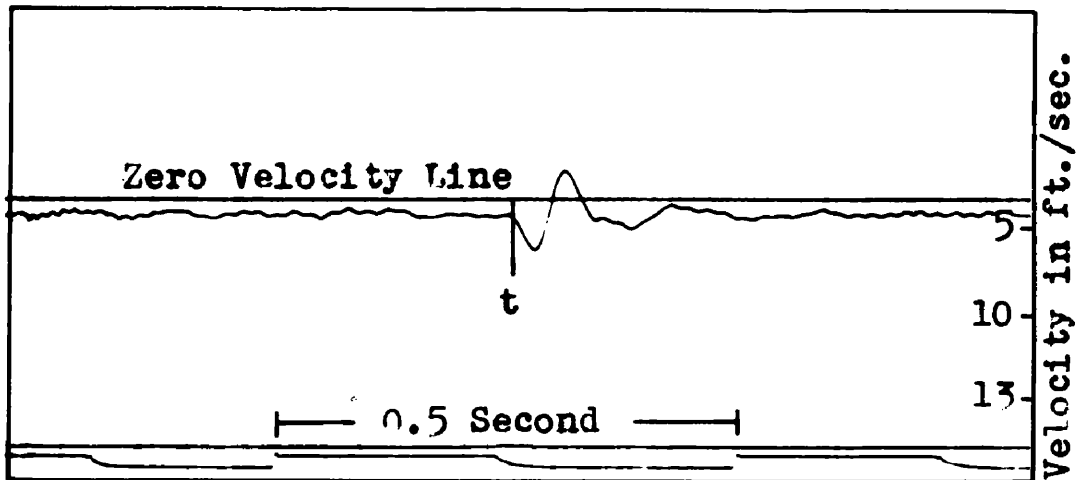


Fig. 35. Air velocity variation in the roadway, due to cage passing inset at time  $t$ .  $R_1=9$  and  $R_3=9$ . Attached volume 250 cu. ft.

ground it might have a period of 30 or 40 seconds which, although having no net effect, may reverse the flow of air for 15 to 20 seconds. The oscillations underground would tend to be more complicated with reflections from all obstructions and road junctions. It will be noticed in Fig. 33 that the reversed air flow is 2 to 3 times the magnitude of the steady flow.

No signs could be seen which might be attributed to the excess air, after expansion, flowing out. This excess air could have a maximum volume of 0.9 cu.ft. which, if it flowed out entirely at the inset, into the shaft, could reduce the normal velocity in the roadway by 1 ft/sec. for 14 seconds or 7 ft/sec. for 2 seconds etc. In order that any such effects would be clearly seen it was decided to replace the 45 cu.ft. box by one of 250 cu.ft. Fig. 35 shows the velocity head in the roadway recorded under similar conditions to that shown in Fig. 32. It will be seen that, although the 45 cu.ft. of volume has been replaced by 250 cu.ft., the waveforms are almost identical. This is due to the fact that changing the boxes only changed the length from the inset to the reflecting end of the box by 10%. The frequency of the oscillations, when the larger box is in circuit is measured as 16 c/s while the two modes of oscillation described before have frequencies of 15 c/s and 14 c/s respectively.

Decreasing the resistance  $R_3$ , as before, increases the amplitude, decay time and steady velocity. Again, as for the 45 cu. ft. box, decreasing resistance  $R_1$  merely increases the steady velocity.

Since the resonant frequency of the system is higher than the the frequency of the effect which is sought, the measuring system was severely damped by connecting a condenser across the galvanometer. In Fig. 36 is shown a velocity head recorded (a) without damping and (b) with the condenser in circuit. It will be seen that the high frequency component has been completely eliminated while the low frequency effect is not appreciably attenuated.

Using the recorder damped in this way, resistance  $R_2$  was set to zero and  $R_1$  and  $R_3$  were varied over wide ranges. When  $R_2$  is zero the cage pressure drop is the largest component of the pressure loss in the main shaft branch of the ventilating network. When, therefore, the cage moves from one side of the inset to the other the pressure difference between the ends of the branch containing the volume changes considerably. This means that the steady velocity before moving the cage is much different from that after the movement. It was found that the change in velocity due to this effect was superimposed on the change due to the expansion, so masking the effect completely. For this reason these results were considered inconclusive.

When  $R_2$  was made large ( = 7 ) the cage pressure drop then represented only a fraction of the total drop and the velocity in the inset with the cage upstream was not markedly different from that when the cage was downstream. This eliminated the masking effect described in the last paragraph and the tests were repeated.

Fig. 37 shows the effect of decreasing the resistance of  $R_3$

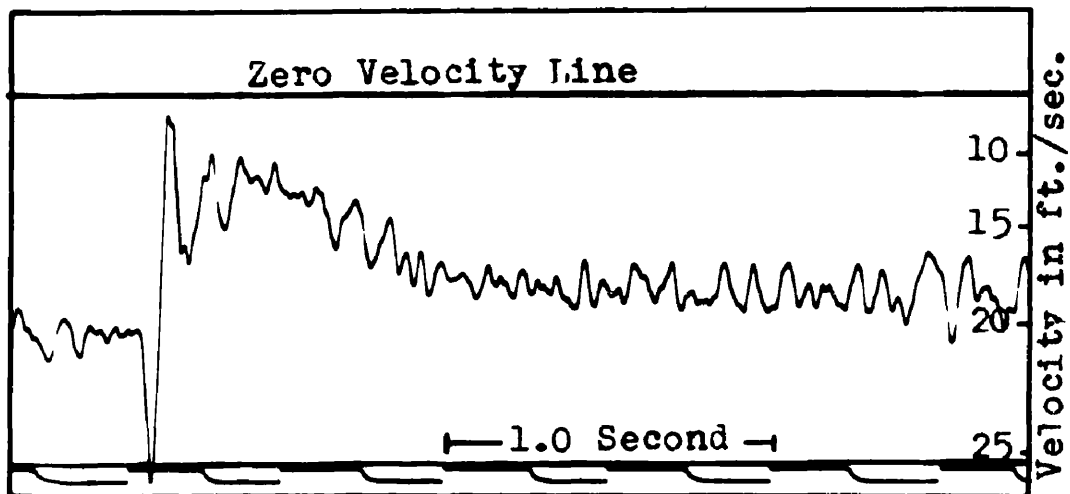


Fig. 36(a). Pressure recorded using the micromanometer with electrical damping out of circuit.

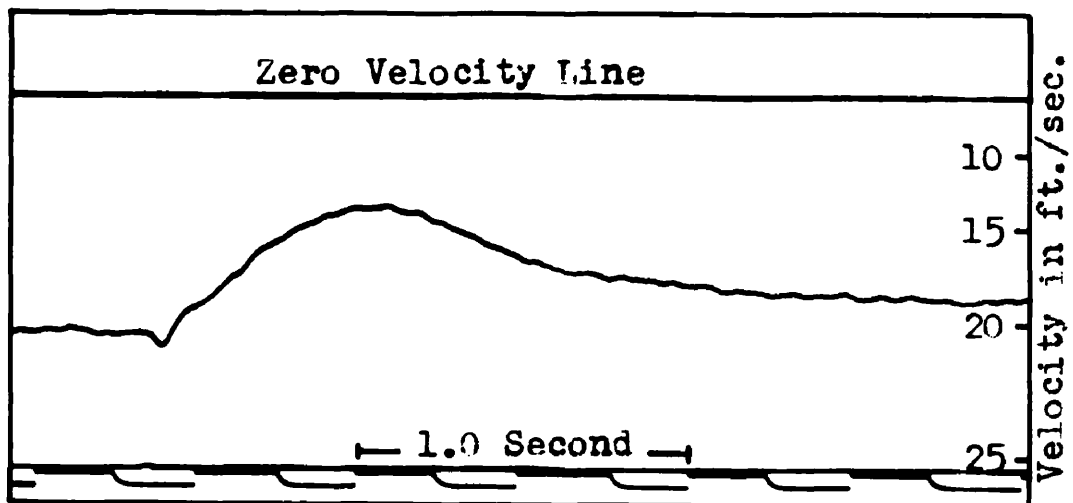


Fig. 36(b). Pressure as above recorded with electrical damping in circuit.

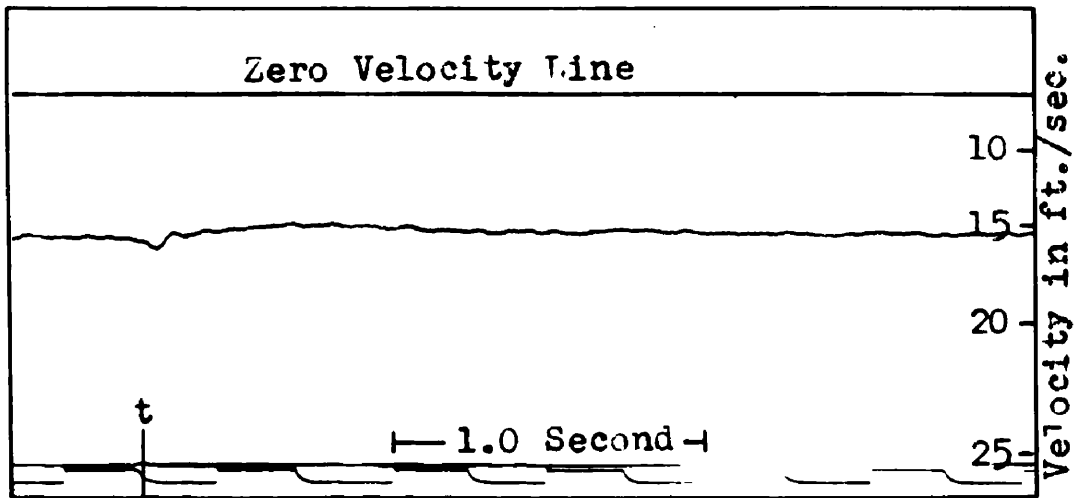


Fig. 37(a). Air velocity variation in the roadway. due to cage passing inset at time  $t$ .  $R_1=5$  and  $R_3=5$ .

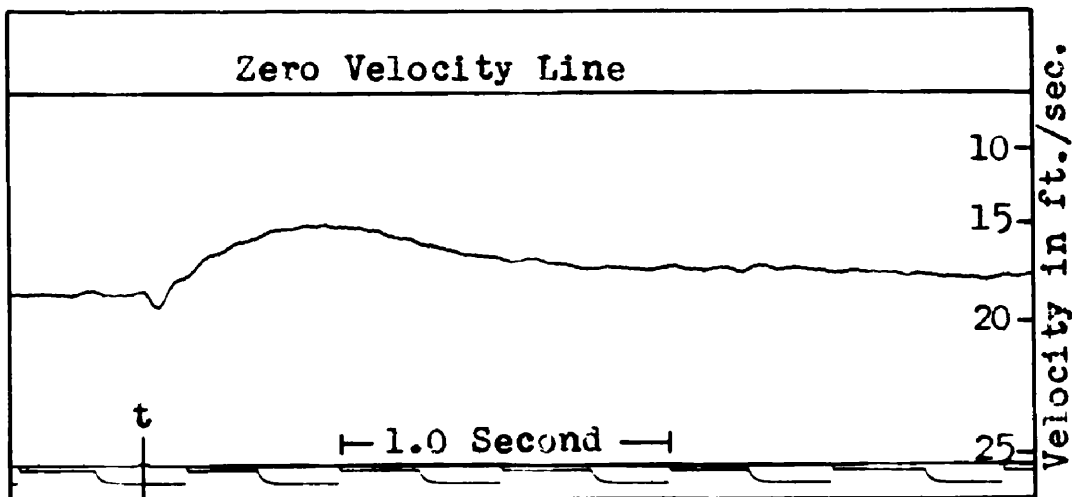


Fig. 37(b). Air velocity variation in the roadway. due to cage passing inset at time  $t$ .  $R_1=5$  and  $R_3=3$ .

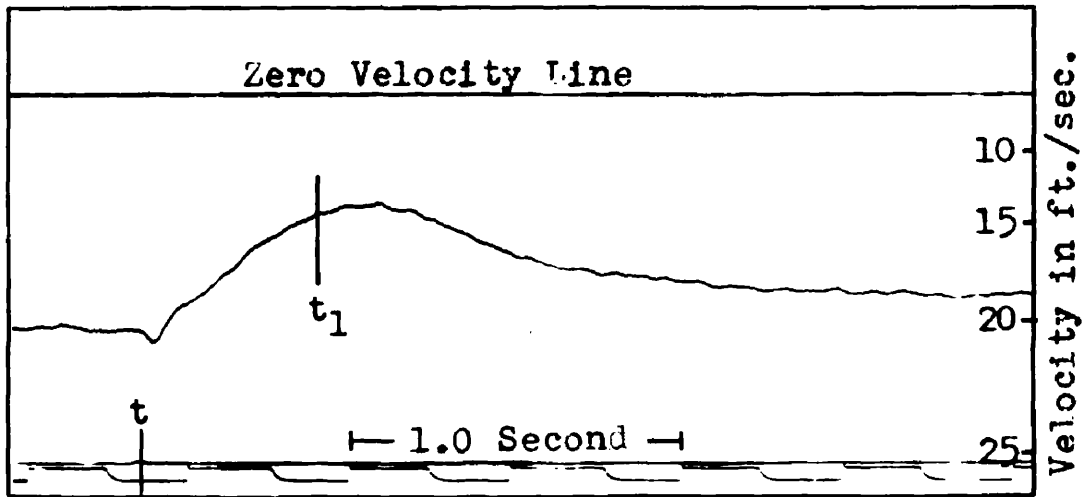


Fig. 37(c) and 38(a). Air velocity variation in the roadway. due to cage passing inset at time  $t$ .

$R_1=5$  and  $R_3=1$ . The cage stops travelling at time  $t_1$ .

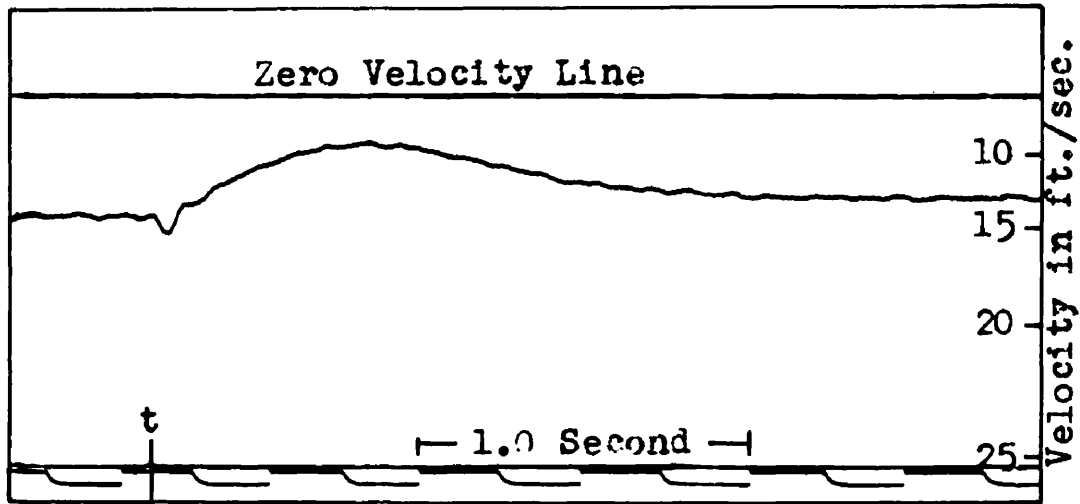


Fig. 38(b). Air velocity variation in the roadway, due to cage passing inset at time  $t$ .  $R_1=6$  and  $R_3=1$ .

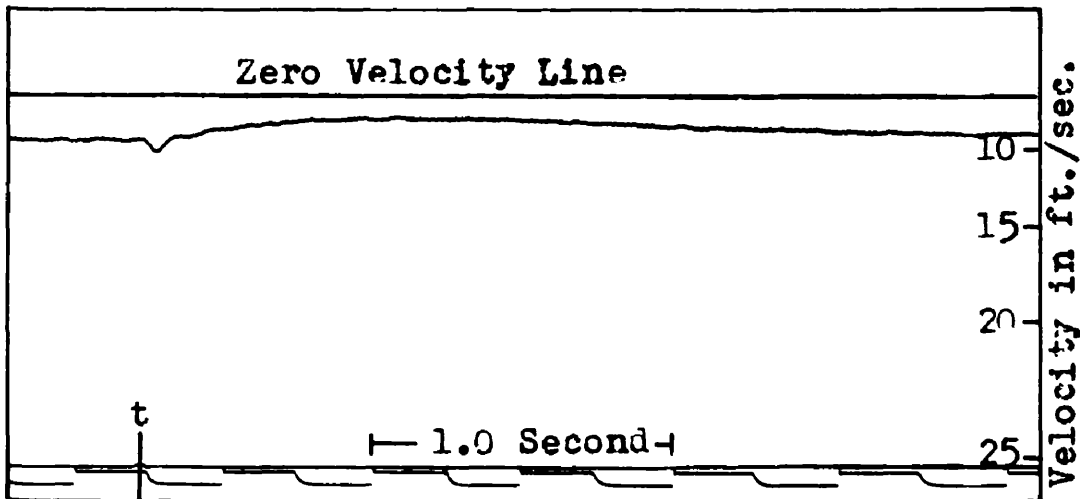


Fig. 38(c). Air velocity variation in the roadway, due to cage passing inset at time  $t$ .  $R_1=7$  and  $R_3=1$ .

while maintaining  $R_1$  at a value of 5. It can be seen that the steady velocity is increased, together with the disturbance. For these tests the cage speed was 12 ft/sec. and the air velocity in the shaft was approximately 15 ft/sec. which would mean that the moving cage produced a pressure drop of 0.17" W.G. and the stationary cage produced a pressure drop of 0.06" W.G. If the volume had been subjected to these pressure drops for a sufficient length of time it would have meant expansions of 0.10 and 0.04 cu.ft. respectively.

By integrating the area under the graphs in Fig. 37 we can calculate the volume of air which must have been produced by expansion. The figures are  $\leq$  0.01, 0.1, 0.2 cu.ft. for Fig. 37 (a), (b) and (c) respectively. These figures would suggest that some other factor is involved and leakage of air into the volume could produce this result. If the cage were moved from one side of the inset to the other, the static pressure in the volume would be changed and so, therefore, would the rate of leakage into the volume. This change of rate would only change the steady velocity conditions but the fact that the cage lowered the static pressure by 0.17" W.G. and then settled at a value only 0.06" W.G. lower than the original value would mean that additional leakage would be drawn into the box which would be redundant when the pressure settled at the new value. It may be this additional air which is upsetting the calculations.

In Fig. 38 we see the effect of increasing the resistance of  $R_1$  when  $R_3 = 1$ . This is simply to decrease the steady velocity and the disturbance. We notice, here, the difference between the

effect of  $R_1$  on this disturbance and its effect on the oscillation first investigated. In the first case  $R_1$  had no effect, whereas in this case the effect is reduced by increasing  $R_1$ .

In Fig. 33 (a) the instant when the cage stopped has been marked. The velocity stops decreasing very soon after this point and it is not possible, from these results, to tell how much the shape of the curve is due to the combination of volume shape and resistance or how much it might be due to the cage velocity.

It would be possible, with the same length of shaft, to allow the cage to run up to three times the distance beyond the inset at present run. This would require an automatic cage controlling mechanism since the cage would be running for only an additional 0.7 seconds. Alternatively the sections of the shaft could be rearranged to situate the inset near to one end.

From the limited scope of these tests few conclusions can be drawn but we may conclude that until all leakage has been eliminated no accurate measurements can be made and certain results may be quite invalid.

From the few results to which importance may be attached we see that the resistance between the pressure disturbance and the volume and the resistance between the volume and the fan both affect the velocity disturbance. These resistances are lumped elements simulating the distributed resistance in actual practice. It seems unlikely that conclusions drawn with the lumped resistances could be related in any way to the effect of distributed resistance. Since the distribution of the resistance

may have a marked effect on the velocity disturbance some method of investigating it should be sought.

## Chapter 9

### THEORETICAL PREDICTION OF VELOCITY DISTURBANCES —

#### METHOD 1

The effect with which we are concerned is the behaviour of a gas under the action of a varying pressure. No matter how complex this behaviour may be it can be described by one or more mathematical equations. This method of description has the advantage that when the correct equations have been found the description is very simply adapted to any set of conditions and the behaviour of the air at any time can be predicted with certainty. It has the disadvantages that it may be difficult to determine the correct equations and, when they have been determined, extracting the data from them in a useful form may be very tedious. In this case it was felt that little difficulty would be met in determining the necessary equations since procedures involving fluid flow and gas dynamics have been well established.

We are concerned with the pressure ( $p$ ), the specific volume or the density ( $w$ ) and the velocity ( $u$ ) of the gas. When wall friction is considered the heat produced alters the temperature ( $\theta$ ) and the specific entropy ( $s$ ) of the gas. We have five dependent variables

$p$ ,  $w$ ,  $u$ ,  $\phi$  and  $s$ , together with two independent variables  $x$  and  $t$  so that five equations are required. These are,

The Continuity Equation,

$$M \cdot \frac{\partial w}{\partial t} + \frac{\partial (w u M)}{\partial x} = 0 \quad \text{Equn. 2}$$

The Momentum Equation,

$$\frac{\partial u}{\partial t} + u \cdot \frac{\partial u}{\partial x} = -\frac{1}{w} \frac{\partial p}{\partial x} - \frac{4fu^2}{2d} \quad \text{Equn. 3}$$

The Equation of State,

$$p = w R \phi \quad \text{Equn. 4}$$

The Entropy conditions,

$$\frac{\partial s}{\partial t} + u \cdot \frac{\partial s}{\partial x} = \frac{4fu^3}{2d g J \phi} \quad \text{Equn. 5}$$

A relation between entropy, pressure and temperature given by,

$$s - s_1 = C_p \log_e \frac{\phi}{\phi_1} - \frac{R}{gJ} \log_e \frac{p}{p_1} \quad \text{Equn. 6}$$

The derivation of these equations will be found in most text books on sound or gas dynamics such as references 6, 7 and 8. They are also derived in Appendix A.

These equations are similar to those used in the theory of sound. However, in sound, the velocity  $u$  is generally very small -- Stewart and Lindsay (Ref. 13) mention velocities of the order of  $10^{-2}$  to  $10^{-3}$  ft/sec. -- and the term  $\frac{\partial u}{\partial x}$  is also small so that, in comparison with  $\frac{\partial u}{\partial t}$ ,  $u^2$  and  $u \cdot \frac{\partial u}{\partial x}$  may be neglected. This

implies that frictional effects may be neglected. It is found experimentally that the heat produced due to the compressions in sound waves does not have time to be conducted away, so that the process, other than at very high frequencies is isentropic. This allows equations 4, 5 and 6 to be replaced by the single equation,

$$p = K v^k \quad \text{Equn. 7}$$

This simplification means that in the theory of sound we are dealing with linear partial differential equations and their solution is straightforward. However, in the case being considered it was felt that the effects of friction could not be ignored, thus implying that  $u$  was not a small quantity. This, in turn, prevents our neglecting terms like  $u \cdot \frac{\partial u}{\partial x}$  so that we are now dealing with non-linear partial differential equations.

A method of solving these equations has been developed in recent years from the original method of Riemann (ref. 10). The original method has been improved along several different lines and the version described by Rudinger (ref. 8) has been used here. This is given in Appendix B.

Five factors were thought to affect the behaviour of the air near the source of pressure disturbance and each was considered in detail. The factors are,

- 1) The volume of the air in the workings.
- 2) The shape of the workings,
- 3) The friction factor of the workings.

- 4) The magnitude of the applied pressure
- 5) The shape of the applied pressure waveform.

1) The volume of the air in the workings

In the report concerning the disturbance in colliery R the estimated volume was  $10^6$  cu.ft. The volume indicated by the results was  $10^7$  cu.ft. When determining the effect on the airflow of different volumes, therefore, it was volumes of this order which were considered.

2) The shape of the workings

In this theoretical treatment the air in the workings was represented by one large volume which was, for convenience, circular at every section. In a mine, as we proceed inbye, the number of parallel roadways increases and so, therefore, does the total cross sectional area. It is the rate of increase of the cross section, as we move further from the source, which is thought to influence the behaviour of air. This is deduced from the fact that the front of the pressure disturbance will proceed inbye at a constant speed - the speed of sound. It will reduce the pressure, and hence increase the volume, of each section of air as it reaches it. The rate of increase in volume at any instant will be proportional to the cross sectional area at the wave front. Hence the rate at which excess air must flow out of the workings will be affected by the area.

Two cases have been dealt with in this treatment. The first

The first is where the diameter of the theoretical model increases linearly as we proceed inbye until it reaches a maximum at the point furthest inbye and then decreases linearly to the end of the volume representing the upcast shaft. In the second case it is the square root of the diameter which increases linearly. If the exact law were known in any particular case it is easily applied.

### 3) The friction factor of the workings

In the case of the friction factor there are really two variables. The first is the friction factor itself, the effect of variation in which is easily determined. If the value in any case being investigated is known it may be used in the calculation.

The second variable is the distribution of the friction throughout the workings. The effect of changing the distribution is determined and the standard distribution, used when studying other variables is obtained from the assumption that the rate of pressure drop from the downcast to the upcast shaft is constant. Fig. 39 shows the rate of pressure drop for a typical horizon mine as quoted by Fritzsche and Potts (ref. 11). Fig. 40 shows the rate of pressure drop as plotted from a pressure survey by Cooke and Statham (ref. 12). Both these examples indicate that a constant rate of pressure loss is a reasonable assumption.

The rate of pressure loss per unit length is given by

$$\frac{dp}{dl} = \frac{4fu^2}{2d}$$

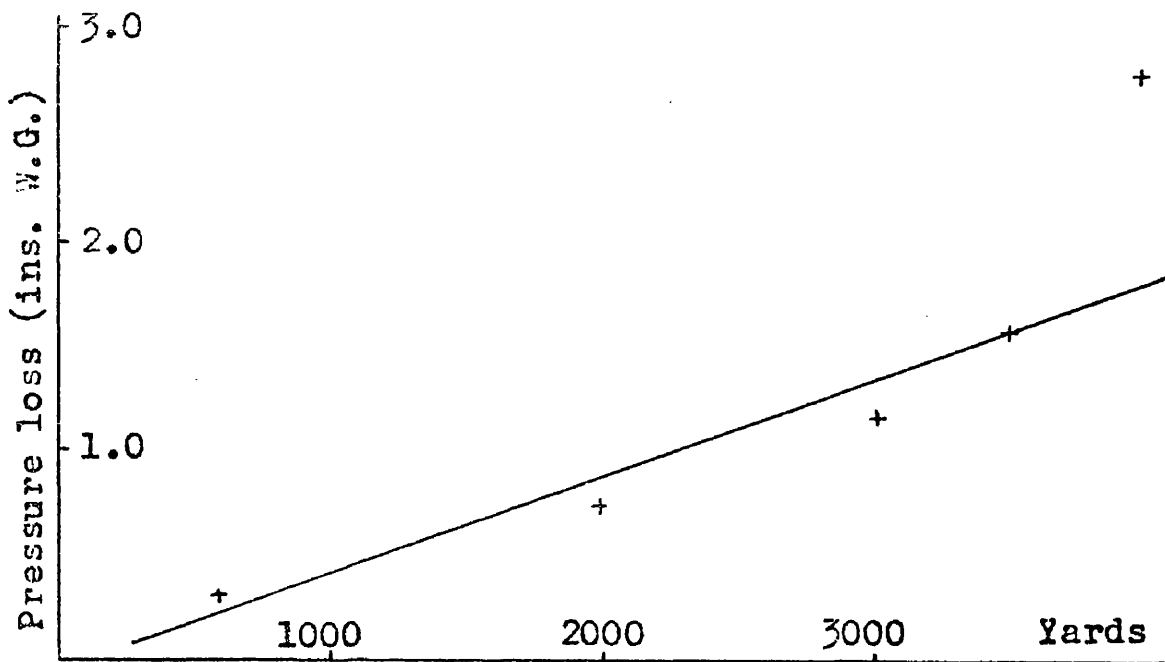


Fig. 39. Rate of pressure loss with distance underground ( Fritzsche and Potts, ref. 11 ).

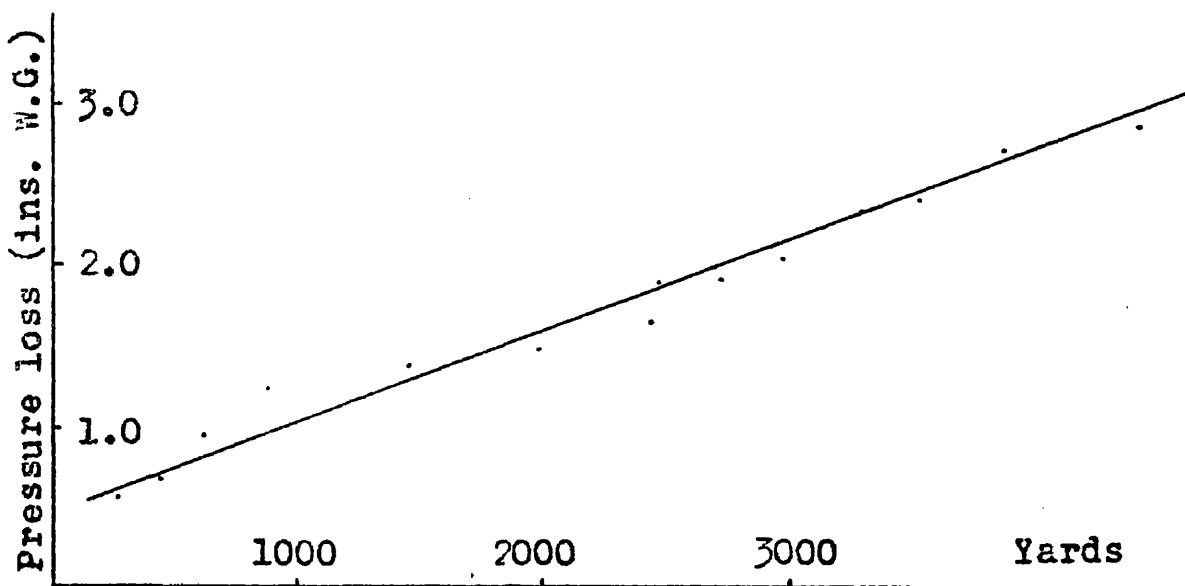


Fig. 40. Rate of pressure loss with distance underground ( Cooke and Statham, ref. 12 ).

If we assume that this is constant we have

$$u \propto \frac{1}{A} \propto \frac{1}{d^2}$$

$$\therefore f \propto d^5$$

The power to which  $d$  is raised may be increased or decreased to allow for a more or less rapid loss of pressure, respectively, as we proceed inbye.

4) The magnitude of the applied pressure.

This is the pressure drop due to the cage and was, in the case of colliery R, approximately 1" W.G. The effect of varying the magnitude around pressures of this order has been determined.

5) The shape of the applied pressure waveform.

This may be either a sudden drop, as in the case of a cage passing an inset at high speed, or a pressure drop which increases slowly as the cage leaves the inset and then decreases again as the cage slows down at the surface. Both cases have been investigated and the rate of increase and decrease in the second case has been varied.

Several other factors, such as the effect of heat in deep mines, may affect the behaviour of the gas to a marked extent. This, and other factors, could be taken into account but those described were the only ones considered.

## Results

The results illustrated in Figs. 41 to 48 have been obtained using the theory described in this chapter and the computation was done on an English Electric Dauce electronic digital computer. The output provided a complete description of the behaviour of the air at any point in the workings at any instant of time. The only information which has been used here is the velocity of the air flowing out of the volume subsequent to the change in pressure.

The behaviour of the air at colliery R suggested that the return end of the workings was acting as a closed end to the pressure pulses. The first method of calculation, drawn up for the computer, worked on this assumption. It was intended to develop the work to cover various end conditions but this was not possible, although the results include an example in which the return end has been treated as completely open. Since, in the case of the closed end, no steady velocity could be flowing, the results have only a qualitative significance, although the extent to which they may be used quantitatively is discussed.

In order to study the effect of each factor separately, a set of standard conditions has been assumed. When any one factor is being varied the others have this standard value. The factors investigated have been discussed and Table VI lists these factors together with the standard conditions.

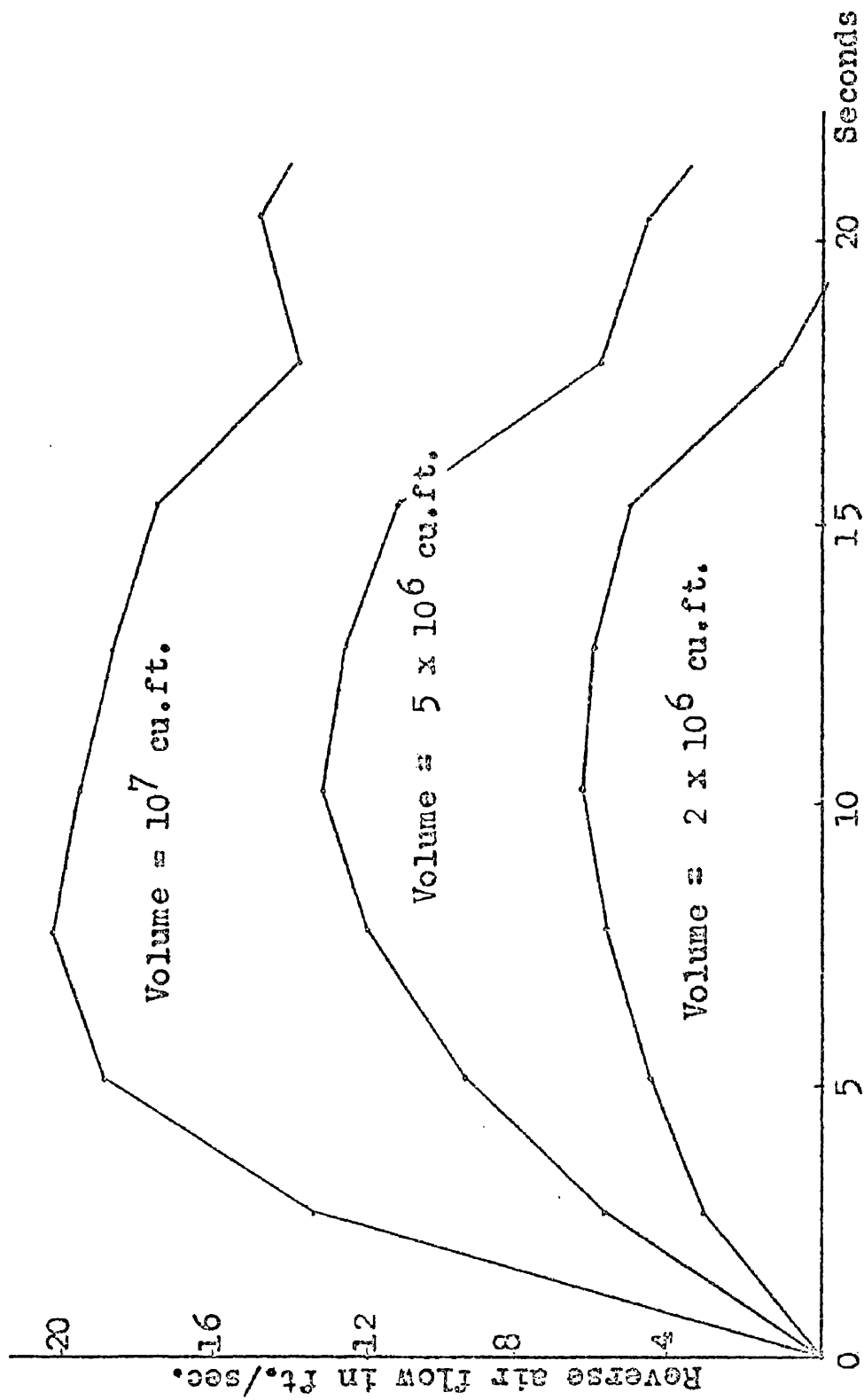


Fig. 41. The effect, on the ventilation disturbance, of changing the volume of the workings, other conditions being standard.

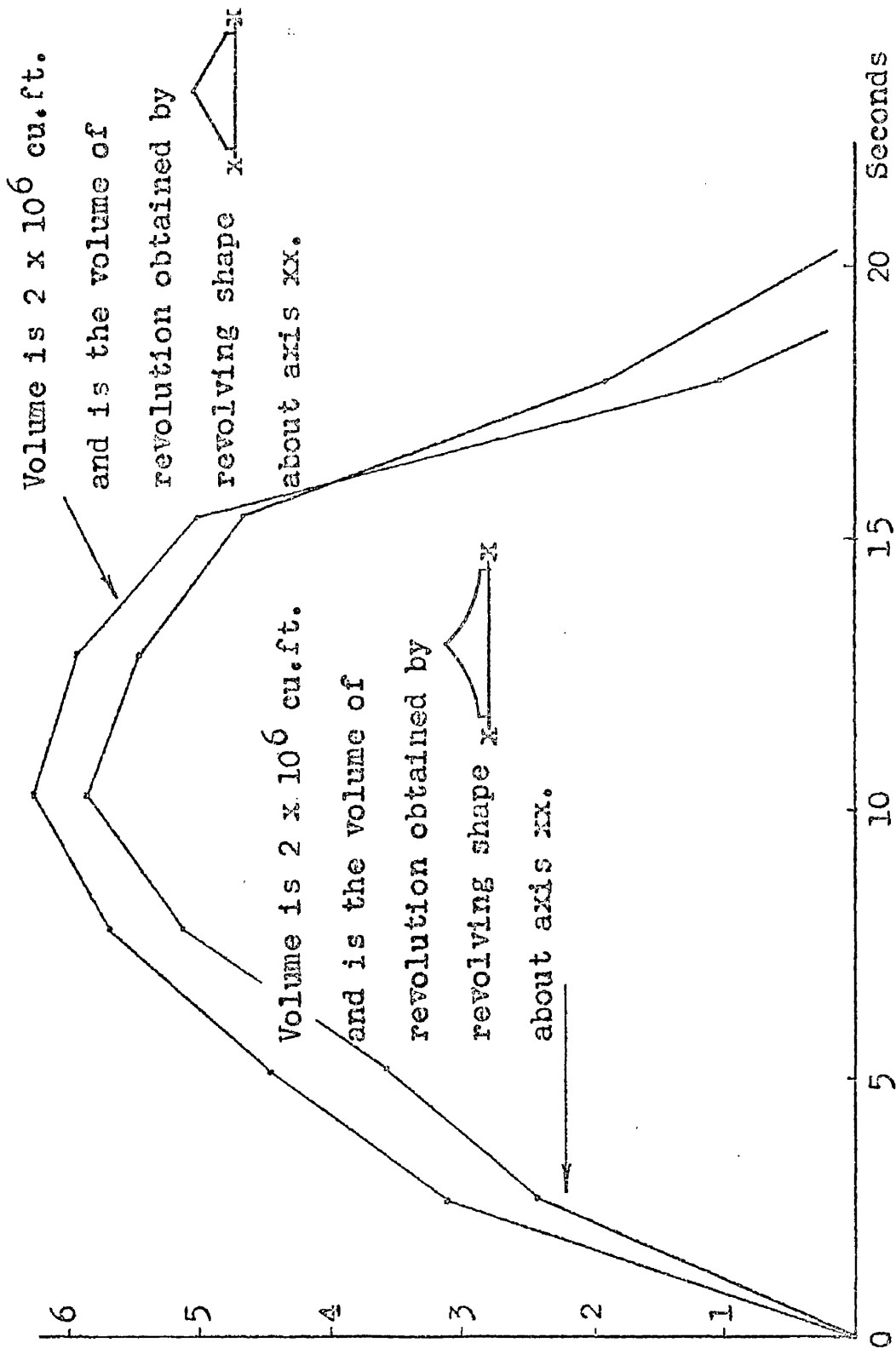


Fig. 42. The effect, on the ventilation disturbance, of changing the shape of the volume, other conditions being standard.

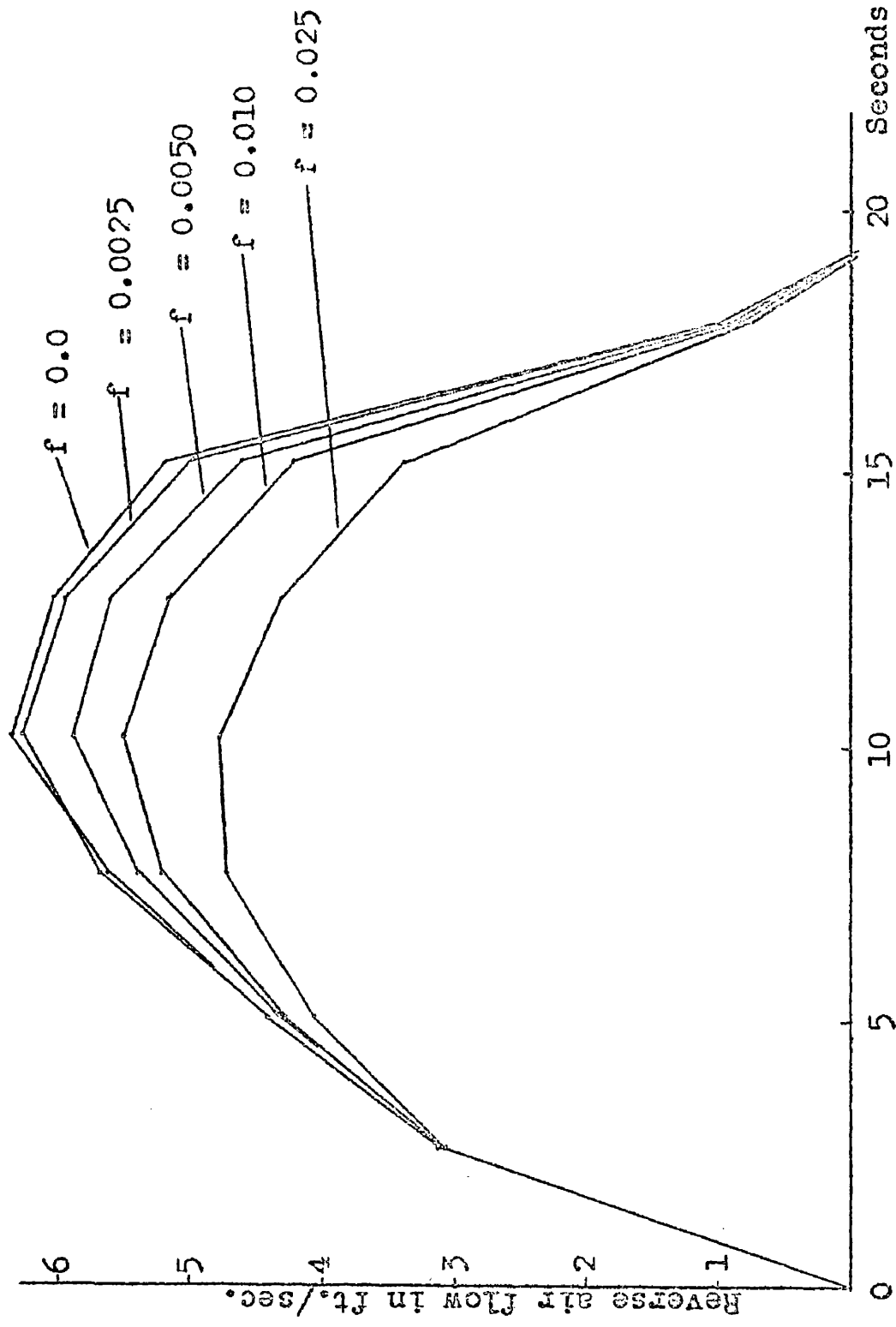


Fig. 43. The effect, on the ventilation disturbance, of changing the friction factor, other conditions being standard.

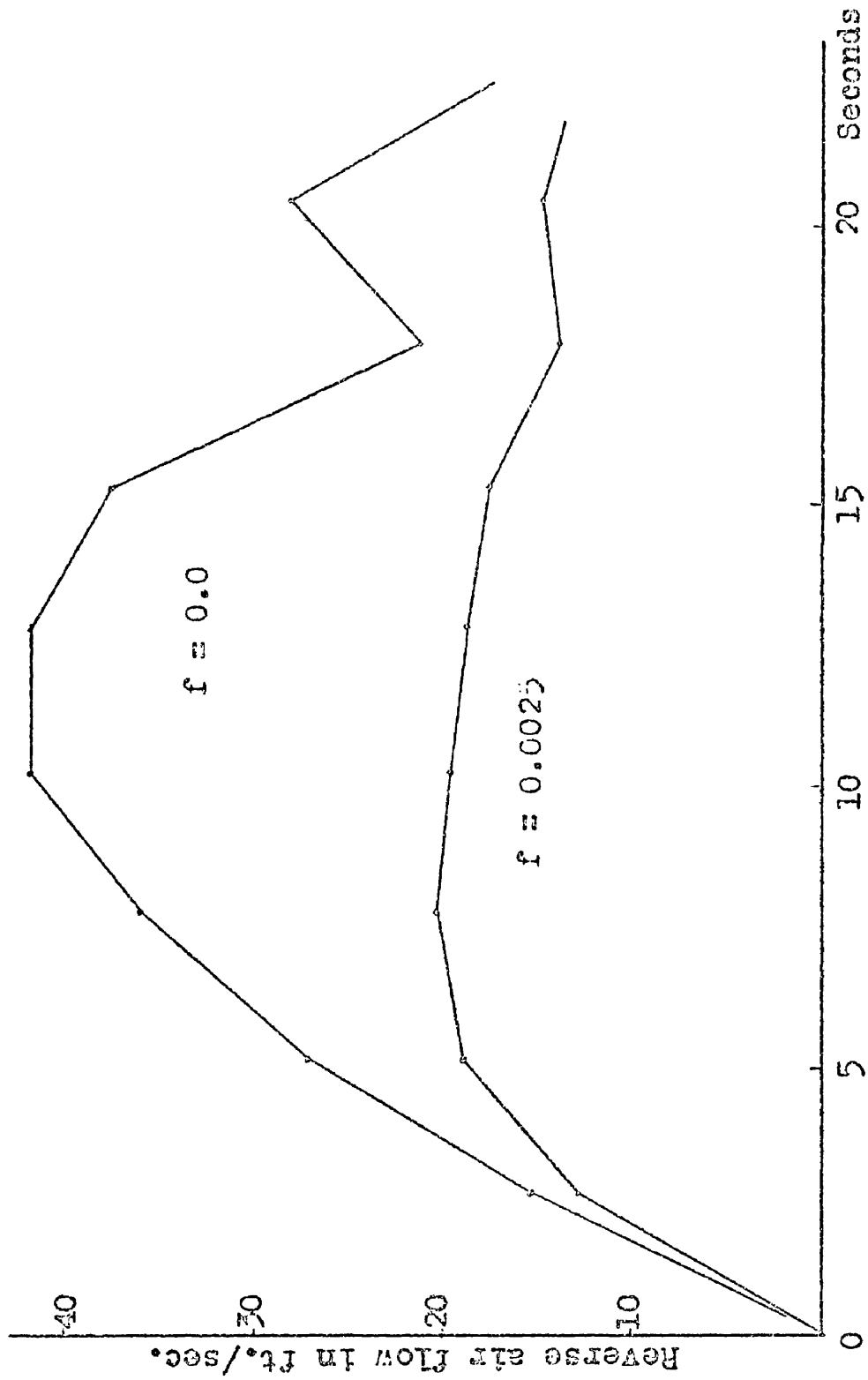


Fig. 44. The effect, on the ventilation disturbance, of changing the friction factor when the volume is 107 cu.ft., other conditions being standard.

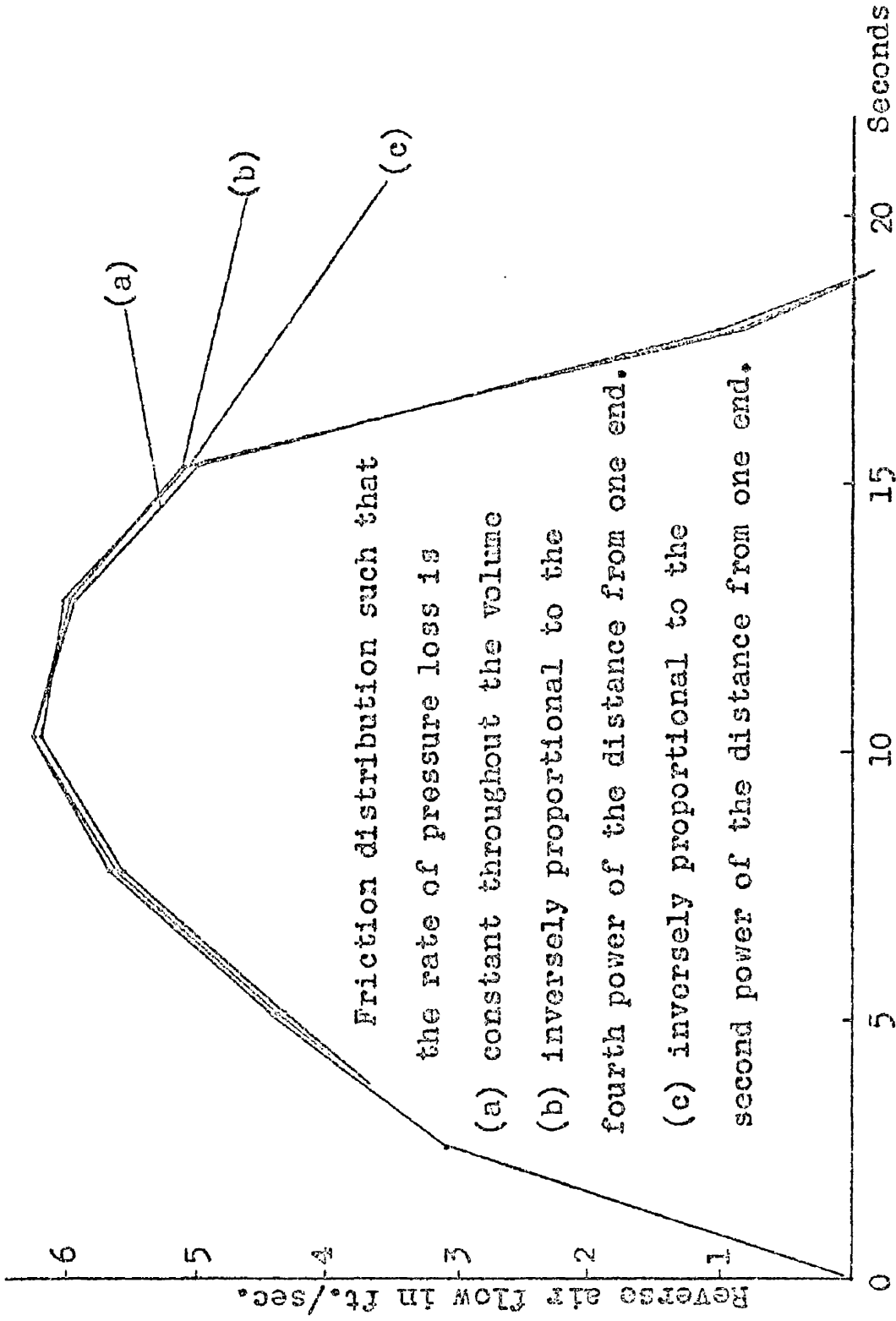


Fig. 45. The effect on the ventilation disturbance of changing the friction distribution, other conditions being standard.

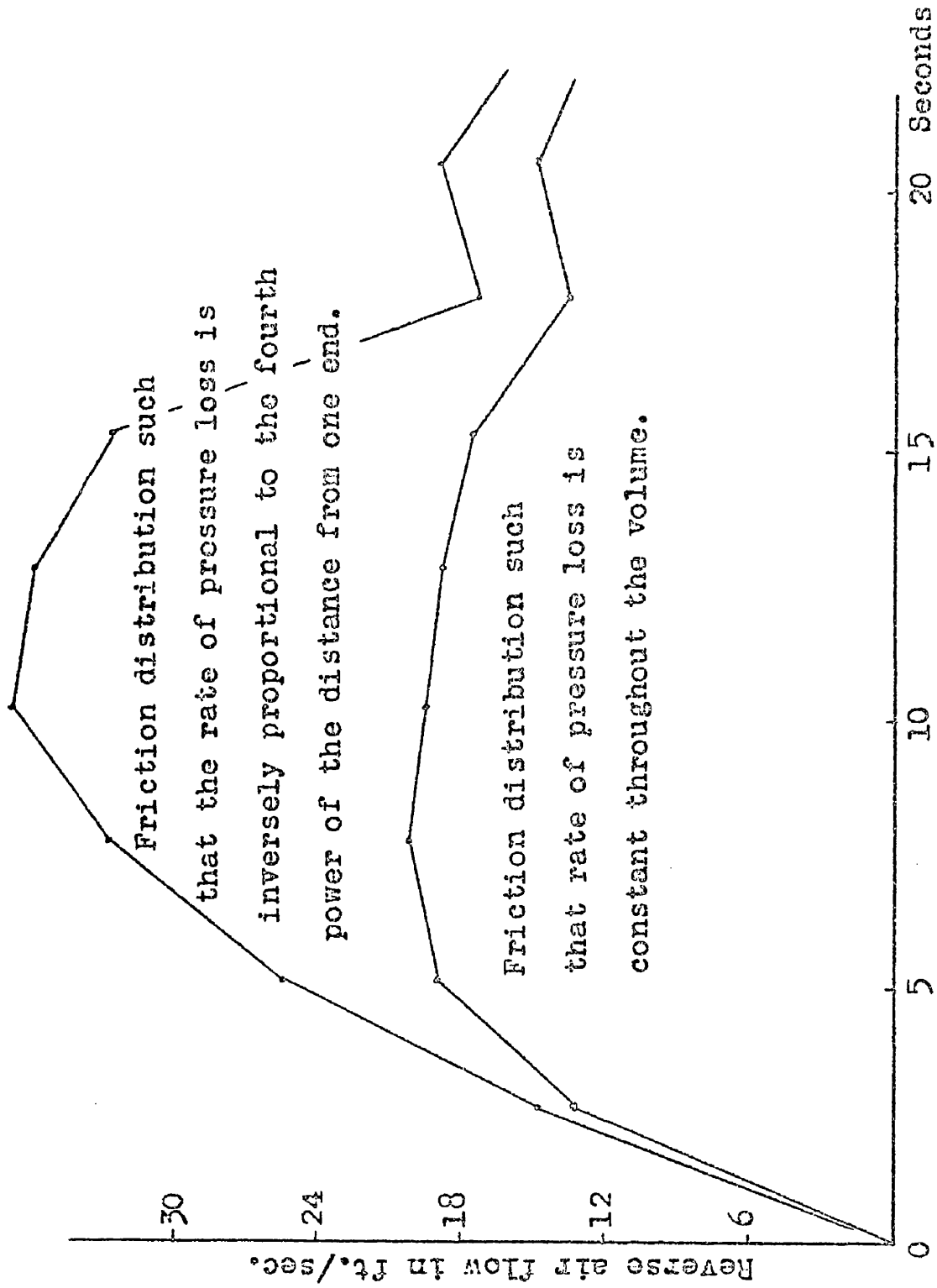


FIG. 46. The effect, on the ventilation disturbance, of changing the friction distribution when the volume is 10<sup>7</sup> cu.ft., other conditions being standard.

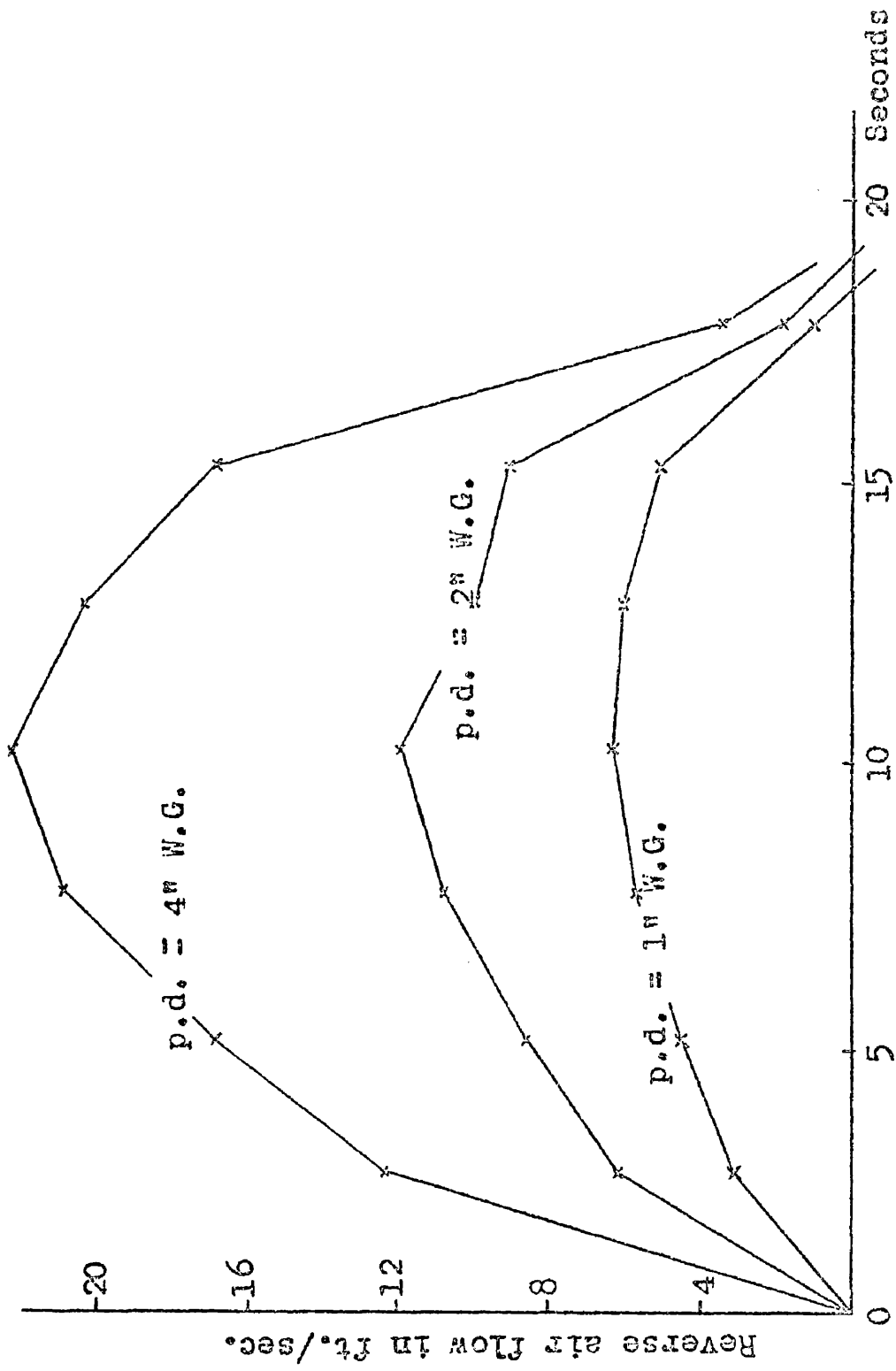


Fig. 47. The effect, on the ventilation disturbance, of changing the magnitude of the applied pressure drop, other conditions being standard.

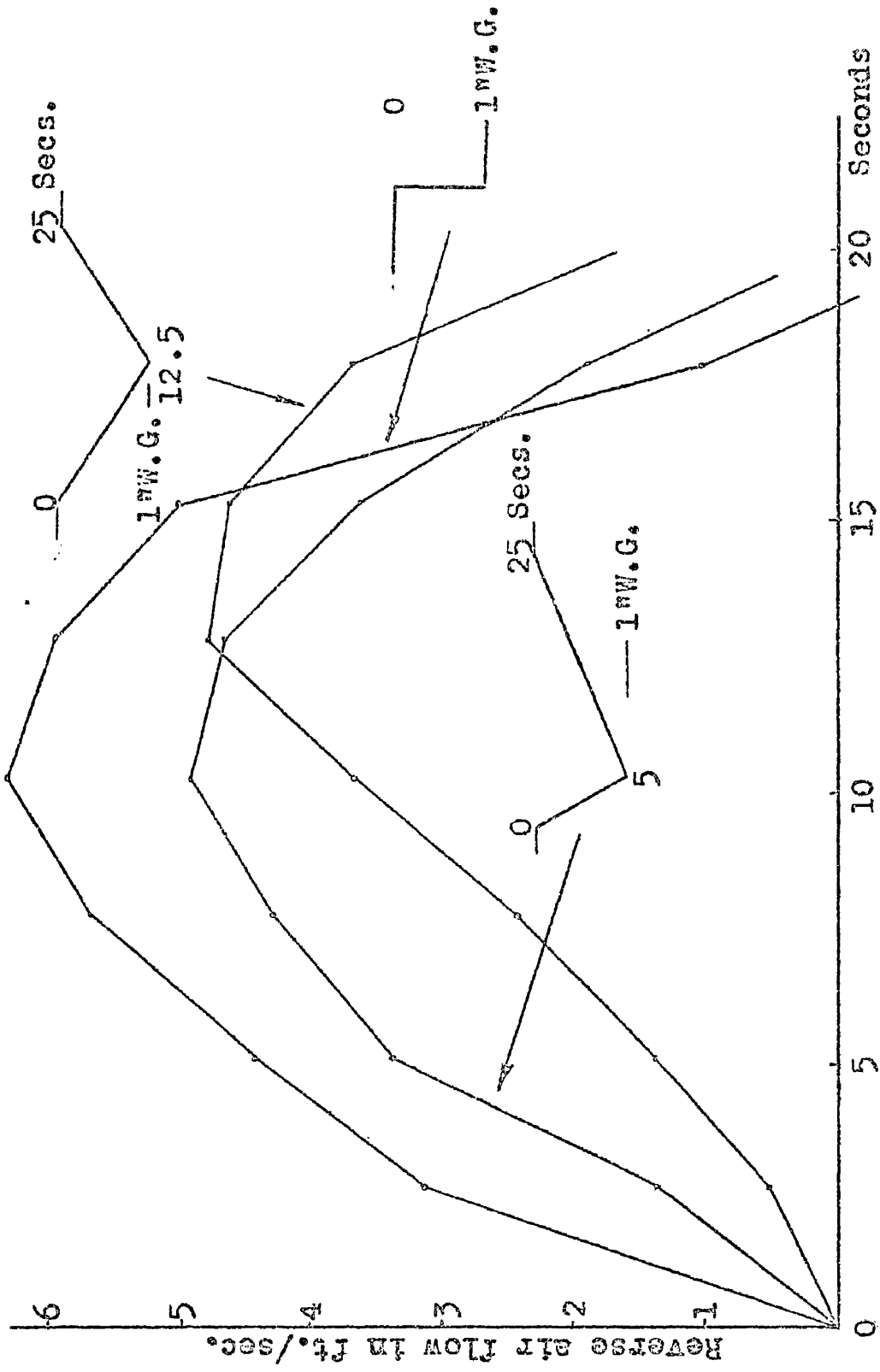


Fig. 48. The effect, on the ventilation disturbance, of changing the applied pressure waveform, other conditions being standard.

T A B L E VI

Variable Factor	Standard-conditions
Volume of workings	$2 \times 10^6$ cu.ft.
Shape of workings	Circular at every section, 10' in diameter increasing linearly to 21.2' in diameter at 5,000' then decreasing linearly to 10' in diameter at 10,000'.
Friction factor	$f = 0.0025$
Distribution of friction	$\frac{dp}{dl}$ is constant, therefore $f \propto d^5$
Magnitude of applied pressure drop	1" W.G.
Shape of pressure waveform	<p>401" W.G.</p>  <p>400" W.G.</p> <p><math>t = 0</math></p>

Volume of Workings

The effect of altering the volume is shown in Fig. 41. It will

be seen that increasing the volume increases the velocity very considerably and a volume of  $10^7$  cu.ft. can produce a very large velocity flow out of the workings into the downcast shaft. It should, however, be pointed out that the standard friction factor of  $f = 0.0025$  is rather low and a more realistic figure may reduce the effect of increasing the volume.

### Shape of Volume

In Fig. 42 the effect of changing the shape of the volume has been shown. In one case it was assumed that the diameter increased linearly to a maximum at the centre and in the other case it was the square root of the diameter which increased linearly. This difference in shape is not large but the effect produced by it is obvious. It seems probable that a greater change of shape will have a correspondingly greater effect on the velocity.

### Friction Factor

The effect of this factor is shown in Fig. 43. The maximum factor,  $f = 0.025$ , is a reasonably large friction factor and, in a new mine, we may expect a lower figure. It can be seen that although a high friction factor reduces the velocity produced, the friction factor is not one of the more important factors. Fig. 43 shows the effect of the friction factor in the standard volume of  $2 \times 10^6$  cu.ft. In Fig. 44 is shown the effect of a low friction factor in the case of a volume of  $10^7$  cu.ft. It can be seen that

the effect is very much more marked and we may conclude that the influence of the friction factor depends to a large extent on the velocity of the air.

### Distribution of Friction

It was shown earlier in this chapter that the pressure drop throughout a mine is reasonably constant. This is simulated in this calculation by having a friction factor which is proportional to the fifth power of the diameter. In Fig. 45 this has been compared with the case where the friction factor is proportional to the first power of the diameter. The case of the friction factor proportional to the diameter is rather meaningless in practice but it does illustrate the effect of changing the distribution of friction. As can be seen no change of any importance is noticed.

In Fig. 46 the same conditions have been applied to a volume of  $10^7$  cu.ft. Here we see a very marked change of velocity. Hence it would seem that, as for the friction factor, the effect of the friction distribution depends to a very large extent on the velocity of the air flowing.

### Magnitude of Pressure Drop

The effect of this factor is shown in Fig. 47. It can be seen that the magnitude of the velocity bears an almost linear relationship to the pressure drop applied. This is not unexpected and may be very serious where high shaft air velocities produce a

large pressure drop past a large cage.

### Shape of Pressure Waveform

In all the results so far a sudden pressure drop has been assumed but in Fig. 48 is shown the effect of different pressure waveforms. We see that the sudden drop produces the greatest velocity of outflowing air with the slowly applied pressure drops producing a lower maximum velocity and a slower rate of rise to this maximum. The more slowly the pressure drop is applied the slower is the rate of rise to the maximum.

In all the results discussed here the diameter of the inset has been taken, conveniently, as 10 feet. It is probable that this should be higher - perhaps 50% higher - so that the area might be twice that used in these calculations. This means that the velocity, as shown, would be halved, producing a less serious disturbance.

### The Upcast Shaft as an Open End

It was not possible to examine fully the condition where the upcast shaft acts as an open end, but one example has been worked out. In this case the fan end is assumed to act as a completely open end, that is, the reflected pressure pulse is opposite in sign to the incident pulse. In Fig. 49 is shown the variation of the air flowing in the inset under the standard conditions in Table VI except that the friction factor in this case is zero and a steady velocity of 10 ft/sec. at a diameter of 10 feet flows through the volume from the

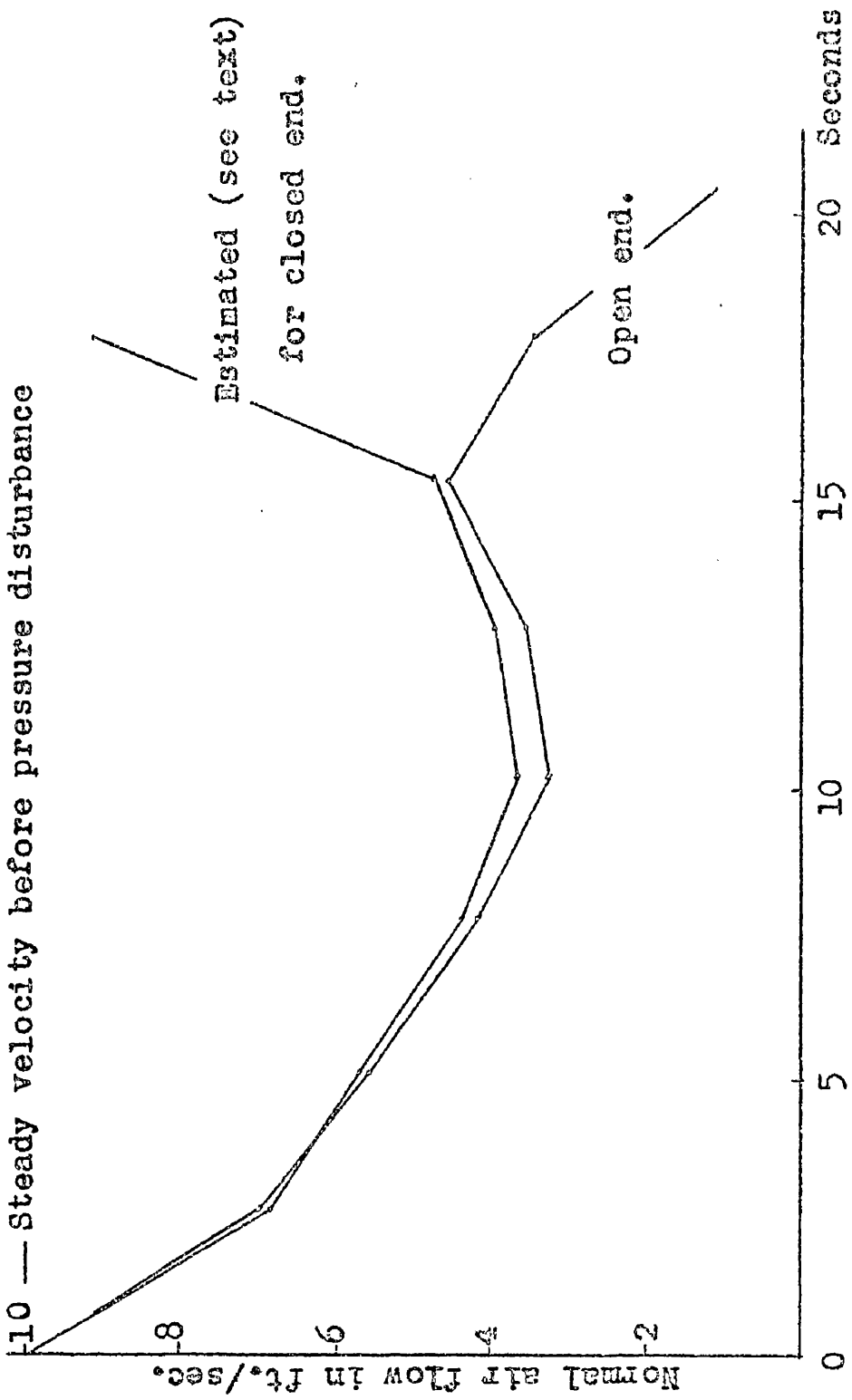


FIG. 49. The effect, on the ventilation disturbance, of different end conditions ( that is, the end other than that to which the pressure is applied ) other conditions being standard.

downcast to the upcast end. Also shown is the graph obtained by subtracting the outflow of air under these conditions, but with a closed end, from a steady velocity of 10 ft/sec. It is seen that the graphs coincide closely until the reflection from the open end returns to the inset. At this instant the velocity of the air, in the open end case, drops very suddenly. It seems likely that this open end condition is not a true estimate of the conditions at the upcast shaft. It is probable that, while being open to the extent of permitting airflow, the fan will act as a closed end to a pressure pulse.

Hence the results obtained with a closed end may give a good quantitative estimate of the behaviour of the air, simply by subtracting them from the steady velocity. This result could have been predicted by noting that, where friction is not the important factor, and therefore the inertia of the air is, the pressure in the system will be a function of  $\frac{du}{dt}$  and not of  $u$ . Hence a steady velocity could be added to the results without affecting their validity. Thus in all the results given, except where friction is of prime importance, the results may be used quantitatively to assess the effect of the pressure disturbances on a steady velocity.

THEORETICAL PREDICTION OF VELOCITY DISTURBANCES -

METHOD 2

In Chapter 9 the importance of the wall friction in the calculation was determined. It was found (see Fig. 43) that, when the volume of the workings was  $2 \times 10^6 \text{ ft}^3$ , even a moderate friction factor produced only a slight change of velocity as compared with the velocity when the friction factor was zero. This was not the case (see Fig. 44) when the volume was  $10^7 \text{ ft}^3$ . It can also be seen that, for all the velocity diagrams, the rate of change of velocity with respect to time  $\frac{du}{dt}$  at any point is much greater ( $10^2$  to  $10^3$  times) than the product of the velocity and the rate of change of velocity with respect to distance  $u \cdot \frac{du}{dx}$ .

Although friction can, by no means, be neglected in all cases there are cases in which this assumption is justified. In such cases the non-linear terms may be omitted from equations A.1 and A.2 [see Appendix A] and equations A.3, A.4 and A.5 may be replaced by equation 4 so that we are reduced to the simplified set of equations used in the theory of sound.

$$\frac{\partial w}{\partial t} + w \cdot \frac{\partial u}{\partial x} = 0 \quad \text{Equn. 8}$$

$$\frac{\partial u}{\partial t} + \frac{1}{v} \cdot \frac{\partial p}{\partial x} = 0 \quad \text{Equn. 9}$$

$$\frac{p}{v k} = \text{constant} \quad \text{Equn. 10}$$

The basic equations of Appendix A have been further simplified by the assumption of constant area. When we later consider a system in which the area varies it is divided into sections in which the area is assumed to remain constant.

Equation 8 is the conservation of mass equation which states that the mass of gas flowing into an element, minus the mass of gas flowing out, is equal to the increase in mass of the element. Considering Fig. 50 this may be rederived in the form

$$Mu_1 \cdot dt - Mu_2 \cdot dt = dV$$

If we let  $V_1$ ,  $V_2$  and  $V_3$  be the volume changes at sections 1, 2 and within the element respectively then we may write.

$$V_1 - V_2 = V_3$$

$$\text{or } \frac{dV_1}{dt} - \frac{dV_2}{dt} - \frac{dV_3}{dt} = 0 \quad \text{Equn. 11}$$

Equation 9 may be written,

$$dp + \frac{w M \cdot dx}{M^2} \cdot \frac{d(uM)}{dt} = 0$$

$$\therefore dp + \frac{m}{M^2} \cdot \frac{d^2 V_2}{dt^2} = 0 \quad \text{Equn. 12}$$

Differentiating equation 10 we get

$$dp = k \bar{w}^{k-1} \cdot dw$$

---

Mass flowing in

is  $\underline{Au_1 dt \cdot w}$

$\bar{v}$

Mass flowing out

is  $\underline{Au_2 dt \cdot w}$

---

Since  $w$  is assumed to be constant,  
this means that the walls can move  
freely to accommodate any additional  
mass admitted to an element.

Fig. 50.

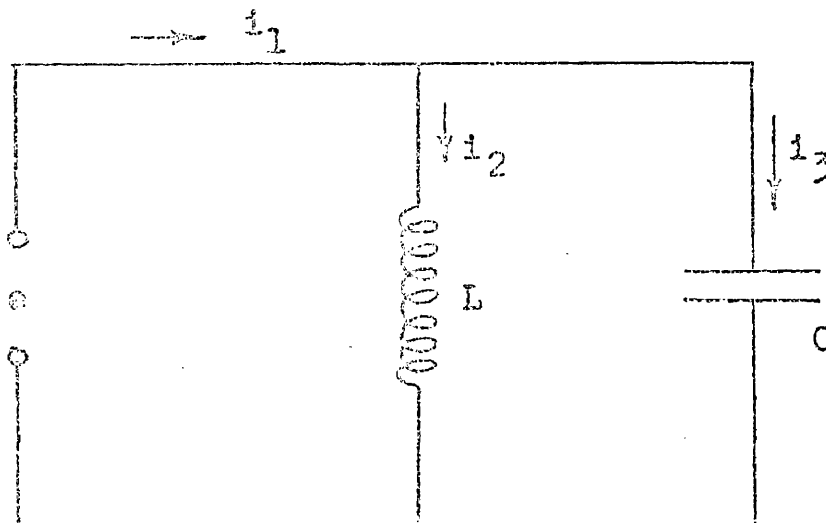


Fig. 51.

$$= \frac{kp}{v} \cdot dv$$

$$\therefore dp = a^2 dv \quad \text{where the velocity of sound } a = \sqrt{\frac{kp}{v}}$$

$$\therefore dp = \frac{a^2 v}{v} \cdot dv$$

$$= \frac{c^2 v}{v} \int \frac{dv}{dt} \cdot dt \quad \text{Equn. 13}$$

Consider the electrical circuit in Fig. 51. We have three unknown currents which are determined from the three equations,

$$i_1 = i_2 + i_3 \quad \text{Equn. 14}$$

$$e = L \cdot \frac{di_2}{dt} \quad \text{Equn. 15}$$

$$e = \frac{1}{C} i_3 \cdot dt \quad \text{Equn. 16}$$

We see that equations 14, 15 and 16 are the differential equations 11, 14 and 13 with different coefficients. The acoustical system is therefore analogous to the electrical system with acoustical pressure  $p$  analogous to electrical voltage  $e$ , volume flow  $\frac{dv}{dt}$  analogous to current  $i$ , acoustical capacitance  $C_a \left( = \frac{v}{a^2 v} \right)$ , which opposes a change in pressure, analogous to electrical capacitance  $C$ , which opposes a change in voltage and acoustical inductance  $L_a \left( = \frac{m}{M^2} \right)$ , which opposes a change in volume flow, analogous to electrical inductance  $L$ , which opposes a change in current.

In equation 12 we see that  $\frac{dV_2}{dt}$  is the volume flow which, together with the mass or inertia of the air, opposes a change in pressure. Hence  $i_2$  is the current flowing through the inductance in the electrical analogue.

It is therefore possible to represent any acoustical system by means of an equivalent electrical network. The methods of solution applicable to the latter may then be used.

Consider the acoustical system in Fig. 52 where the volume shown is circular at every section. It can be split into lumped elements (three have been chosen) which represent the acoustical capacitance and inductance. Table VII shows how the elements are calculated and in Fig. 53 they are represented by an analogous electrical circuit. In order to determine what the rate of discharge of air will be when a sudden pressure drop of 1" W.G. is applied to the open end of the system in Fig. 52 it is necessary to determine  $i_4$  for a corresponding sudden reduction in voltage applied to the circuit in Fig. 53.

#### Method of Solution

To determine the effect of a sudden pressure drop let the steady voltage applied to the circuit in Fig. 53 be  $e_1$  and let this drop suddenly to  $e_2$  at a time  $t = 0$ .

$e_c$  is the voltage on capacitance  $C$ , and

$e(0+)$  is the voltage immediately after  $t = 0$ .

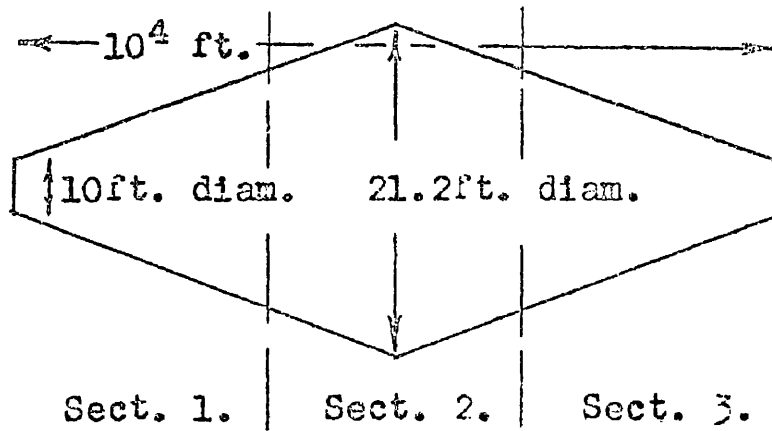


Fig. 52.  
Biconical  
volume.

Table VII

Section	Volume $V$ ft <sup>3</sup> .	Mass of air $m$ lbs.	Mean area $M$ ft <sup>2</sup>	$C =$ $V/a^2w$	$L =$ $m/M^2$
1.	$5.1 \times 10^5$	$3.8 \times 10^4$	150	5.4	1.8
2.	$9.9 \times 10^5$	$7.4 \times 10^4$	290	10.5	0.86
3.	$5.1 \times 10^5$	$3.8 \times 10^4$	150	5.4	1.8

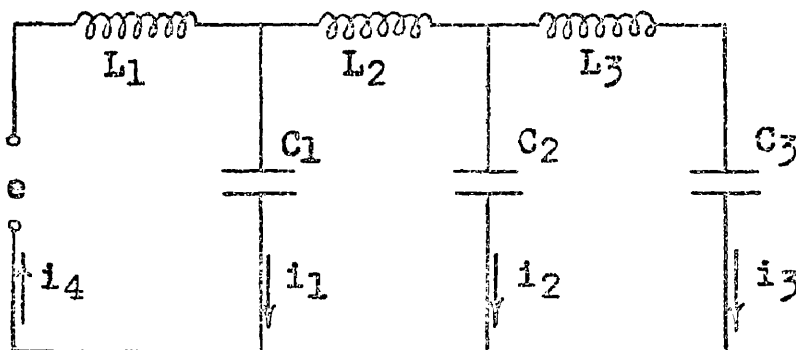


Fig. 53.

The four equations describing the four unknown currents are then :

$$i_4 = i_1 + i_2 + i_3$$

$$-e + L_1 \frac{di_4}{dt} + \frac{1}{C_1} \int i_1 dt + e_{C_1}(0+) = 0$$

$$-e + L_1 \frac{di_4}{dt} + L_2 \frac{d}{dt} (i_4 - i_1) + \frac{1}{C_2} \int i_2 \cdot dt + e_{C_2}(0+) = 0$$

$$-e + L_1 \frac{di_4}{dt} + L_2 \frac{d}{dt} (i_4 - i_1) + L_3 \frac{di_3}{dt} + \frac{1}{C_3} \int i_3 \cdot dt + e_{C_3}(0+) = 0$$

If we let  $E, I$  be the Laplace transforms of  $e, i$  respectively we may use the method of Laplace transformation to rewrite these equations as algebraic equations.  $s$  is here used as the Standard Laplace variable.

$$I_4 = I_1 + I_2 + I_3$$

$$-E + sL_1 I_4 - i_4(0+) + \frac{1}{C_1 s} I_1 + \frac{e_1}{s} = 0$$

$$-E + sL_1 I_4 - i_4(0+) + sL_2(I_4 - I_1) - (i_4 - i_1)(0+) +$$

$$\frac{1}{C_2 s} I_2 + \frac{e_1}{s} = 0$$

$$\begin{aligned}
 -E + sL_1 I_4 - i_4(0+) + sL_2(I_4 - I_1) - (i_4 - i_1)(0+) \\
 + sL_3 I_3 - i_3(0+) + \frac{1}{C_3 s} I_3 + \frac{e_1}{s} = 0
 \end{aligned}$$

At  $t = 0+$  all current will be zero.

From these four equations we may extract  $I_4$ ,

$$\begin{aligned}
 I_4 = -s^2 C_2 L_3 E - s^4 C_2 L_2 L_3 C_1 E + s^3 C_2 L_2 L_3 C_1 e_1 + \\
 C_2 L_3 s e_1
 \end{aligned}$$

$$-\frac{C_2}{C_3} E - \frac{C_2}{C_3} s^2 L_2 C_1 E + \frac{C_2}{C_3} sL_2 C_1 e_1 + \frac{C_2}{C_3} \frac{e_1}{s} - E$$

$$-Es^2 L_2 C_1 + sL_2 C_1 e_1 + \frac{e_1}{s} - C_1 s^2 L_3 E$$

$$-\frac{C_1}{C_3} E + C_1 L_3 s e_1 + \frac{C_1}{C_3} \frac{e_1}{s}$$

$$-s^3 C_2 L_3 L_1 - s^3 C_2 L_3 L_2 - s^5 C_2 C_1 L_1 L_2 L_3 - \frac{C_2}{C_3} s L_1$$

$$-\frac{C_2}{C_3} s L_2 - \frac{C_2}{C_3} s^3 L_1 L_2 C_1 - sL_1 - sL_2 - s^3 L_1 L_2 C_1$$

$$-sL_3 - \frac{1}{C_3s} - s^3 C_1 L_1 L_3 - s \frac{C_1}{C_3} L_1$$

Substituting the values for C,L given in Table VII we have,

$$I_4 = -\left(-sE + e_1\right) \frac{84.6 s^4 + 41.4 s^2 + 3.96}{148 s^6 + 88.2 s^4 + 11.2 s^2 + 0.19}$$

which may be rewritten

$$I_4 = -\left(-sE + e_1\right) \left[ \frac{0.098}{s^2 + 0.425} + \frac{0.068}{s^2 + 0.151} + \frac{0.406}{s^2 + 0.0196} \right]$$

In the acoustical case the pressure is assured to drop from 400" W.G. to 399" W.G. Since the voltage is analogous to the pressure in pounds/ft<sup>2</sup>, the voltage drops from  $6.7 \times 10^4$  pdls./ft<sup>2</sup> to  $(6.7 \times 10^4 - 167)$  pdls./ft<sup>2</sup>. A positive unit step function, i.e. a function which jumps from 0 to +1 when it reaches  $t = 0$ , is conventionally written  $U(t)$ . Thus the voltage applied to the circuit may be written  $e = 6.7 \times 10^4 - 167 U(t)$

$$\therefore E = \frac{6.7 \times 10^4}{s} - \frac{167}{s}$$

We also have  $e_1 = 6.7 \times 10^4$

Therefore,

$$I_4 = -167 \left[ \frac{0.098}{s^2 + 0.425} + \frac{0.068}{s^2 + 0.151} + \frac{0.406}{s^2 + 0.0196} \right]$$

which may be rewritten,

$$I_4 = -167 \left[ 0.150 \frac{0.625}{s^2 + (0.625)^2} + 0.175 \frac{0.388}{s^2 + (0.388)^2} + 2.90 \frac{0.140}{s^2 + (0.140)^2} \right]$$

The inverse transformation of this equation gives

$$i_4 = -167 \left[ 0.150 \sin 0.625t + 0.175 \sin 0.388t + 2.90 \sin 0.140t \right]$$

This describes  $i_4$  when the voltage is suddenly reduced by 167 volts. Current  $i$  is analogous to volume flow  $\frac{dV}{dt} = Mu$ . Therefore to get  $u$  we must divide  $i$  by the area  $M$ . The open end is 10' in diameter, so the area is 78.5 ft<sup>2</sup>. This provides the final solution to the problem,

$$u = -2.12 \left[ 0.150 \sin 0.625t + 0.175 \sin 0.388t + 2.90 \sin 0.140t \right]$$

This has been plotted in Fig. 54 together with the solution for the same conditions using the alternative method. It is seen that the correspondence is very close and any small discrepancies may be due to the fact that in the electrical case the distributed parameters were represented by only three lumped parameters.

In this calculation it has been assumed that there was no friction between the walls and the air flowing in the system. While the friction effect may be neglected in some cases it is very important in others. The electrical element which causes dissipation of energy is resistance. In electrical circuits, however, the voltage drop across a resistance is proportional to the first power of the current

flowing through it, whereas in mine ventilation the pressure drop across a resistance is proportional to the second power of the velocity. It would be possible to extend this method, using an iterative procedure similar to that used in mine ventilation calculations (ref. 13), to determine the effect of a resistance which caused a pressure drop proportional to the second power of velocity, but the calculations would then become at least as tedious as those in the gas dynamics method.

It will also be realised that, in this case, as opposed to the steady flow ventilation case, instead of successively replacing the resistance in the analogue by a new constant value proportional to the product of the former resistance and the current flowing through it, it would be necessary to replace it by another, again proportional to the product of the former and the current flowing through it, but which would, in this case, be a function of time since the current itself would be a function of time.

This fact notwithstanding, the electrical analogue method may still have many advantages in certain cases. It is, for example, easier to determine what will happen when a roadway, along which a pressure pulse is being propagated, splits into two or more roadways, or joins another roadway along which another pressure pulse is being propagated.

An aspect of the electrical analogue method which might profitably be investigated is the simulation of an acoustical system by an electrical model in which the effects of any voltage changes

could be measured directly. To include the effects of resistance would, however, be very difficult in view of the fact that the resistance would be a function of time.

The electrical analogue method has not been investigated to the same extent as the gas dynamics method, but its possibilities have been indicated so that in future work it may be taken into account.

The work which has been described included the experimental study of the pressure drop produced by stationary and moving cages, together with the theoretical and experimental study of the effects, on the ventilation, of this changing pressure.

The study of the importance of cage dimensions showed that, within the limits normally used, the ratio of cage length to cage breadth does not affect the pressure loss due to the cage. It was also found that each additional deck, over three, produces, as might be expected, a fairly constant increase in pressure loss. But the frontal area has the greatest effect and produces a pressure loss proportional to its third power, so that an increase in area of 10% will increase the pressure loss by 33%. It becomes very obvious that the area of any cage must be given the fullest consideration in any discussion of pressure loss. It is not possible to suggest what kind of balance should be struck to maintain a high winding tonnage with a low cage pressure loss between, for example, cage area and the number of decks, since every installation will have its own economics and special conditions.

Investigation into the components of the pressure loss showed that re-expansion is the largest single factor. This re-expansion takes place between the decks and behind the cage. It was found that if the mine cars filled the cage well enough to avoid re-expansion between decks, the pressure loss would be reduced by approximately

one sixth. The re-expansion behind the cage contributes greatly to the pressure loss and streamlining can reduce this loss considerably. It has been shown (ref. 4) that a properly streamlined shape can reduce the pressure loss by 50%, while simple straight-sided fairings can reduce it by up to 45%. Streamlining may introduce many constructional difficulties at the pit top and bottom, as well as with the cage. However, it is possible that a combination of economical considerations may make streamlining worthwhile.

The study of the pressure drop produced by a moving cage resulted in an expression being developed which indicates the relative importance of the air and cage velocities. From it, for example, we may deduce that, in the case of the cage at colliery R travelling in an air velocity of 40 ft/sec., a reduction in cage speed from 40 ft/sec. to 20 ft/sec. should produce a reduction in pressure drop of 40%. A comparison of fig. 3 and fig. 4 shows that the maximum pressure drop has been reduced by approximately 45%.

Having studied the pressure drop produced by the cage the effect of communicating this pressure to a volume of air, such as is found underground, was investigated. The first conclusion which was drawn from these tests is that any changing pressure tends to set in oscillation the air in the system. An infinite number of modes of oscillation are possible and those which are least attenuated have the greatest effect on the airflow. In the model it was possible to determine the frequency of the oscillations and, by inspection, deduce which mode of oscillation was prevalent. Underground this

would be very much more difficult due to the complex system of airways and it would be almost impossible to predict which mode of oscillation was likely to occur. It seems probable, however, that any oscillation involving a long length of roadway will be severely attenuated by partial reflections from obstructions and openings, and hence will give no trouble. Any oscillation involving a short length of roadway will be of relatively high frequency and should not disturb the airflow to any marked extent. It was found that, in the model, any oscillation could be made to decay rapidly by inserting a resistance in the oscillating air.

The second, and perhaps more important, effect of the moving cage is to cause large volumes of air suddenly to change in pressure. A reduction in pressure will cause an expansion and consequent outflow of air. If this air flows out in the opposite direction to the ventilating air it may seriously interfere with normal ventilation. In the model a large volume was used to simulate the air in the underground workings and resistances on either side of the volume simulated the distributed resistance of the workings. The velocity of the air flowing from the shaft through this volume was recorded as the cage moved past the inset. It was possible, by a suitable combination of the resistances on either side of the volume, to get a serious reduction of the ventilating air velocity. However, leakage into the volume prevented any conclusive results from being obtained although it was possible to conclude that the resistances on either side of the volume affected the degree of disturbance of the airflow. Hence we may

deduce that both the friction factor and the distribution of the friction underground will affect the disturbance. In the model the cage stopped moving too soon after passing the inset to simulate conditions in a mine shaft in this respect. It was, therefore, not possible to determine any close relationship between the cage speed and the shape of the air velocity time curve. This point may be of importance.

The possibility of predicting the degree of disturbance mathematically was studied simultaneously with the experimental tests. The solution of the basic equations for the gas dynamics of non-steady compressible flow was obtained and produced information about several factors. It was, however, not possible to verify the method of calculation by any field tests. The report on the disturbance at colliery R does not give sufficient details to check that particular case, but the results predicted for a similar case are of a similar type.

These calculations indicate that friction is important only where high velocities are involved and that the volume of the air and the cage pressure drop are the important factors. It is also probable that the shape of the volume can modify, to a large extent, the shape of the velocity disturbance waveform.

An alternative method of solving modified equations was explained but its possibilities were not fully studied. It was suggested that an electrical analogue could be constructed which would facilitate the solution of these equations.

It was found from the calculations that the fan was acting as a closed end to pressure pulses, while permitting the flow of air through it. It follows that if the fan could be moved closer to the source of the disturbance it would confine any velocity variations to a shorter length of roadway. It is difficult to see how this principle may be employed, but it might be possible to construct, near the source of the disturbance, in the main airway, a doorway through which mine cars etc. could pass. The rest of the section of the roadway, at this point, could be rotating vanes driven at such a speed as neither to give energy to nor take energy from the air. This would permit the free passage of the air, while offering an almost closed end to pressure pulses.

It has been suggested (ref. 1) that a second, parallel, shaft should be provided, where possible, to act as the main downcast shaft. Reference 14 describes the conditions at colliery S where a second shaft is in existence. Shafts No.1 and No.2 are downcast, No.2 serving two levels and No.1 going only to the upper level. No.3 shaft is the upcast for both levels. Balanced skips wind coal in No.3 shaft, balanced cages are used in No.1 shaft but No.2 shaft has a large cage and counterweight. Fig. 55 shows the layout of the roadways around the shafts at the upper level. Air velocity measurements were taken at stations 1-8 and A, B, C, D while the cage was winding in No.2 shaft. Fig. 56 shows the variation of velocity with time measured at station 2 and is typical of stations 1-8.

One of the first conclusions drawn from these measurements is

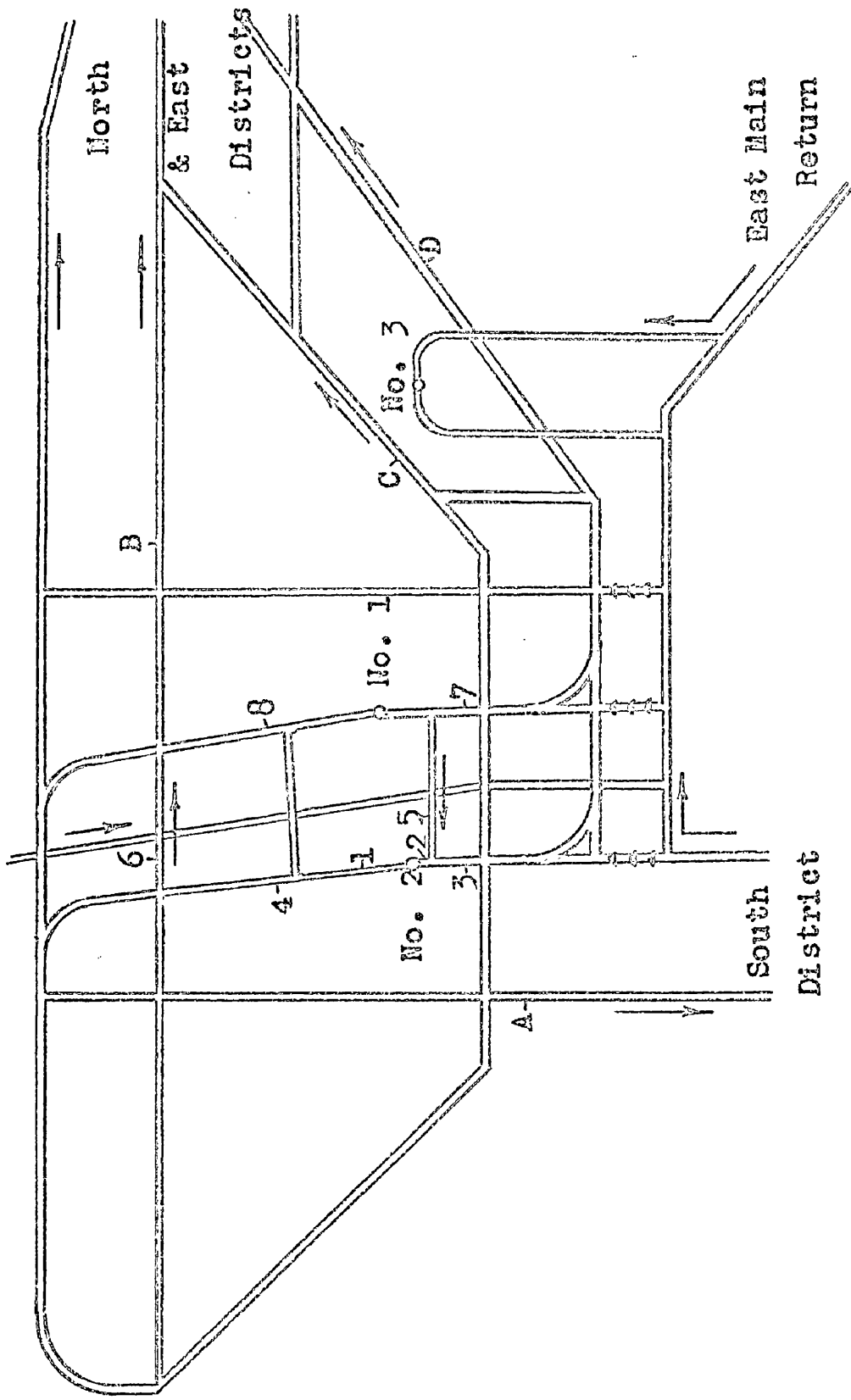


Fig. 55. Layout of roadways around the shafts at the Top Hard pit bottom, colliery S, showing the positions of the measuring stations.

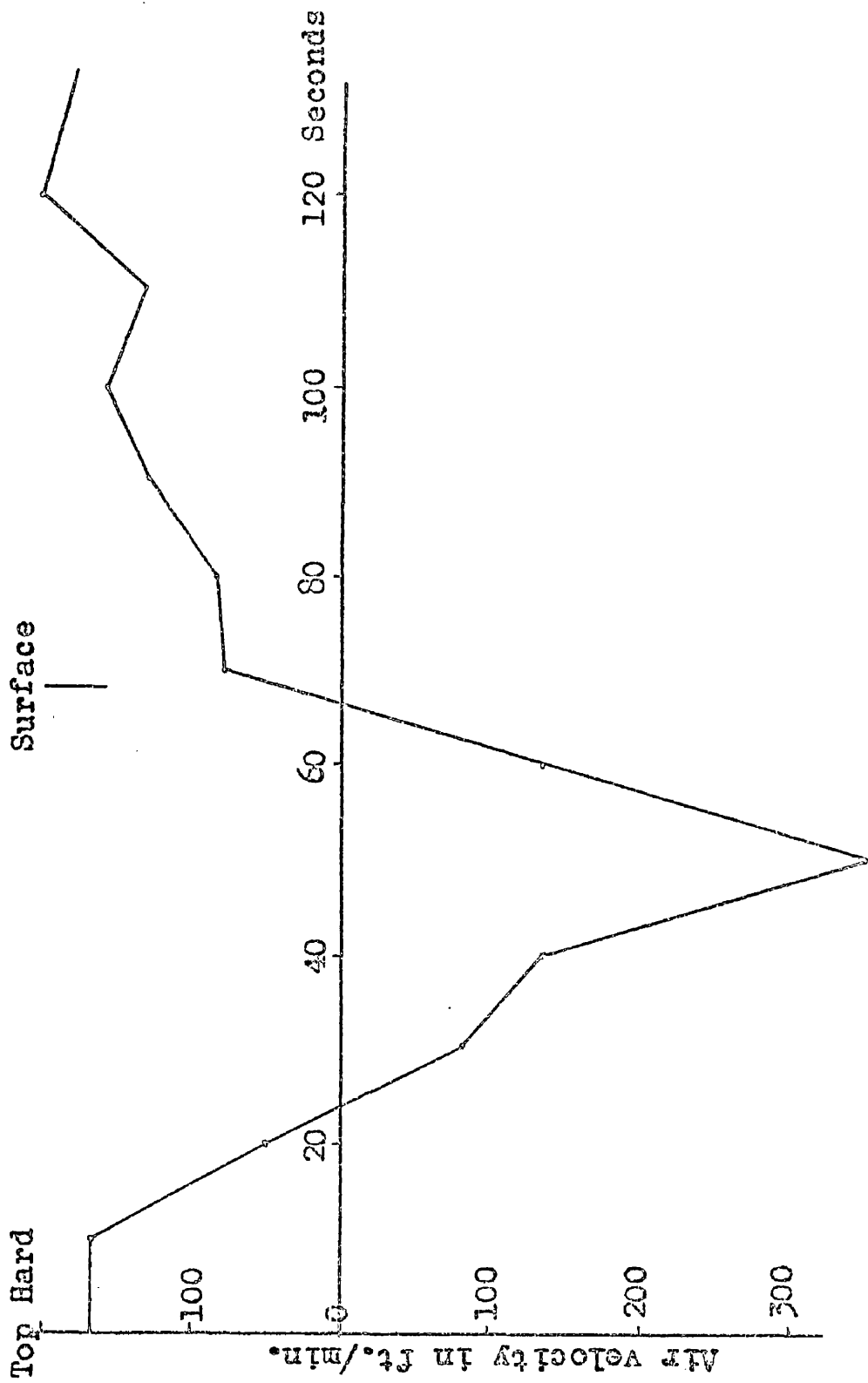


Fig. 56. Airflow measurements at station 2, colliery S, as cage ascends from Top Hard to surface at 49 ft./sec.

that no disturbance exists in the main intakes at stations A, B, C and D, hence a parallel shaft does effectively prevent disturbances being propagated inbye. It does not, however, lessen the disturbances close to the downcast shaft and tends to increase them. There is no evidence of any detrimental effects of this fluctuating airflow round the downcast shafts. It should be noticed that, in this case, expansion of the air plays little or no part in these disturbances. It is simply changes of pressure between two sources of air, that is, the two downcast shafts, which cause the change of airflow.

The investigation has not considered whether any disturbances present a hazard to health or safety, since that will depend very much on local conditions. However, the following suggestions apply both to existing cases, where trouble has been met, and to new installations.

- 1) Provide a parallel shaft.
- 2) Use a high cage speed or larger number of decks,  
in preference to a large cage frontal area.
- 3) Streamline the cage.
- 4) Use balanced-cage winding.
- 5) Use a single skip which will have a much smaller  
area for the same payload.

The limitations of the investigation have generally been discussed where they were important. Future work may overcome several of these and, in particular, the investigation of the effects of the cage pressure drop on a large volume of air will require to be carried out

in much more detail, paying close attention to the similarity between the model and actual practice.

More field tests will require to be done to verify the methods of calculation used and the results obtained. The construction of an electrical analogue might be of great assistance in solving the equations when the methods have been verified.

## A P P E N D I X A

### DERIVATION OF BASIC EQUATIONS

In order to make a solution of the basic equations possible they have been derived in a one dimensional form. This treatment is valid when the other dimensions of the system are small compared with the length. It is also assumed that the gas will follow the ideal gas law.

#### 1) The Continuity Equation.

Consider Fig. A.1. The mass entering the section  $dx$  in time  $dt$  is  $(w\mu)dt$  and the mass leaving is  $(w\mu + \frac{\partial(w\mu)}{\partial x} \cdot dx)dt$ . The rate of increase of the mass in section  $dx$  is  $dx \cdot \frac{\partial \mu}{\partial t} \cdot dt$  which must be equal to the difference between outflow and inflow.

$$\text{Hence } dx \cdot \frac{\partial \mu}{\partial t} \cdot dt = - \frac{\partial (w\mu)}{\partial x} \cdot dx \cdot dt$$

Since, in our case,  $\mu$  is independent of  $t$  we have,

$$\mu \cdot \frac{\partial w}{\partial t} + \frac{\partial (w\mu)}{\partial x} = 0 \quad \text{Equn. A.1}$$

#### 2) The Momentum Equation.

Consider Fig. A.2. The sum of forces acting on element  $dx$  is

$$p\mu - \left[ p\mu + \frac{\partial p\mu}{\partial x} \cdot dx \right] + p \cdot d\mu - \frac{4fu^2}{2d} \cdot w\mu dx$$

which, by Newton's Law, is equal to the product of the mass and the acceleration, which is  $\frac{Dw}{Dt} \cdot \mu \cdot dx \cdot w$

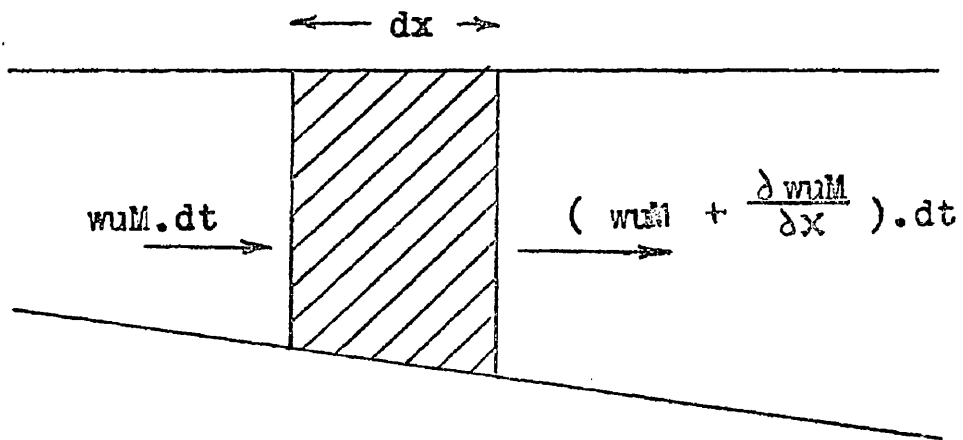


Fig. A.1. Mass flow into and out of an elemental volume.

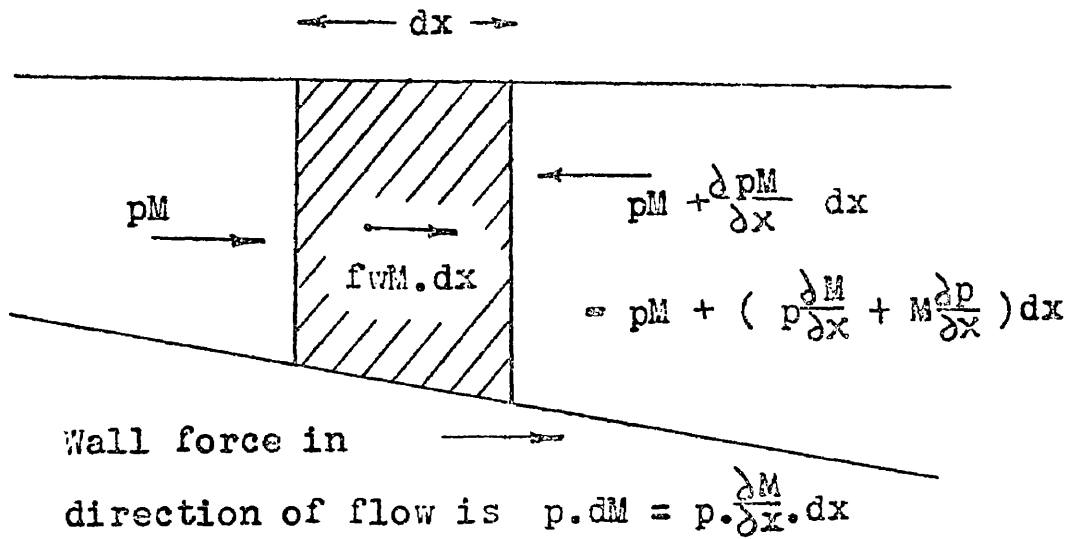


Fig. A.2. The forces acting on the fluid in an elemental volume.

Hence we get,

$$\frac{Du}{Dt} = \frac{\partial u}{\partial t} + u \cdot \frac{\partial u}{\partial x} = -\frac{1}{\rho} \cdot \frac{\partial p}{\partial x} - \frac{4fu^2}{2d} \quad \text{Equn. A.2}$$

### 3) Entropy Conditions.

The work done by friction

$$= \left( \frac{4fu^2}{2d} \cdot u \right) / \text{lb/sec.}$$

$$\therefore \text{Heat added / lb / sec.} = \frac{4fu^3}{2d\rho J} = \frac{Dq}{Dt}$$

By definition  $\frac{Ds}{Dt} = \frac{1}{\rho} \cdot \frac{Dq}{Dt}$

$$= \frac{4fu^3}{2d\rho J \rho}$$

$$= \frac{\partial s}{\partial t} + u \cdot \frac{\partial s}{\partial x}$$

Equn. A.3

### 4) The equation of state.

This is  $p = \rho R \theta$

From the definition of the local velocity of sound we have

$$a^2 = k \frac{p}{\rho} = kR\theta \quad \text{Equn. A.4}$$

### 5) Relation between entropy, pressure and temperature.

This is simply obtained by integrating the first law of thermodynamics, which may be written,

7

$$ds = \int_{s_1}^s c_p \cdot \frac{d\theta}{\theta} - \frac{R}{J} \log_e \frac{p}{p_1}, \quad \text{on the assumption}$$

of constant specific heat. This gives

$$s - s_1 = c_p \cdot \log_e \frac{\theta}{\theta_1} - \frac{R}{J} \log_e \frac{p}{p_1} \quad \text{Equn. A.5}$$

The equation involving the specific heat at constant pressure is useful in the following form,

$$c_p = \frac{k}{k-1} \cdot \frac{R}{J} \quad \text{Equn. A.6}$$

By combining equations A.4, A.5 and A.6 we can obtain two other useful relationships,

$$\frac{p}{p_1} = \left( \frac{A}{A_1} \right)^{\frac{2k}{k-1}} e^{-k(S-S_1)} \quad \text{Equn. A.7}$$

$$\frac{w}{w_1} = \left( \frac{A}{A_1} \right)^{\frac{2}{k-1}} e^{-k(S-S_1)} \quad \text{Equn. A.8}$$

In these equations the variables have been used in their non-dimensional form.

A P P E N D I X B

METHOD OF SOLVING THE BASIC EQUATIONS

Equations A.1 and A.2 may be written

$$\frac{\partial \log w}{\partial t} + u \cdot \frac{\partial \log w}{\partial x} + \frac{\partial u}{\partial x} = -u \cdot \frac{\partial \log H}{\partial x} \quad \text{Equn. B.1}$$

$$\frac{\partial u}{\partial t} + u \cdot \frac{\partial u}{\partial x} = -\frac{a^2}{k} \cdot \frac{\partial \log p}{\partial x} - \frac{4fu^2}{2d} \quad \text{Equn. B.2}$$

where use has been made of  
equation A.4. Equation A.5 may be rearranged, using equations A.4  
and A.6, to give

$$d \log p = \frac{2k}{k-1} d \log a - \frac{GJ}{R} ds = \frac{2k}{k-1} \cdot \frac{da}{a} - \frac{GJ}{R} \cdot ds$$

$$\text{and } d \log w = \frac{2}{k-1} d \log a - \frac{GJ}{R} ds = \frac{2}{k-1} \cdot \frac{da}{a} - \frac{GJ}{R} ds$$

Substituting these expressions for  $d \log p$  and  $d \log w$  in  
equations B.1 and B.2 we get

$$\frac{2}{k-1} \cdot \frac{\partial a}{\partial t} + \frac{2}{k-1} \cdot u \cdot \frac{\partial a}{\partial x} + a \cdot \frac{\partial u}{\partial x} = -au \frac{\partial \log H}{\partial x} + a \cdot \frac{GJ}{R} \cdot \frac{Ds}{Dt} \quad \text{Equn. B.3}$$

$$\text{and } \frac{\partial u}{\partial t} + u \cdot \frac{\partial u}{\partial x} + \frac{2}{k-1} \cdot a \cdot \frac{\partial a}{\partial x} = a^2 \cdot \frac{GJ}{kR} \cdot \frac{\partial s}{\partial x} - \frac{4fu^2}{2d} \quad \text{Equn. B.4}$$

If equation B.4 is added to and subtracted from equation B.3

we get,

$$\begin{aligned} \frac{\partial}{\partial t} \left( \frac{2}{k-1} a \pm u \right) + (u \pm a) \frac{\partial}{\partial x} \left( \frac{2}{k-1} a \pm u \right) = \\ - au \frac{\partial \log M}{\partial x} + a \cdot \frac{GJ}{R} \left( \frac{Ds}{Dt} \pm \frac{a}{k} \cdot \frac{\partial s}{\partial x} \right) \pm \frac{4fu^2}{2d} \end{aligned} \quad \text{Equn. B.5}$$

The left hand side of this equation is the derivative of the parameters

$\left( \frac{2}{k-1} a \pm u \right)$  in the  $x, t$  plane in a direction such that

$$\frac{dx}{dt} = u \pm a$$

$$\text{Now } \frac{D}{dt} = \frac{\partial}{\partial t} + u \cdot \frac{\partial}{\partial x}$$

$$\text{and } \frac{\delta \pm}{\delta t} = \frac{\partial}{\partial t} + (u \pm a) \frac{\partial}{\partial x}$$

$$\therefore a \cdot \frac{\partial}{\partial x} = \frac{\delta \pm}{\delta t} - \frac{D}{dt} = - \frac{\delta \mp}{\delta t} + \frac{D}{dt}$$

Using this to eliminate  $\frac{\partial s}{\partial x}$  from equation B.5 we get,

$$\begin{aligned} \frac{\delta \pm}{\delta t} \left( \frac{2}{k-1} a \pm u \right) = - au \frac{\partial \log M}{\partial x} + a \cdot \frac{GJ}{kR} \cdot \frac{\delta \mp}{\delta t} s + \\ (k-1)a \cdot \frac{GJ}{kR} \cdot \frac{Ds}{Dt} \mp \frac{4fu^2}{2d} \end{aligned}$$

By multiplying both sides of this equation by  $\frac{l}{s_0^2}$  it may be written in a non-dimensional form.

Thus,

$$\frac{\delta + P}{\delta T} = -AU \frac{\partial \log M}{\partial X} + A \frac{\delta + S}{\delta T} + (k-1)A \frac{DS}{DT} - \frac{4fU^2 l_0}{2d A_0^2}$$

Equn. B.6

$$\frac{\delta - Q}{\delta T} = -AU \frac{\partial \log M}{\partial X} + A \frac{\delta - S}{\delta T} + (k-1)A \frac{DS}{DT} + \frac{4fU^2 l_0}{2d A_0^2}$$

Equn. B.7

Since 
$$\frac{\delta \pm \log M}{\delta T} = \frac{\partial \log M}{\partial T} + (U \pm A) \frac{\partial \log M}{\partial X},$$

then 
$$-AU \frac{\partial \log M}{\partial X} \text{ can be written } - \frac{AU}{(U \pm A)} \frac{\delta \pm \log M}{\delta T}$$

Also, from the non dimensional form of equation A.3 we have

$$\frac{DS}{DT} = \frac{4f l_0 U^3}{2d A^2} \frac{U}{|U|} \text{ where the last term has been added to give the correct sign to } \frac{DS}{DT} \text{ independently of the direction of } U.$$

Therefore, along a line given by  $\frac{dX}{dT} = U \pm A$  we have, for points 1 and 2 separated by  $\Delta T$ ,

$$P_2 = P_1 - \frac{AU}{U \pm A} \left[ \log M_2 - \log M_1 \right] + A \left[ S_2 - S_1 \right] + (k-1) \frac{4f l_0 U^3}{2d A} \cdot \frac{U}{|U|} - \frac{4fU^2 l_0}{2d A_0^2} \cdot \Delta T$$

and along a line given by  $\frac{dX}{dT} = U - A$  we have, for points 2 and 3 separated by  $\Delta T$ ,

$$Q_2 = Q_3 - \frac{AU}{U - A} \left[ \log M_2 - \log M_3 \right] + A \left[ S_2 - S_3 \right] + (k-1) \frac{4f l_0 U^3}{2d A} \cdot \frac{U}{|U|} +$$

$$+ \frac{4fU^2 l_0}{2d A_0^2} \Delta T$$

$\frac{DS}{DT}$  is the variation of particle entropy measured along the path taken by the particle — namely  $\frac{dX}{dT} = U$ . Hence for two points 2 and 4 on a line given by  $\frac{dX}{dT} = U$  we have  $S_2 = S_4 + \frac{DS}{DT} \Delta T$

The lines  $\frac{dX}{dT} = U \pm A$

and  $\frac{dX}{dT} = U$  are called characteristics and a plot of them is called a wave diagram.

### Procedure

Consider the wave diagram in Fig. A.3. In this  $T$  is positive in the upward direction,  $X$  is measured to the right and  $U$  is positive as the air is flowing from left to right. In our case  $A$  will be very nearly 1.0 and  $U$  will be small so that the  $P$  and  $Q$  characteristics will be lines at approximately  $45^\circ$  to the axes sloping upwards to the right and left respectively.

If we have two points 1 and 2 (see Fig. A.4) which do not lie on the same characteristic and whose properties  $X, T, A, U, S$  are known then we may draw a  $P$  characteristic, with slope  $U_1 + A_1$ , through point 1 to meet, at point 3, the  $Q$  characteristic with slope  $U_2 - A_2$ , drawn through point 2. Through point 3 we may now draw a line having a slope equal to the mean particle path slope of points 1 and 2, i.e.  $\frac{U_1 + U_2}{2}$ . This line will intersect the line joining points 1 and 2 at point 4. Line 3-4 will therefore be a

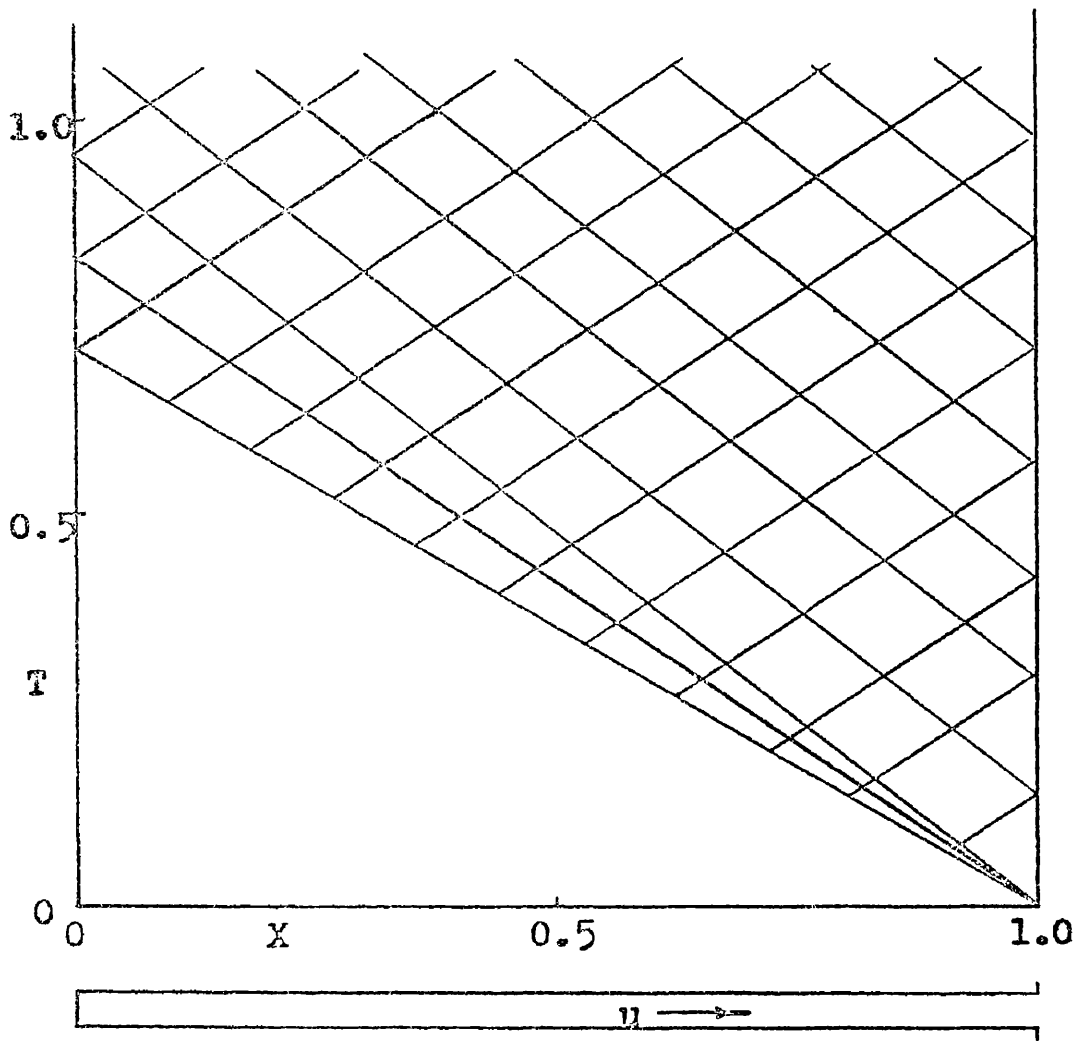


Fig. A.3. Wave diagram resulting from sudden release of compressed air from a cylinder.

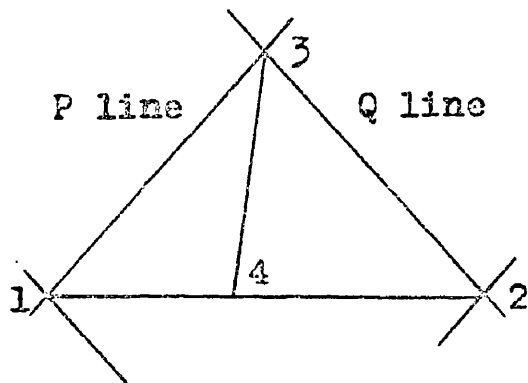


Fig. A.4.  
Determination  
of one point.

particle path along which  $\frac{DS}{DT}$  is known. By linear interpolation between points 1 and 2 we may determine  $S_4$  and hence  $S_3$ . Using, as a first approximation, the  $U$  and  $A$  values at one end of each line 1-3 and 2-3 we may determine  $P_3$  and  $Q_3$ . By adding and subtracting  $P_3$  and  $Q_3$  we may determine  $A_3$  and  $U_3$  respectively. We now know what the slope of line 1-3 should be at point 3 and we may redraw the line with a mean slope. We may similarly redraw lines 2-3 and 3-4 with mean slopes.  $P_3$  and  $Q_3$  are again determined, this time using mean values of  $U$  and  $A$ . This process may be repeated until  $A_3$  and  $U_3$  have been determined to a sufficient accuracy. Points 1 and 3 or 2 and 3 may then be used to find further points in the  $X/T$  field. Hence the properties of the gas may be determined at any position and time.

### End Conditions

At the closed end of a duct we determine from the approaching  $P$  or  $Q$  characteristic the  $P$  or  $Q$  value at the closed end. It is also known that at a closed end  $U = 0$ , therefore  $A$  may be determined.

At an open end we may have either of two conditions — namely inflow or outflow. In the case of outflow it is assumed that the pressure just inside the end of the duct is the same as that of the atmosphere outside the end of the duct. Thus  $P$  or  $Q$  is determined as for a closed end and, knowing  $A$  this time, we determine  $U$ .

In the case of inflow it is assumed that flow across the end

section of the duct is steady, and since there can be no friction loss across a section we consider  $\frac{du}{dt}$  and  $f$  as zero.

Equation A.2 becomes

$$u \cdot du + \frac{dp}{\rho} = 0 \quad \text{Equn. B.8}$$

It is also assumed that the inflow is isentropic so that  $S$  is known and  $\frac{P}{\rho^k} = \text{constant}$ . Equn. B.9

Combining equations B.8 and B.9 and integrating, we get

$$\frac{k}{k-1} \frac{P}{\rho} + \frac{u^2}{2} = \text{constant.}$$

$$\therefore \frac{2}{k-1} A_0^2 + U_0^2 = \text{constant} = \frac{2}{k-1} A_E^2 + U_E^2 \quad \text{Equn. B.10}$$

We also have, for the right hand end open,

$$P_0 = \frac{2}{k-1} A_0 + U_0 \quad \text{Equn. B.11}$$

Equations B.10 and B.11 may be combined to yield

$$A_0 = \frac{P_0 + \sqrt{\frac{k+1}{k-1} A_E^2 - \frac{k-1}{2} P_0^2}}{\frac{k+1}{k-1}}$$

The positive sign is that which corresponds to outflow. Hence  $P_0$  is determined as before and, knowing the external conditions and therefore  $A_E$ , we may determine  $A_0$  from the above expression and hence  $U_0$ .

## R E F E R E N C E S

1. DURHAM DIVISIONAL  
VENTILATION ENGINEER "Ryhope Colliery An Investigation  
into the Effects of Single Cage  
Winding". National Coal Board  
Report Feb. 1957
2. WILKIE, A. "Study of the Effects of Moving  
Cages in Shafts". Mining Dept.  
Library, R.C.S.T. Glasgow 1959
3. TABACK, I. "The Response of Pressure  
Measuring Systems to Oscillating  
Pressures". H.A.C.A. Tech.  
Rep. 1819, 1949
4. STEVENSON, A. "Mine Ventilation Investigations"  
Mining Dept. Library, R.C.S.T.  
Glasgow 1956
5. BLAHO, M. "Drag of Trains in Tube Tunnels"  
Acta. Tech. Hung. Vol. VIII  
3 4 1954
6. FRIEDLANDER, F.G. "Sound Pulses" Cambridge  
University Press, 1958
7. LIEPMANN, H.W. and  
PUCKETT, A.E. "Introduction to Aerodynamics  
of a Compressible Fluid"  
John Wiley and Sons, Inc. 1947

8. RUDINGER, G. "Wave Diagrams for Non-steady Flow in Ducts" D. Von Nostrand and Co. Inc. 1955
9. STEWART and LINDSAY "Acoustics" p.22 Chapman and Hall Ltd. 1931
10. RIEMANN, B. "Über die Fortpflanzung ebener Luftwellen von endlicher Schwingungsweite". Gött. Abh. 8 (Math.), 43-65 1858-59
11. FRITZSCHE, C.R. and POTTS, E.L.J. "Horizon Mining" p.538 George Allen & Unwin Ltd. 1954
12. COOK, W.E. and STATHAN, I.C.F. "Practical Examples of Surveys and Interpretation of Results" T.I.M.E. Vol. 81 1931
13. SCOTT, D.R., HUDSON, R.F. and HINSLEY, F.B. "A Calculator for the Solution of Ventilation Network Problems" T.I.M.E. Vol. 112, p.624 1952-53
14. EAST MIDLANDS NO.3 AREA VENTILATION ENGINEER "The Effects on the Ventilation of the Movement of the Cage in No.2 Shaft at Rufford Colliery" National Coal Board Report Nov. 1959